

ABSTRACT

Title of Document: FEASIBILITY OF BINDING
ANTIOXIDATIVE FOOD PIGMENTS USING
RIBULOSE-1,5-BISPHOSPHATE
CARBOXYLASE OXYGENASE.

Sarah Michelle Yachetti, Master's in Science,
2010

Directed By: Y. Martin Lo, Ph.D.
Nutrition and Food Science

Antioxidative food pigments during manufacturing are subjected to harsh conditions that can attenuate the antioxidant benefits and alter its color significantly. Thus, stabilization of these pigments is desired to increase the product's nutritional and commercial value. Ribulose-1, 5-bisphosphate carboxylase oxygenase (RuBisCO), an abundant protein with a balanced amino acid profile, may serve as a good binding agent to increase stability of pigments due to the fact that it is naturally bound to chlorophyll in plants besides its highly stable structure. This research investigated the binding capacity of purified RuBisCO to riboflavin, annatto extract, and beta-carotene. Protein-pigment complexes were promoted with mixing, sonicating, heating and freeze thawing techniques. Raman spectroscopy, surface plasmon resonance, and UV-Vis were used to measure binding potential. A method to extract RuBisCO from

tobacco with paramagnetic antibody-coated beads was also investigated. Not only does this exploratory research provide the baseline understanding of the challenges and hurdles in forming a protein-pigment complex, but the detection techniques established could also be of value for developing quantitative measurements of such complexes. While further research is still needed to elucidate the interaction between the pigments and RuBisCO, it was confirmed that the binding ability of RuBisCo to the pigments investigated could be greatly hindered by the structural conformation of RuBisCo.

FEASIBILITY OF BINDING ANTIOXIDATIVE FOOD PIGMENTS USING
RIBULOSE-1,5-BISPHOSPHATE CARBOXYLASE OXYGENASE

By

Sarah Michelle Yachetti.

Thesis submitted to the Faculty of the Graduate School of the
University of Maryland, College Park, in partial fulfillment
of the requirements for the degree of
Master's in Science
2010

Advisory Committee:
Dr. Y. Martin Lo, Chair
Dr. Jeffrey DeGrasse
Dr. Stacey DeGrasse
Dr. Mark Kantor
Dr. Betsy Jean Yakes

© Copyright by
Sarah Michelle Yachetti
[2010]

Acknowledgements

I would like to acknowledge the support and guidance of Dr. Y. Martin Lo, committee chair, without whose support I would never have finished my degree. I also thank the members of my graduate committee for their guidance and suggestions.

This thesis would not have been possible without the generous use of instruments and supplies from the Food and Drug Administration (FDA), provided with support and direction by Stacey Degrasse, Jeffrey Degrasse, and Betsy Jean Yakes. I am in debt and thankful of the mentorship all three of you have provided to me over the years.

To Stacey I am truly grateful for the dedication to help me become a better scientist. I am thankful to Betsy for teaching me that there are no problems, but only challenges to be overcome. And thanks to Jeff for teaching me that something in the lab can always be done faster, but understanding what is going on behind it is what counts. I also want to thank John Callahan for his help in securing my ability to complete my research at the FDA. Thanks to Kevin Reuter for help in processing tobacco samples.

A special thanks to my lab mates who helped keep me sane through all of this.

Finally, I would like to thank family members and friends for encouraging me every step along the way and making sure that I knew I can accomplish anything I set my mind to.

Table of Contents

Acknowledgements.....	ii
Table of Contents.....	iii
List of Tables	iv
List of Figures	v
Chapter 1: Introduction.....	1
Chapter 2: Literature Review.....	4
2.1 Antioxidative Pigments.....	4
2.1.1 Riboflavin	7
2.1.2 Annatto Extract.....	10
2.1.3 Beta-Carotene	12
2.2 RuBisCO.....	15
2.2.1 Properties and Interest.....	15
2.2.2 Structure and Stability.....	16
2.2.3 Extraction and Purification Methods	17
2.3 Tools to Assess Binding.....	19
2.3.1 Raman Spectroscopy.....	19
2.3.2 Surface Plasmon Resonance	23
2.3.3 UV-Vis.....	26
Chapter 3: Objectives.....	30
Chapter 4: Materials and Methods.....	31
4.1: Materials	31
4.1.1 Antioxidative Pigments and Standard RuBisCO	31
4.1.2: Tools to Assess Binding	31
4.1.3 Tobacco RuBisCO Extraction.....	33
4.2 Methods.....	39
4.2.1 Evaluation of Binding.....	39
4.2.2 Extraction.....	48
4.2.3 Purification of Protein.....	49
Chapter 5: Results and Discussion.....	63
5.1 Binding Effectiveness	63
5.1.1 Raman Spectroscopy.....	63
5.1.2 Surface Plasmon Resonance	69
5.1.3 UV-Vis.....	89
5.2 Extraction.....	111
5.3 Purification.....	112
5.3.1 Confirmation of Protein using Paramagnetic Antibody Beads.....	112
5.4 Recommendations to Continue Research	126
5.4.1 Binding Promotion.....	126
5.4.2 Completion of Protein Purification.....	127
Chapter 6: Conclusion.....	129
Bibliography	130

List of Tables

- Table 1: Factors that affect antioxidant power (Yanishlieva, 2001).
- Table 2: Comparison of extraction buffers for tobacco protein extraction optimization.
- Table 3: Protein-Pigment Complex sample description.
- Table 4: Instrument Setup for all pigments with Raman spectroscopy.
- Table 5: Comparison of different experimental setup for RuBisCO powder with Raman Spectroscopy.
- Table 6: Standard RuBisCO and pigment solutions used for heating and freeze thaw cycles in protein-pigment complex formation for UV-Vis study.
- Table 7: Results for Kinetics 1:1 Binding for standard RuBisCO.
- Table 8: Heterogeneous Analyte Binding values for molecular weight and concentration.
- Table 9: Results for Kinetics 1:1 Binding for standard RuBisCO with riboflavin.
- Table 10: Results for Kinetics 1:1 Binding for standard RuBisCO with annatto extract.

List of Figures

Figure 1: Chemical Structure of riboflavin.

Figure 2: Chemical Structure of annatto extract.

Figure 3: Chemical Structure of beta-carotene.

Figure 4: Modified schematic of one subunit of RuBisCO. Cylinders show α -helices and arrows show β -strands. Circled portion represent TIM barrel. (Schneider et al., 1986); Reprinted with permission from Macmillan Publishers Ltd: [The EMBO Journal] (Schneider et al.), copyright (1986).

Figure 5: Block diagram of Raman spectroscopy instrument.

Figure 6: Surface plasmon resonance sensorgram for association and dissociation of analyte to ligand in order to determine kinetics with (1) ligand (antibody) immobilized to surface with buffer flowing over surface, (2) association of analyte (RuBisCO), (3) dissociation of analyte, (4) regeneration of surface, (5) signal back to baseline with just ligand immobilized on surface.

Figure 7: UV-Vis absorption of spinach RuBisCO in PBS at pH 7.9 with peaks matching well with data published by Fashui, et al. where there are major peaks corresponding to between 215 and 220nm and the second at 274nm.

Figure 8: UV-Vis Spectrum for Riboflavin in water (0.034mg/mL) with peaks matching with data published by Eitenmiller et al (2008).

Figure 9: Setup for freezing tobacco extract in liquid nitrogen, details discussed in section below.

Figure 10: Example of 50mL tube with holes.

Figure 11: Final Tobacco Extract Pellets to be stored at -80°C .

Figure 12: Setup for grinding of tobacco pellets into fine powder for further use in extraction.

Figure 13: Example of beads on magnetic rack to aid in washing and removal of solution.

Figure 14: RuBisCO spectrum with no baseline adjustment and an exposure time of 1 second with 3 total exposures and following experiment setup seen in Table 5, value A (780nm).

Figure 15: Riboflavin image, Raman microscope (10X, light field).

Figure 16: Beta carotene image, Raman microscope (10X, light field).

Figure 17: Annatto Extract image, Raman microscope (10X, light field).

Figure 18: Standard RuBisCO image, Raman microscope (10X, dark field).

Figure 19: Riboflavin spectrum with baseline adjustment and an exposure time of 5 seconds with 3 total exposures and following experiment setup seen in Table 4 (780nm).

Figure 20: Beta-carotene spectrum with no baseline adjustment and an exposure time of 0.1 seconds with 3 total exposures and following experiment setup seen in Table 4 (780nm).

Figure 21: Annatto Extract spectrum with baseline adjustment and an exposure time of 1 second with 3 total exposures and following experiment setup seen in Table 4 (780nm).

Figure 22: General sensorgram information with antibody binding, RuBisCO injection for association and dissociation measurements, followed by regeneration to

establish baseline to allow chip to be reused. Data shown is from 0.5mg/mL standard RuBisCO in PBS at pH 7.9 for initial trials with antibody binding.

Figure 23: Sensorgram for RuBisCO Kinetics with anti-RuBisCO antibody (mouse monoclonal) and standard RuBisCO in PBS solution at pH 7.9.

Figure 24: Standard curve for RuBisCO samples.

Figure 25: Kinetics results for standard RuBisCO using a 1:1 binding model. Colored lines are experimental; black lines are fit.

Figure 26: Standard RuBisCO with Riboflavin.

Figure 27: Comparison of standard RuBisCO/riboflavin complex and standard RuBisCO.

Figure 28: Kinetics for standard RuBisCO with riboflavin using a 1:1 binding model. Colored lines are experimental; black lines are fit.

Figure 29: Standard RuBisCO with annatto extract.

Figure 30: Comparison of standard RuBisCO to standard RuBisCO with annatto extract.

Figure 31: Comparison of standard RuBisCO to annatto extract in solvent solution (calibration 2).

Figure 32: Kinetics for standard RuBisCO with annatto extract using a 1:1 binding model. Colored lines are experimental; black lines are fit.

Figure 33: UV-Vis spectra for standard RuBisCO in PBS at pH 7.9 at varying concentrations.

Figure 34: UV-Vis spectra normalized for standard RuBisCO in PBS at pH 7.9.

Figure 35: UV-Vis spectra for standard RuBisCO in PBS at pH 7.9 and solvent solution for riboflavin (water).

Figure 36: UV-Vis spectra comparing standard RuBisCO in PBS at pH 7.9, riboflavin in solvent solution, standard RuBisCO with riboflavin, and the additive values of standard RuBisCO in PBS at pH 7.9 and riboflavin in solvent solution.

Figure 37: UV-Vis spectra comparing the normalization of standard RuBisCO with riboflavin and the additive values of standard RuBisCO in PBS at pH 7.9 with riboflavin in solvent solution.

Figure 38: UV-Vis spectra for annatto extract in solvent solution.

Figure 39: UV-Vis spectra comparing standard RuBisCO in PBS at pH 7.9, annatto extract in solvent solution, standard RuBisCO with annatto extract, and the additive values of standard RuBisCO in PBS at pH 7.9 and annatto extract in solvent solution.

Figure 40: UV-Vis spectra comparing the normalization of standard RuBisCO with annatto extract and the additive values of standard RuBisCO in PBS at pH 7.9 with annatto extract in solvent solution.

Figure 41: UV-Vis spectra for beta-carotene in solvent solution.

Figure 42: UV-Vis spectra for standard RuBisCO in PBS at pH 7.9 with and without sonication.

Figure 43: UV-Vis spectra for riboflavin in solvent solution with and without sonication.

Figure 44: UV-Vis spectra comparing standard RuBisCO and riboflavin with sonication (normalized) to the additive value of standard RuBisCO in PBS at pH 7.9 with sonication plus riboflavin in solvent solution with sonication (normalized).

Figure 45: UV-Vis spectra comparing normalization values of standard RuBisCO with riboflavin with heating to additive values of standard RuBisCO in PBS at pH 7.9 and riboflavin in solvent solution both with heating.

Figure 46: Solutions for final trial of heating and freeze thaw cycles with pigments added directly to standard RuBisCO in PBS at pH 7.9 for a final concentration of 1:100 mole ratio (protein: pigment), with (1) beta-carotene, (2) beta-carotene with MgCl₂, (3) bixin, (4) bixin with MgCl₂, (5) riboflavin, (6) riboflavin with MgCl₂, and (7) standard RuBisCO .

Figure 47: UV-Vis spectra comparing normalized values of standard RuBisCO with riboflavin after heating and freeze thaw cycles to additive values of standard RuBisCO in PBS at pH 7.9 plus riboflavin in solvent solution.

Figure 48: UV-Vis spectra comparing normalized values of standard RuBisCO with beta-carotene after heating and freeze thaw cycles to additive values of standard RuBisCO plus beta-carotene in PBS at pH 7.9.

Figure 49: UV-Vis spectra comparing normalized values of standard RuBisCO with bixin after heating and freeze thaw cycles to additive values of standard RuBisCO plus bixin in PBS at pH 7.9.

Figure 50: Comparison of bixin and beta-carotene in PBS at pH 7.9 and ethanol with (1) beta-carotene in ethanol, (2) beta-carotene in PBS, (3) bixin in ethanol, (4) bixin in PBS.

Figure 51: (a) UV-Vis results for beta-carotene in ethanol, (b) UV-Vis results for bixin in ethanol.

Figure 52: UV-Vis results comparing standard RuBisCO with riboflavin after heating and freeze thaw cycles with and without MgCl₂.

Figure 53: Results for Western Blot and stained membrane, (A) standard RuBisCO (1mg/mL); (B) molecular weight marker; (C) standard RuBisCO with beads before wash; (D) standard RuBisCO with beads after, no wash; (E) standard RuBisCO with beads after, with wash; (F) standard RuBisCO with beads, final; (G) tobacco supernatant with beads after, no wash; (H) tobacco supernatant with beads after, with wash; (I) tobacco supernatant with beads, final; (J) molecular weight marker; (K) molecular weight marker.

Figure 54: Results for Western Blot and stained membrane A molecular weight marker; (B) standard RuBisCO control (0.5μL); (C) standard RuBisCO control (1μL); (D) Pellet A; (E) Pellet B; (F) Molecular weight marker; (G) supernatant A; (H) supernatant B.

Figure 55: Poncaeu stain of samples from tobacco powder extraction with methanol extraction: (A) standard RuBiSCO; (B) supernatant A; (C) pellet A; (D) supernatant B; (E) pellet B.

Figure 56: Silver stain comparison of supernatant from extraction buffer B with methanol extraction and dilutions, (A) supernatant from extraction with buffer B; (B) standard RubisCO; (C) supernatant with methanol extraction; (D) 15μL supernatant with methanol extraction in loading buffer (1X) plus 5μL loading buffer (1X); (E) 10μL supernatant with methanol extraction in loading buffer (1X) plus 10μL loading buffer (1X); (F) 5μL supernatant with methanol extraction in loading buffer (1X) plus

15 μ L loading buffer (1X); (G) 1 μ L supernatant with methanol extraction in loading buffer (1X) plus 19 μ L loading buffer (1X).

Figure 57: Western results for (A) standard RubisCO; (B) 15 μ L supernatant with 5 μ L loading buffer (1X); (C) 15 μ L supernatant with 3 μ L loading buffer (1X) and 2 μ L reducing agent (10X); (D) 10 μ L supernatant with 10 μ L loading buffer (1X); (E) 10 μ L supernatant with 8 μ L loading buffer (1X) and 2 μ L reducing agent (10X); (F) 5 μ L supernatant with 15 μ L loading buffer (1X); (G) 5 μ L supernatant with 13 μ L loading buffer (1X) and 2 μ L reducing agent (10X); (H) 1 μ L supernatant with 19 μ L loading buffer (1X); (I) 1 μ L supernatant with 17 μ L loading buffer (1X) and 2 μ L reducing agent (10X).

Figure 58: (a) Western blot results for standard RuBisCO followed by dilutions of beads and supernatant not incubated in beads and (b) Silver stain results. (A) standard RuBisCO; (B) 20 μ L beads incubated in supernatant; (C) 15 μ L beads incubated in supernatant with 5 μ L loading buffer, 1X; (D) 10 μ L beads incubated in supernatant with 10 μ L loading buffer, 1X; (E) 5 μ L beads incubated in supernatant with 15 μ L loading buffer 1X; (F) supernatant from ground tobacco powder.

Figure 59: Silver stain results for bead conjugation study, (A) supernatant with beads conjugated (10mg/mL RbcL anti-rabbit, polyclonal for RuBisCO); (B) PBS at pH 7.9 with beads conjugated (10mg/mL RbcL anti-rabbit, polyclonal for RubisCO); (C) PBS at pH 7.9 with non-conjugated beads.

Figure 60: (a) Western blot results for final bead and supernatant trials and (b) silver stain results. (A) standard RuBisCO; (B) supernatant with conjugated beads (10mg/mL anti-rabbit, polyclonal for RuBisCO); (C) PBS at pH 7.9 with conjugated

beads (10mg/mL anti-rabbit, polyclonal for RuBisCO); (D) PBS at pH 7.9 with non-conjugated beads; (E) supernatant; (F) supernatant 1:10; (G) supernatant 1:100; (H) supernatant 1:1000.

Figure 61: Western blot results from (1) *Spinacia oleracea*; (2) *Synechococcus* PCC 7942; (3) *Cyanophora paradoxa*; (4) *Heterosigma akashiwo*; (5) *Thalassiosira pseudonana*; (6) *Euglena gracilis*; (7) *Micromonas pusilla* (8) *Chlamydomonas reinhardtii* (9) *Prophyra* sp; (10) *Gonyaulax polyedra*; (11) *Emiliana huxleyi*.
Permission from www.agrisera.com.

Chapter 1: Introduction

The health benefits of dietary antioxidants have been extensively investigated, in particular their role in reducing oxidative stress in biological systems (Liu, 2003). Higher consumption of antioxidant-rich fruits and vegetables has been associated with lower risk of coronary heart disease, diabetes, and other chronic diseases (Liu, 2003). Growing knowledge about the health promoting properties of dietary antioxidants has driven a strong interest in supplementing or enhancing these bioactive compounds in the human diet.

Antioxidative pigments such as riboflavin, annatto extract (bixin), and beta-carotene are common, natural additives found in a variety of foods including dairy, baked goods, and beverages. Riboflavin, or vitamin B₂, is a member of the flavin group associated with protection against cardiovascular disease by reducing oxidation of low density lipoproteins additional to anti-carcinogenic effects in the intestine (Yanishlieva et al., 2001). Both beta-carotene and annatto extract are carotenoids known to provide cell communication components and macular protection besides acting as immune function enhancers and UV skin protectants (Rao et al., 2007). However, these three pigments are unstable in food products (Delgado-Vargas et al., 2003; Yanishlieva et al., 2001). Riboflavin, annatto extract, and beta-carotene may degrade due to high heat, oxygen exposure, or interactions with other compounds in food (Nisha et al., 2005; Delgado-Vargas et al., 2003; Agte et

al., 2002; Ranhotra et al., 1995). Therefore, there is growing interest in the food industry to identify an effective binding agent capable of stabilizing these antioxidative pigments.

Ribulose 1,5-bisphosphate carboxylase oxygenase (RuBisCO), an enzyme involved in the Calvin cycle and the most abundant protein on earth (Reinhard and Höcker, 2005), is found in the chloroplast of plants in nature and makes up at least 50% of all proteins in plant leaves (Schneider et al., 1992). To date, many methods exist for extracting RuBisCO from various plant sources, such as the use of Sephadex extraction or high performance liquid chromatography (HPLC) separation (Holler et al. 2007; Wang et al., 2006 and 2003; Chang 1972). RuBisCO can be purchased commercially as a partially purified powder from spinach (Sigma-Aldrich). It is our hypothesis that such a natural pigment-binding protein, as seen in similar complexes found in invertebrates as well as in plants (Zhang et al., 2008; Heras et al., 2007; Mimuro et al., 2004), could serve as an ideal binder for the antioxidative pigments of interest.

Additionally, along with the possibility of providing stability, RuBisCO could also be employed as a protein source for a variety of food applications. Over the last 20 years, leaf concentrates and isolates have been viewed as nonconventional protein sources, and with a balanced amino acid profile, ubiquitous nature, and abundance, RuBisCO could provide a good source of

protein (Pedone et al., 1995). Montanari et al. (1993) demonstrated a crude extraction process that shows fraction I (precipitated at pH 5.6) of RuBisCO from tobacco to provide good nutritional characteristics which are defined below.

In the present study, various attempts were made to facilitate the formation of RuBisCO-pigment complexes using mixing, sonicating, heating, and freeze-thaw techniques. The properties of RuBisCO-pigment complexes were investigated using Raman spectroscopy, surface plasmon resonance biosensors, as well as UV-VIS spectroscopy. If binding proved successful, the next step would be to determine the bioavailability of the antioxidative pigments once bound, as well as establish information on the potentially improved stability of the protein-pigment complexes. A protocol for extracting a highly proteinaceous supernatant from tobacco leaves was established in hope that RuBisCO could be extracted from this abundant source while providing a value-added application for such an ill-imaged crop in dire needs of alternative uses (Fu et al., 2010; Yancy, 2004). An exploratory research assessing the challenges and hurdles in forming a stable protein-pigment complex will enable further development in stabilizing antioxidative pigments, whereas the detection techniques established could be of value for quantitative measurements of such complexes.

Chapter 2: Literature Review

2.1 Antioxidative Pigments

The consumer associates the color of his or her food with safety and quality, as well as a measure of good processing (Delgado-Vargas et al., 2003). Currently there is a trend toward the use of natural colorants because of public concern that synthetic colorants are potentially harmful (Wissgott et al., 1996). Most natural colorants or pigments used in food products are also antioxidants and provide benefits to human health. An antioxidant is a substance that is capable of delaying, retarding, or preventing the development of rancidity in food or other flavor deterioration due to oxidation (Yanishlieva et al., 2001). Antioxidants occur in or can be extracted from plant and animal tissues (Yanishlieva et al., 2001). Some of these natural colorants can be created in the lab, but they must be completely identical to those found in the natural environment in order to be allowed in food products. Synthetic colorants are used in foods but are limited by the federal government due to safety concerns. While synthetic colorants are less expensive than natural colorants and pigments, the benefits offered by natural colorants as antioxidants offer a reason for use and possible growing interest among industry and consumers.

It has been shown that nearly 75% of all food in developed countries is processed in some form before it reaches the consumer (Delgado-Vargas et al., 2003). It is because of this processing and transportation that additives are

needed. Overtime degradation and loss of normal appearance may occur in the food product, so pigments and stabilizers are attractive (Delgado-Vargas et al., 2003). There are several common reasons why pigments and antioxidants are added to foods. These reasons include the restoration of foods original appearance, assurance of color uniformity, protection of other components with antioxidants, and preservation of food appearance and characteristics. It is important to note that color additives can never be used to mask poor processing or manipulation of a product during processing (Delgado-Vargas et al, 2003). There are also several factors that affect the ability of antioxidants to function (Table 1).

Table 1: Factors that affect antioxidant power (Yanishlieva, 2001).

Factor	Antioxidant Power
↑ Concentration	↑ power
↑ Oxygen	↓ power
↑ Light	↓ power

Specific pigments or antioxidants are chosen to be added to a food product for various reasons. When considering a natural color additive, one must take into account the color or hue required, the physical form of the food (liquid, solid, emulsion), the properties of the food to be colored (oil or water based, pH, etc.), and the processing conditions (heating and storage) (Delgado-Vargas et al., 2003). Also, each pigment or antioxidant has specific regulations determining what food it can be used in and for what purpose. Because of these considerations the three pigments of riboflavin, annatto extract, and

beta-carotene were chosen, as they are commonly used antioxidants. They impart specific colors (mainly yellow or orange hues) and are used in a wide variety of products ranging from dairy to bakery goods to beverages and snacks.

As already mentioned, color is one of the most important first impressions to a consumer; however, natural colorants can be unstable in food products.

Generally, antioxidants are thought to be products that stabilize foods, as they can help prevent oxidation by destroying free radicals. However, these antioxidants are prone to degradation and deterioration themselves, thus a stabilizer would be beneficial in certain food products.

There are several ways that antioxidants can undergo degradation. A major disadvantage of natural antioxidants is that they have low resistance to oxygen, especially when also exposed to light, high temperature, and dry conditions (Yanishlieva et al., 2001). Unfortunately these are all possible conditions that the food may be exposed to during storage or use by the consumer. In addition, there is relatively little information on how an antioxidant might change as it interacts with other food components and how these changes affect the foods' ability to resist oxidation (Yanishlieva et al., 2001). In addition it is important that a food is protected against oxidation, as this process can result in rancidity and off flavors.

Overall, there is a desire to provide stability to these colorants to enhance the likelihood that their antioxidant capabilities remain intact and stable throughout the processing of foods. To address this issue, RuBisCO was selected for evaluation as a pigment stabilizer given that it is an inherently stable protein (Reinhard and Höcker, 2005). RuBisCO is not only investigated as a possible binder to pigments, but also as a supplemental protein enhancer in foods.

2.1.1 Riboflavin

Riboflavin is part of the family of flavonoids or flavins. These compounds are efficient antioxidants and have been proposed to protect against cardiovascular disease by the reduction of oxidation of low density lipoproteins (Yanishlieva et al., 2001). Flavonoids have also been found to show anti-carcinogenic effects in the intestine (Yanishlieva et al., 2001). Overall, flavonoids are found in various foods naturally and provide not only the health benefits as listed above, but also nutrients that are precursors to vitamins.

Riboflavin, or vitamin B₂, is normally an orange-yellow color (Figure 1). It is commonly used in baby foods, cereals, sauces, processed cheeses, and fruit drinks (“Natural Food Colors”, 2009).

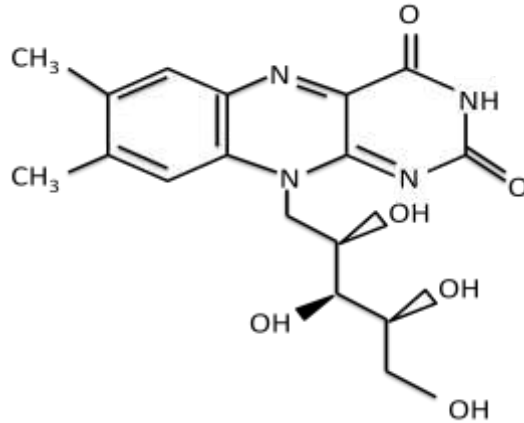


Figure 1: Chemical Structure of riboflavin.

This pigment is water soluble, meaning that it will be miscible with water soluble RuBisCO and easier to work with because solubility will not pose a problem during further studies. Riboflavin is stable in neutral and acidic solutions and aerated or oxygenated environments, but it is unstable in alkaline solutions, light, and heat (“Natural Food Colors”, 2009). Thus riboflavin may degrade during food processing or storage, making a stabilizer desirable. For example, one report showed that 10-20% of riboflavin was lost during processing/cooking steps during production of ready-to-eat food products (Agte et al., 2002).

There is a report of binding riboflavin to zein-bound particles in order to have better entry into a fish larvae diet (Onal et al., 2005) and reduce the loss of riboflavin into the water. Zein is a non-toxic, edible protein that is soluble in alcohol (Onal et al., 2005). There have been several different studies seeking to increase the delivery of water-soluble nutrients to fish. There is a high

amount of leaching that occurs in the fish foods, so preparation of microencapsulated foods is a new field of research. While their research did find that riboflavin could be bound to the Zein, it unfortunately also uncovered that under certain conditions the complex could not be optimized and so the amount of riboflavin that was leached out of the food was not reduced significantly (Onal et al., 2005). The continued leaching may be due to the fact that the riboflavin was not coupled completely with the Zein protein; however, with the addition of methyl palmitate the leaching was reduced (Onal et al., 2005). This report shows that if the pigments are to be stabilized in various food matrixes then there needs to be significantly strong binding of the protein to the pigment.

Another study on riboflavin focused purely on its stability in spinach foods during heating. This study showed the need for a stabilizer to help keep riboflavin from leaching and degrading. Using kinetic modeling, Nisha et al. (2005) found that spinach puree provides a more stable environment for riboflavin. At 120°C for 60 minutes the degradation of riboflavin from a pure solution of spinach is 27.5% and from the spinach puree it is 22.8% (Nisha et al., 2005). It was reported that spinach puree phytochemicals may exert protection over the riboflavin, as it is exposed to heat treatment (Nisha et al., 2005). It is hopeful that other kinds of stabilizing methods, such as the one explored here, will have the same effect.

Overall, riboflavin is an important nutrient in the consumers' diet, but it can leach out or degrade in foods easily when exposed to high water content or heating. There have been several efforts to stabilize riboflavin in foods as discussed above, but both studies discussed had limited success. The goal of this project is to stabilize riboflavin with the protein RuBisCO for the purpose of making it less susceptible to degradation during food processing so that it would be present to provide antioxidant benefits to consumers.

2.1.2 Annatto Extract

Annatto extract is the most widely used carotenoid extract and is notably used in high amounts in dairy, bakery, and confectionery products (Delgado-Vargas et al., 2003). Annatto seeds are the only natural source of bixin, a xanthophyll carotenoid. Mainly, the trees from which the seeds are harvested are grown in Brazil or other South American countries. The structure for annatto extract is a long double bonded carbon chain with oxygen functional groups on either end (Figure 2). This pigment is relatively inexpensive as compared to other natural pigments (Cardarelli et al., 2008).

bixin dispersed in vegetable oil and stored at temperatures below freezing had a loss of about 20-25%. Balaswamy et al. (2006) studied the stability of bixin in annatto oleoresin and dye powder during storage. The annatto pigment was stored in the form of dye powder or annatto oleoresin, which is a mixture of both oil and resin from plants, in glass jars for 360 days in three different conditions: cold (5-8°C) temperatures in the dark, room temperature in the dark, and room temperature in daylight (Balaswamy et al., 2006). Data showed that the dye powder form had much higher losses than oleoresin for all forms of storage. Overall, degradation of bixin was seen, demonstrating concern for its stability during the application of food processing and storage (Balaswamy et al., 2006).

2.1.3 Beta-Carotene

This carotenoid is the most abundant of all, as it is highly involved in the photosynthesis process and is found in most plant species. Beta-carotene was first isolated in 1817 and is a precursor to vitamin A (Bartley et al., 1995). An oil soluble pigment, beta-carotene is used to color a variety of foods ranging from beverages to baked goods to frozen foods to candies. This pigment is stable through variable heat and light conditions and also has a large pH range of 2.0 to 14.0. The structure of beta-carotene is similar to annatto extract as they are both from the carotenoid family (Figure 3).

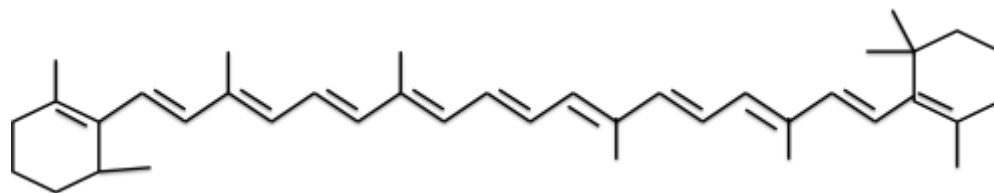


Figure 3: Chemical Structure of beta-carotene.

As a precursor to vitamin A, beta-carotene, is beneficial to the healthy development of individuals and promotes disease prevention (Yanishlieva et al., 2001). Several epidemiological studies which provided higher amounts of beta-carotene than normal have been completed and only one found that beta-carotene had protective effects against cancer (Yanishlieva et al., 2001). Other studies indicated that smokers are at a higher risk for cancer with the use of beta-carotene (van de Berg et al., 2000). These results suggest a possible biphasic response to beta-carotene, in that it promotes health when consumed at normal dietary levels, but may have adverse affects when consumed at an increased amount (Rao et al., 2007). Regardless, it is still advisable to provide stability to beta-carotene for better control of the amount used to supplement foods.

A study completed in 1999 reviewed the stability and antioxidant activity of beta-carotene in different cooking oils. Beta-carotene has been shown to protect lipids from free radical autoxidation, since it can inhibit propagation with the termination of oxidation chain reactions by reacting with peroxy radicals (Goulson et al., 1999). The stability of beta-carotene was measured

using normal phase HPLC. Data showed that in either oil, conventional canola oil, or high oleic canola oil, the rate of beta-carotene loss was lower with increasing concentrations of the pigment (Goulson et al., 1999). These results show that at higher concentrations beta-carotene is a more efficient quencher of oxygen.

Finally, the stability of beta-carotene in whole wheat bread and crackers can be used as an example of this pigment in food products. In wheat and most other grains there are very low levels of beta-carotene, but through fortification these grain foods, a dietary staple, can become a good source of carotene in the diet (Ranhotra et al., 1995). The study by Ranhotra and coworkers was completed with an interesting goal in mind: by adding beta-carotene to whole wheat products, the already impressive nutritional profile of many bakery products can be enhanced, provided the supplemented beta-carotene remains stable (Ranhotra et al., 1995). It was found that the beta-carotene stability was reduced during the baking process for whole wheat bread and crackers. The losses for the bread ranged from 4.3% to 14.8% and for the crackers there was a loss of 17.9% to 22.8% (Ranhotra et al., 1995). The resulting higher loss in the crackers may be due to a greater surface area and therefore more heat reaching the cracker than the bread. Overall, it can be seen that there needs to be a better way to provide stability for beta-carotene if it is to fortify foods such as bread or crackers.

2.2 RuBisCO

2.2.1 Properties and Interest

As the most abundant protein on earth, RuBisCO is a significant protein of interest. This protein makes up at least 50% of all proteins in plant leaves (Reinhard and Höcker, 2005). RuBisCO is involved in the Calvin Cycle to help the leaf produce energy during photosynthesis. As such, this protein is linked with chlorophyll, the main pigment of photosynthesis, in the chloroplast of the plant, meaning that during extraction processes it is difficult to remove chlorophyll from the protein. The activation of RuBisCO occurs on the carboxyl end of the β -strand of the barrel of one of the large subunits (Schneider et al., 1992). Both CO_2 and Mg^{2+} are required in order to activate the protein (Reinhard and Höcker, 2005) which indicates that a metal ion may be needed in order to allow RuBisCO to bind to other pigments.

Fraction I, precipitated at pH 5.6, of RuBisCO from tobacco provides good nutritional characteristics (Montanari et al., 1993). RuBisCO protein is tasteless and offers good palatability; furthermore, the RuBisCO fraction does not contain sugars, fats, or salt (Montanari et al., 1993). It is also a well defined protein molecule with a complete amino acid profile (Montanari et al., 1993). Containing a balanced amino acid profile, RuBisCO can enhance the protein content of a product and may possibly be used to provide protein fortification to a product.

2.2.2 Structure and Stability

The protein RuBisCO is inherently stable, which could provide stability to bound pigments, as they undergo processing in food products as discussed above. The RuBisCO enzyme is made up of 8 large subunits (56 kDa) and 8 small subunits (14 kDa) (Schneider et al., 1986). The structure of each subunit of RuBisCO has an alpha/beta barrel configuration where eight parallel beta-strands create the core of the barrel and are surrounded by eight alpha-helices (Schneider et al., 1986) (Figure 4). When there are eight strands involved in this motif it is called a TIM barrel (circled in red, Figure 4), so named because it was first identified in the enzyme triosephosphate isomerase.

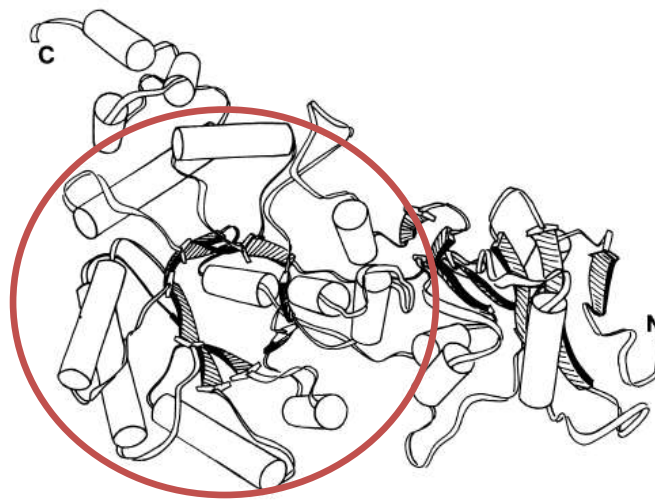


Figure 4: Modified schematic of one subunit of RuBisCO. Cylinders show α -helices and arrows show β -strands. Circled portion represent TIM barrel.

(Schneider et al., 1986); Reprinted with permission from Macmillan Publishers Ltd: [The EMBO Journal] (Schneider et al.), copyright (1986).

The TIM barrel is one of the most common enzyme folds and offers stability due to the interactions in the secondary structure, such as hydrogen bonds between the main chains of the beta-strands, between the intra-helical strands, and between the side chains and salt bridges, along with the dipole-dipole interactions between the alpha-helical structures and the beta-strands (Yang et al., 2009 and Reinhard and Höcker, 2005). Also, the TIM barrel offers enhanced thermo-stability to proteins (Reinhard and Höcker, 2005).

2.2.3 Extraction and Purification Methods

RuBisCO can be extracted into various forms including crystals or precipitates from the green biomass of the leaves. The first crystallographic studies to understand the structure of RuBisCO were completed in protein extracted from tobacco plants (Schneider et al., 1992). The protein is normally categorized into two fractions and each will elute at different pH levels. The first fraction has a pH of around 5.6 and the second a pH of 3.5 (Fu et al., 2009), with this first fraction offering a pure form without lipids, carbohydrates or salts (Pedone et al., 1993).

There are numerous methods in the literature for extracting and purifying RuBisCO and other plant proteins from various sources (Holler et al. 2007; Wang et al., 2006 and 2003; Chang 1972); most of the techniques involve heating, harsh chemicals, expensive equipment, and time consuming procedures. The aims of all these protocols are to remove other proteins,

carbohydrates, nucleic acids, phenolics, alkaloids, phytic acid, starch, salt, and any other impurities (Holler et al., 2008). Wang et al. (2005) have developed a universal and rapid method for protein extraction from plant tissues which could prove to be a useful extraction method for this research. However, this procedure uses harsh chemicals (i.e. phenol) as does many of the above mentioned methods, which denature proteins. So, while this and other recent protocols may provide a purified protein, they are not beneficial to this project due to the possible reduction in protein activity. Our goal is to maintain RuBisCO structure and folding capability or not irreversibly denature the protein, in order to provide the stability offered in motifs such as the TIM barrel.

Chlorophyll, along with other proteins, starches, and fats, can be somewhat difficult to remove from RuBisCO samples. If RuBisCO is interacting tightly to chlorophyll or other impurities, even after extraction, then it might inhibit the binding of the pigments being investigated here. As such, the purest form of RuBisCO possible is sought for further analysis. Furthermore, the crude extraction process, used initially in our work, that avoided harsh chemicals and used pH precipitation of fractions (Fu et al., 2009) did not yield the purest form product, and chlorophyll could not be removed completely from the fractions. Because of this lack purified protein a different method was used for the research of this project.

An alternate use of the tobacco crop is needed, due to the tobacco buyout of the 90s, which meant that more than half of farmers in the state of Maryland switched to more life sustaining crops (Holler et al., 2007). However, for the farmers still growing tobacco the possibility of extracting this protein from tobacco leaves to bind to pigments may provide usefulness to the crop.

Tobacco is a non-food/non-feed crop, so using this plant imposes no problems in subverting the regular food supply (Holler et al., 2007). The tobacco crop is only harvested during the summer and fall months, yet harvested material can be stored to preserve the tissue without degradation or microbial contamination. A buffer using salts, magnesium, Tris (pH 8.0), and protease inhibitor complex (to reduce denaturation) was used to store the homogenized tissue in liquid nitrogen at -80°C from tobacco plants that were harvested in the summer of 2009.

2.3 Tools to Assess Binding

2.3.1 Raman Spectroscopy

Raman spectroscopy was first discovered in 1928 by Sir C. V. Raman and has since developed into a powerful method of analysis in all fields of science (Ingle, 1988). This technique allows one to determine detailed and specific information about a sample at a molecular level with non-destructive results and minimum sample preparation (Schmitt, 2006). It is an emerging tool for the food industry because of these attributes in combination with the ability to interrogate aqueous samples. Raman can be used on a wide range of foods,

including macrocomponents (proteins, lipids, carbohydrates, and water), minor components (carotenoid pigments or synthetic dyes), microorganisms, or even packaging materials that may contact food (Li-Chan, 1996).

The Raman phenomenon is based on the scattering of electromagnetic radiation when an incident photon is absorbed by a molecule and the subsequent relaxation of an electron occurs inelastically (Ingle and Crouch, 1988). Raman scattering comprises frequency shifts that are independent of scattering angle and are caused by rotational and vibrational transitions in molecules (Ingle and Crouch, 1988). In order for Raman scattering to occur, there needs to be a change in polarizability in the molecule at the equilibrium bond distance (Ingle and Crouch, 1988). The overall intensities obtained in Raman scattering are based on the source of irradiance and wavelength, and spectra give information as to the vibrational structure of the molecules interrogated (Ingle and Crouch, 1988). Figure 5 shows a block diagram of a general Raman spectroscopy instrument.



Figure 5: Block diagram of Raman spectroscopy instrument.

Raman is a vibrational spectroscopy technique and is a complementary method to infrared (IR) spectroscopy (Li-Chan, 1996). For Raman, non-polar groups that are in nonsymmetric molecules, such as C=C, C-C, and S-S, have strong intensity bands, while in IR polar groups like C=O, N-H, and O-H have strong stretching (Li-Chan, 1996). It is because of these selection criteria that Raman spectroscopy can be used to evaluate aqueous solutions, as the water bands are extremely weak in Raman. As water bands in IR can obscure other vibrational bands, IR normally uses samples that are dry or non-aqueous (Li-Chan, 1996). This makes Raman useful for studies of biological systems as well as for food products which normally have an increased water activity level content.

There are several other benefits to Raman spectroscopy, along with a few limitations that must be mentioned. First, this technique can be used to study samples in aqueous solutions, non-aqueous liquids, fibrous forms, films, surfaces, powders, precipitates, gels, and crystals (Li-Chan, 1996). While high concentrations are needed to provide strong bands, only small quantities are required to analyze samples (Li-Chan, 1996); as little as 1 μ L of solution or 1mg of solid sample may be needed. Also, Raman samples require little to no preparation before data collection can begin. Some of the limitations surrounding Raman spectroscopy include the fact that fluorescence may occur and obscure the weaker Raman scattering bands (Li-Chan 1996). This is especially common in large macromolecular samples such as proteins or

sugars. While generally a nondestructive technique, some samples may be photodegraded due to the intense power of the laser at the sample. This limitation is easily overcome by reducing laser power or increasing the laser spot size, but it is important to watch for degradation to ensure correct spectra are acquired and to enable further sample analysis.

Overall, Raman spectroscopy has been shown to provide reliable analytical results when studying proteins as well as smaller molecules such as pigments and antioxidants. The most beneficial aspect of Raman for this project is that it can be used to analyze aqueous or other types of solutions. The samples of RuBisCO and pigments will be either created in water or oil suspensions, so Raman could be an advantageous analytical tool for studying binding. Each sample measured under Raman spectroscopy will offer a unique spectrum based on structural components.

The major challenges that may occur in the studies herein will be the fluorescence and potential photodegradation of the RuBisCO sample; however, this may be avoided with extraction and purification methods that provide a pure form for study. Raman will also possibly help provide an intricate look at the binding process of the molecules in RuBisCO and pigments to be used, as the vibrational spectra may yield information on binding based on possible shift or change in spectra.

2.3.2 Surface Plasmon Resonance

In 1902 surface plasmon resonance (SPR) was discovered, but the physical interpretation of this phenomenon was not fully refined until 1968 by Otto, Kretschmann, and Raether who reported on the excitation of surface plasmons on metal surfaces (Schasfoort et al., 2008). The development of SPR biosensors has allowed for the study of proteins, nucleic acids, lipids, carbohydrates, whole cells such as microorganism, and complex mixtures of samples with little purification (Biacore, 2002).

In simple terms, SPR is based on polarized light being reflected off a thin metal film. Upon changing the angle of incidence, there is a decrease in intensity of reflected light where the surface plasmons are excited. The wavelength of this SPR dip is dependent on the refractive indices of the substrate and the biosensor surface/solution. The SPR dip can be tracked over time to create a sensorgram that provides information (e.g., concentration and kinetics) about analyte binding to the biosensor surface (Schasfoort et al., 2008).

While there are a variety of companies offering SPR instruments, this research was performed on a Biacore T100. Biacore sensor chips provide a variety of benefits that include: reproducible results, stable baselines, high chemical stability, and low non-specific binding (Biacore, 2002). The fact that the chips are stable means that regeneration can be provided over many cycles, an

important factor that will be explained below. The instrument used has an autosampler and automatic injection system which gives results that have less laboratory technician error. Overall, SPR offers a great resource, as it can be used in a broad range of research, from macro to micro molecules. SPR is used for ligand determination, protein function understanding, binding of proteins, evaluating DNA damage, and many more applications relating to the life sciences (Biacore, 2002). It can also be used in food and drug applications in quality control, safety analysis, hormone identification and drug development (Biacore, 2010).

The assay to be used for the following research involves an immobilized antibody as the ligand and the RuBisCO protein as the analyte (Figure 6).

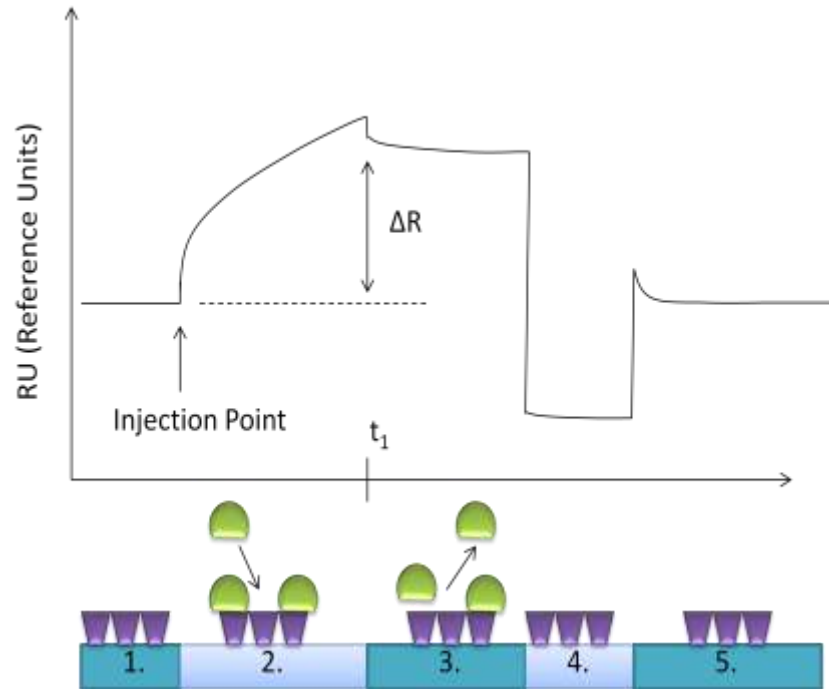


Figure 6: Surface plasmon resonance sensorgram for association and dissociation of analyte to ligand in order to determine kinetics with (1) ligand (antibody) immobilized to surface with buffer flowing over surface, (2) association of analyte (RuBisCO), (3) dissociation of analyte, (4) regeneration of surface, (5) signal back to baseline with just ligand immobilized on surface.

First the buffer flows over the chip to provide a baseline; at this point the ligand is already bound to the surface (in this case, the antibody for RuBisCO) (Schasfoort et al., 2008). Next, association of the analyte occurs (RuBisCO) causing a measurable change in response units as the angle changes depending on what is bound to the surface (Schasfoort et al., 2008). The analyte then dissociates as buffer is again injected over the chip, thus creating a decrease in signal response and providing information on the kinetics of the system (Schasfoort et al., 2008). The SPR system then provides the ability to

regenerate, which is the removal of the analyte by breaking the bond to the ligand and essentially clearing to the original surface made, so each chip can be used multiple times. SPR was used in this project to determine the binding of RuBisCO to antibody as well as the potential binding of protein to pigment based on a change in kinetics cause by the creation of a protein pigment complex.

2.3.3 UV-Vis

Ultraviolet-visible spectrometry (UV-Vis) measures the transmittance, T , (or absorbance, A) of a solution in a transparent cell of a given length. This method is used for qualitative and quantitative analysis in various aspects of research. In UV-Vis the photons give energy to the electron of the sample and in turn promote them to a higher energy level. The energy obtained from the light provides the wavelength for absorption.

In order to measure the difference in power there is a reference blank, which is the solution alone that the analyte is then measured in. For UV-Vis the wavelength from the light source can either be set to a specific wavelength or scan the range from 200 nm to 800 nm. When running UV-Vis, there are several factors that may influence the results including: the solvent used the pH of solution, the temperature, electrolyte concentration, as well as the presence of interfering substances (Skoog et al., 2007).

In proteins there are three different distinguishable absorption bands: the peptide bond that links amino acids at 220 nm, several aromatic amino acid bands from 230-300 nm, and absorption in the visible region of the spectrum due to the possible presence of metal ions and prosthetic groups such as chlorophylls, flavins, and heme groups (Nienhaus et al., 2005). UV-Vis provides an excellent method to study the concentration of proteins (Nienhaus et al., 2005) and when working at room temperature in aqueous solutions with a pH ~ 7.0, physiological conditions can be mimicked (Nienhaus et al., 2005).

Fashui et al. (2005) studied spinach RuBisCO, and found the absorption maxima for one peak between 215 and 220nm and for the second peak at 274nm which were also observed in this study (Figure 7).

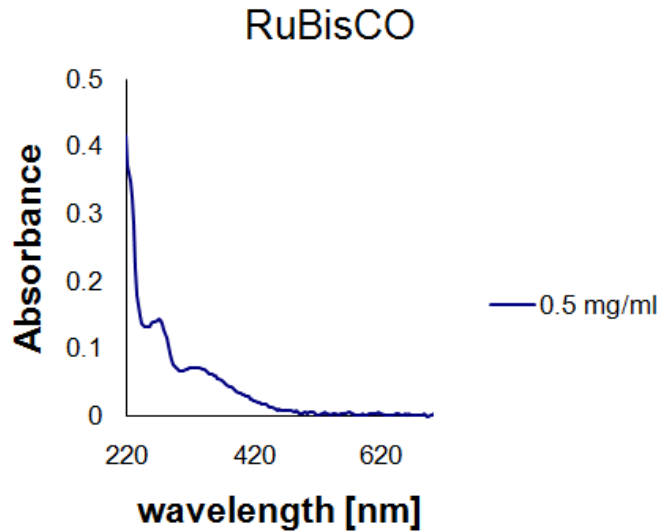


Figure 7: UV-Vis absorption of spinach RuBisCO in PBS at pH 7.9 with peaks matching well with data published by Fashui, et al. where there are major peaks corresponding to between 215 and 220nm and the second at 274nm.

Light absorption spectra are an incredibly useful tool for indentifying and categorizing pigments. Carotenoids contain a long conjugated double-bond structure, as seen in Figures 4 and 5 (Britton et al., 2004). Carotenoids absorb light strongly and show intense absorption bands around the 400-500 nm region (Britton et al., 2004). While most carotenoids absorb strongly in this range, it is important to note that spectral shape differs between carotenoids (Britton et al., 2004). Also, solvents play a key role in the transitional energy and resulting absorbance of a carotenoid, as the maximum peak may vary depending on what solvent is used (Britton et al., 2004). In addition, a shift in absorbance may result due to polarity of solvent (Socaciu et al., 2008). For

riboflavin in aqueous solutions there are several key maximum absorption peaks at 223, 266, 373, and 445 nm (Eitenmiller et al., 2008) as shown in Figure 8.

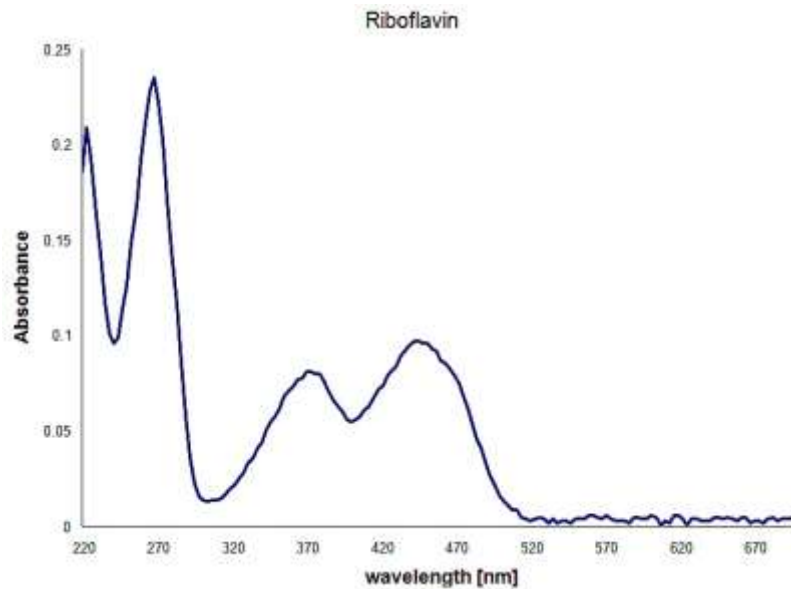


Figure 8: UV-Vis Spectrum for Riboflavin in water (0.034mg/mL) with peaks matching with data published by Eitenmiller et al (2008).

UV-Vis provides identifiable signals for both pigments and proteins. This detection method was used to potentially provide information on the binding of pigments to protein. It was anticipated that if a protein-pigment complex was formed, it would result in a shift in absorption maxima and/or changes in the spectral profile. Also, UV-Vis offers reliable, reproducible results with little sample preparation.

Chapter 3: Objectives

The ultimate goal of this project was to explore the feasibility of binding antioxidative food pigments using ribulose 1-5, biphosphate carboxylase oxygenase (RuBisCO). In order to achieve the goal, three specific objectives were investigated:

- To promote the formation of protein-pigment complex between RuBisCO and the pigments using mixing, sonication, heating, and freeze-thaw techniques.
- To evaluate the potential binding between RuBisCO and the pigments using Raman spectroscopy, Surface plasmon resonance, and UV-Vis spectroscopy.
- To extract and purify RuBisCO from tobacco, promoting an alternative source of protein, using paramagnetic antibody-coated beads.

Chapter 4: Materials and Methods

4.1: Materials

4.1.1 Antioxidative Pigments and Standard RuBisCO

The pigments used were powder beta-carotene (MP Biomedicals, LLC, Solon, OH, Cat. No. 101287), powder riboflavin (Spectrum Chemical, MFG, Corp., Gardena, CA, R1032) and a liquid form of annatto extract (Colorcon.com, Harleysville, PA, Annatto Extract WL 28, Lot no. 081110). The standard RuBisCO was from spinach, 95% pure (Sigma, St. Louis, MO). The solvent solutions used were MilliQ water for riboflavin, 20% methanol (Sigma) for annatto extract and acetone (Sigma) for beta-carotene.

4.1.2: Tools to Assess Binding

Raman Spectroscopy

The Nicolet Almega XR Dispersive Raman Confocal Microscope (Thermo Scientific, Pittsburg, PA) was used for all research with Raman spectroscopy. An aluminum spot slide (Aluminum EZ-Spot Micro Mounts, Thermo Electron North America LLC, Madison, WI) was used to hold all samples and avoid Raman background from a glass slide.

Surface Plasmon Resonance

The Biacore T100 (GE Healthcare, Piscataway, NJ) was used for all research with surface plasmon resonance. Series S sensor chips CM5 along with the Amine Coupling Kit and Mouse Antibody Capture Kit were used for experiments (GE Healthcare). The antibody for SPR was monoclonal, mouse anti-RuBisCO antibody (anti-Spinach RuBisCO Large subunit mAb, 50 μ g from COSMOBIO (Carlsbad, CA)). Standard protocol and buffers from GE Healthcare were used for conjugation of the antibodies to the chip and immunoassay conditions, except where noted. The solutions needed to complete this were NHS/EDC, anti-mouse at 30 μ g/mL in acetate buffer at pH 5, 10mM glycine-HCl pH 1.7, ethanolamine, and running buffer. The running buffers employed in these studies included 1M Tris HCl buffer pH 8.0, HBS-EP+ (10X, 0.01M HEPES, 0.15M NaCl, and 3mM EDTA, pH 7.4) HBS-N (10X, 0.1M HEPES and 1.5M NaCl, pH 7.4) and PBS, phosphate buffered saline, at pH 7.9. The HEPES buffers were purchased from GE Healthcare, and the PBS (Sigma) pH was adjusted from a pH of 7.4 to 7.9 with NaOH and HCl. The Tris buffer (BioRad, Philadelphia, PA) was adjusted with HCl to pH 8.0.

Ultraviolet-Visible Spectrometry

A NanoDrop UV-Vis Spectrometer (Thermoscientific, Waltham, MA) was employed, and the detection was full spectrum (220 to 750 nm). A Sonicor water bath sonicator (7 gal, Wallingford, CT) was used for sonication of

samples. A microwave system (Discover CEM Focused microwave system, Matthews, NC) was used in order to heat samples. The solvent solutions used were water for riboflavin, 20% methanol (Sigma) for annatto extract and acetone (Sigma) for beta-carotene. Bixin (MP biomedical, LLC, Cat. No. 205371) was also used. Magnesium chloride hexahydrate (Sigma, ACS reagent) was used to promote binding. All samples were made up in 1.5mL Eppendorf tubes.

4.1.3 Tobacco RuBisCO Extraction

Tobacco

The tobacco used for this research was a low alkaloid tobacco (*Nicotiana tabacum* cv. MD-609LA) provided by the University of Maryland Central Maryland Research and Education Center in Upper Marlboro, MD. This tobacco plant contained an average nicotine level of 0.6-0.8 mg/g dry weight (Fu et al. 2010).

Freezing Tobacco Tissues

The tobacco leaves were minced upon receiving using a cutting board and a knife. Windex was used to clean the board between batches. A 50mL conical centrifuge tube with flat standing bottom was used for holding 10mL of plant tissues, and 10mL total of 100mM Tris-HCl, pH 8.0, 300mM NaCl, and 5mM MgCl₂ (freezing buffer) were added (buffer from Whitney, SM. 2001. *The Plant Cell*). A Polytron was used to break apart the plant tissue. Plant

protease inhibitor cocktail (PIC, Sigma P9599) [cytotoxic] was used to help prevent denaturation of proteins. PIC was added just before use to the buffer (dilute stock 1:100 into buffer (40mL buffer plus 400 μ L of PIC)). The buffer was kept on ice, and 1mL was used for 30g of tissue. Cheese cloth was used to remove plant tissue from the solubilized protein. A Dewar of liquid nitrogen was used to freeze the tobacco liquid (Figure 9).



Figure 9: Setup for freezing tobacco extract in liquid nitrogen, details discussed in section below.

A 60mL luer-lock syringe with a 20 gauge needle was used to drip the tobacco liquid into the liquid nitrogen in a 50mL flat bottom tube. A spatula was used to separate the pellets formed, and the liquid nitrogen was stored in a CryoCooler (Product Number: CG 08-07, OPS Diagnostics, LLC, Lebanon,

NJ). A cap from a 50mL tube was poked with 8 to 10 holes using the needle, in order to expel liquid nitrogen from the tube before final storage (Figure 10).



Figure 10: Example of 50mL tube with holes.

Sample Preparation

The frozen tobacco liquid was ground using a drill, ceramic mortar, and ceramic pestle attached to drill (CryoGrinder™ Kit, Product Number: CG 08-01, OPS Diagnostics, LLC, Lebanon, NJ). A spatula was used to scrape the inside of the mortar to ensure the formation of a fine powder. Tongs with a protected end were used for holding anything in liquid nitrogen, especially supporting the mortar during grinding. The powder formed was stored in a 50mL polystyrene flat bottom tube with cap.

Antibody Paramagnetic Beads

Dynal Dynabeads, M270 Epoxy, paramagnetic beads were used with anti-RuBisCO antibody (Ab1: anti-Spinach RuBisCO Large subunit mAb, 50ug

from COSMOBIO, monoclonal, mouse and Ab2: RbcL, RuBisCO large subunit, form I and form II (100µg) polyclonal rabbit Anti-RuBisCO, Agrisera, Vännäs , Sweden).

For the conjugation of the beads, 0.1M sodium phosphate at pH 7.4 (Sigma), antibody, 3M ammonium sulfate (Sigma), Stripping buffer (Seppro), 10mM Tris buffer pH 8.8 (Sigma), 10mL dionized water with 114µL triethylamine (Sigma) made fresh, PBS (Sigma), and PBS plus 0.5% Triton (Sigma) were used. The solutions from Dynabeads® Antibody Coupling Kit, Cat. No. 143.11D, Rev 100 (C1, C2, HB, LB, and SB) were also used to create antibody coated beads.

To prepare the tobacco RuBisCO powder extraction buffer with 100mM Tris pH 8.0 (Sigma), 100mM NaCl (Sigma), 0.1% Triton (100X, Sigma), and 0.5mL PIC (EDTA-free, 100X, Thermo Scientific) was added. There were two different extraction buffers used (Table 2).

Table 2: Comparison of extraction buffers for tobacco protein extraction optimization.

Materials	Extraction Buffer A	Extraction Buffer B
Tris	100mM, pH 8.0	100mM, pH 8.0
NaCl	100mM	500mM
Triton	0.1%	0.5%
PIC	0.1mL	0.1mL
pH	Adjusted to 7.9	Adjusted to 7.9

The standard RuBisCO was used as 1mg/mL in PBS adjusted to pH 7.9 with HCl and NaOH. For the RuBisCO extraction and binding to the beads, the dilution, stripping, and neutralization buffer was from the GenWay, Inc. (San Diego, CA) SEPPRO extraction protocol. To prevent nonspecific binding the beads may be washed with 0.01M PBS (Sigma) + 0.05% Tween 20 (Sigma). For samples run on SDS-PAGE, samples were placed in LDS Loading Buffer (4X, Invitrogen NUPAGE®). Reducing agent, Dithiothreitol (DTT), was also used to prepare samples (10X, Invitrogen NUPAGE®). Methanol precipitation was used to determine if protein is present and used 100% methanol (Sigma) and 90% methanol (Sigma).

SDS-PAGE

The NuPAGE® MES or MOPS buffer (Invitrogen) was made up with 475mL of distilled water plus 25mL of NuPAGE® MES or MOPS at 10 X. From this solution 50mL were reserved and 500µL of NuPAGE® antioxidant were added. The running gels used were NUPAGE 10% Bis-Tris gel (1.0mm X 10well) (Invitrogen) and NUPAGE 4-12% Bis-Tris gel (1.0mm X 12well) (Invitrogen). A microwave (Discover CEM Focused microwave system) was used to denature samples at 90°C for 10 minutes. For samples from the pellet of the tobacco extract, centrifugation at 16000×g for 2 minutes was performed. The molecular weight standard used was SeeBlue® plus 2 pre-stained standard (1X, Invitrogen, Carlsbad, CA). A total of 20µL of each sample was added to each well. The gel was placed in a XCell Surelock

Electrophoresis cell, and the voltage was run at 200V with a programmed method (Fisher Scientific FB1000 power source).

Western Blot

The wash buffer contains 45mL of distilled water plus 5mL of Fast Western 10 X Wash Buffer (Thermo Scientific). The primary antibody was made of 10mL of Fast Western Antibody Diluent (Thermo Scientific) or 10mL of milk solution with 10 μ L of antibody for RuBisCO at 1mg/mL (1:1000) regardless of the antibody used. The milk solution was made of 5g of instant nonfat dry milk in 75mL of MilliQ water with 10mL of TBS-T (Tris buffered saline solution with Tween 20, pH 8.0, Sigma, T-9039). The secondary antibody was 9mL of Fast Western Antibody Diluent (Thermo Scientific) plus 1mL mouse or rabbit optimized HRP reagent, PICO (Thermo Scientific). The exposure solution was made of Super Signal West PICO Stable Peroxide Solution (Thermo Scientific) and Super Signal West PCIO Luminol/enhancer Solution (Thermo Scientific) at a ratio of 50/50 to a total of 10mL. The Invitrogen iBlot with iBlot gel transfer PVDF, mini was used to transfer the gel to the membrane.

Silver Stain

The silver staining was conducted using the Pierce Silver Stain Kit available through Thermo Scientific. The fixing solution was made up of 30% ethanol with 10% acetic acid in MilliQ water. The ethanol wash contained 10%

ethanol in MilliQ water. MilliQ water was used to rinse the gel in between washes. The solutions used include SilverSNAP® Sensitizer, Enhancer, Stain, and Developer. The sensitizer working solution was made up of 50µL Sensitizer with 25mL of water. The stain solution was made up of 0.25mL enhancer with 25mL stain. The working developing solution was 0.25mL enhancer with 25mL developer. The stop solution was 5% acetic acid in water.

4.2 Methods

4.2.1 Evaluation of Binding

Creating a Protein-Pigment Complex

Differences exist in creating the protein-pigment complexes based on the solubility of the pigment employed: the carotenoids being oil soluble, while riboflavin is water soluble. Due to the fact that the standard RuBisCO and each pigment need to be prepared in stock solutions of different liquids it is important to understand how the pigment solutions, as well as the standard RuBisCO solution affect the results for SPR and UV-VIS. A variety of solutions were created for each protein-pigment complex (Table 3).

Table 3: Protein-Pigment Complex sample description.

Samples	Standard RuBisCO	Pigment	PBS at pH 7.9	Solvent
Control	X		X	
Calibration 1	X		X	X
Calibration 2		X	X	X
Complex	X	X	X	X

The control contained standard RuBisCO in the PBS at pH of 7.9. The first calibration was half standard RuBisCO in PBS at pH 7.9 and half solubilizing solution (MilliQ water, 20% methanol, or acetone) depending on the pigment used. The second calibration was half the pigment in solubilizing solution and half PBS at pH 7.9. The complex contained half RuBisCO in PBS at pH 7.9 with half pigment in its solubilizing solution. The samples in both PBS at pH of 7.9 and the solubilizing solutions from here on will be described as the solvent solution (calibrations 1, 2, and complex). All of the concentrations of protein to pigment were made at a molar ratio of 1:100 to allow for excessive pigments being available to bind to the large RuBisCO protein molecule. The solutions were made in a total of 1mL final volume from stock solutions of established concentrations based on the final molarity needed for each sample and pigment. The solvent solution also varied depending on which pigment was used.

Raman Spectroscopy

All spectra obtained for riboflavin, annatto extract, and beta-carotene followed the instrument setup shown in Table 4.

Table 4: Instrument Setup for all pigments with Raman spectroscopy.

Parameter	Value
Laser wavelength	780 nm
Laser power	65%
Aperture	100 μm pinhole
Estimated Resolution	24.3 – 40.1 cm^{-1}
Objective	MPlan 10X BD

For the RuBisCO powder two different setups (Table 5) were used to obtain a spectrum.

Table 5: Comparison of different experimental setup for RuBisCO powder with Raman Spectroscopy.

Parameter	Value (A)	Value (B)
Laser wavelength	780 nm	532 nm
Laser power	13%	1%
Aperture	100 μm pinhole	100 μm pinhole
Estimated Resolution	18.7 – 34.6 cm^{-1}	24.3 – 40.1 cm^{-1}
Objective	MPlan 10X BD	MPlan 10X BD

Microscope images of each of the samples were also obtained.

Surface Plasmon Resonance (SPR) Biosensor

The first step to using the SPR biosensor was to create a surface for the ligand, (Mouse anti-RuBisCO) by using the anti-Mouse capture kit. This sensor surface allows for a universal platform for all mouse antibodies and standard regeneration chemistry. First the chip is docked and the instrument primed with the running buffer; in this case HBS-N was chosen for all samples

because it was most compatible with RuBisCO samples. Next, the instrument was normalized using the standard protocol provided by the vendor. In order to create the anti-Mouse surface, the standard Biacore procedure was followed for amine coupling, anti-Mouse conjugation, ethanolamine blocking, and glycine pH 1.7 chip conditioning. The flow rate of 10 μ L/min was used with each step being performed for seven minutes. Flow cell 1 was set as a reference surface (no anti-Mouse) while flow cell 2 was coupled with the anti-Mouse IgG.

The next step was to check for any non-specific binding (NSB) to make sure that the anti-RuBisCO did not bind to the reference surface and was only bound specifically to the anti-Mouse capture sites. In these experiments, NSB was not seen for the RuBisCO antibody or the RuBisCO samples. Next, 150-300 Response Units (RU) of the anti-RuBisCO was captured on the anti-Mouse platform, and it was verified that the surface can be regenerated using 10 mM glycine-HCl at pH 1.7. During these experiments the reference channel was not exposed to the anti-RuBisCO. One mL of each 1 μ g/mL of anti-RuBisCO in the running buffer and glycine was placed into the reagent rack, and the flow rate was set to 10 μ L/min. The procedure began with short time injections of the anti-RuBisCO (12 seconds) in order to determine the rate of binding, and thus the level needed to reach 150-300 RU. The time was increased if the target RU was not obtained, and the values were recorded

until the target value was reached. If the target level was overshoot then the surface was regenerated and the studies performed again.

Once the capture time was determined, and the glycine regenerated the surface back to a stable baseline, surface ligand activity was measured. For these experiments, the anti-RuBisCO surface is exposed to standard RuBisCO protein and binding was evaluated. A Wizard was created using the Biacore software. Three major steps were involved: capture, sample, and regeneration. This was conducted over flow cells 1 and 2, again with flow cell 1 as a reference channel. The ligand (anti-RuBisCO) capture had a contact time of 20 seconds with a flow rate of 10 μ L/min and a stabilization period of 60 seconds. The sample (standard RuBisCO in PBS at pH 7.9) had a contact time of 120 seconds with a flow rate of 30 μ L/min and a stabilization period of 180 seconds. The regeneration (glycine HCl with a pH of 1.7) had a contact time of 180 seconds with a flow rate of 20 μ L/min and a stabilization period of zero seconds. The analysis temperature and sample compartment temperature were both at 25°C. If the chip had not been used recently it was important to prime the system following standard protocols. The concentrations run for the standard RuBisCO in PBS at pH 7.9 were in the following order: 0.0, 0.005, 0.01, 0.05, 0.1, 0.5, 1, 0.05, and 0.0mg/mL.

The Method for each pigment was created using the Biacore software. All trials were completed with the pigments after they had been added to protein

in solution. It is important to note that the beta-carotene was not run with SPR because there were no solvents to dissolve this pigment that are compatible with the instrument fluidics. The first method was for riboflavin. The assay steps included the samples listed in Table 3. For each of these four samples there were three steps: capture, sample, and regeneration. The contact time for the capture solution (anti-RuBisCO) was 90 seconds with a flow rate of 10 μ L/min followed by a stabilization period of 30 seconds. This was only over flow cell 2 as flow cell 1 remained as a reference channel. Next was the sample where the solutions listed in Table 3 were run over the chip with a contact time 180 seconds at 10 μ L/min and a dissociation time of 300 seconds. The sample step was run over both flow cells 1 and 2. The final step was regeneration with glycine HCl at a pH of 1.7 with a contact time of 180 seconds at a flow rate of 10 μ L/min again over both flow cells. There was a stabilization period for regeneration of 20 seconds. The analysis temperature and sample compartment temperature were both at 25°C. The concentrations of standard RuBisCO for each step were 0.5, 0.1, 0.05, and 0.0mg/mL, while the concentrations of riboflavin were 0.034, 0.0068, 0.0034, and 0.0mg/mL in order to reach the mole ratio of 1:100 (protein:pigment).

The second method created was for the annatto extract. The assay steps were the same as the riboflavin method with the only difference being the use of annatto extract for pigment with its given solubilizing solution, 20% methanol, and concentrations of 0.035, 0.007, 0.0035, and 0.0mg/mL.

The final step was to evaluate the kinetics using various concentrations of the standard RuBisCO and pigments with the Kinetics/Affinity assay.

Ultraviolet-visible Spectrometry

All of the solutions shown in Table 3 were evaluated by UV-Vis spectrometry to determine if spectral shifts were observed, indicating protein-pigment complex formation. The NanoDrop was used to obtain spectra and 2 μ L of each sample were added. Deionized water was needed to clean and initiate the instrument. Blanks were used, based on the solution used (Table 3) to establish a zero reading for the baseline. Each of the pigments was made in the following solutions: riboflavin in water, beta-carotene in acetone, and annatto extract in 20% methanol (as described in Table 3).

Further studies were completed with riboflavin to evaluate if sonication or heating and freeze thaw cycles could facilitate binding of the pigments to the protein. All three of the pigments were later tested with heating and freeze thaw. The riboflavin solutions (Table 3) were sonicated for 10 minutes in a water bath sonicator, vortexed, and then sonicated again for 10 minutes. Samples were then measured with the NanoDrop. The heating of the sample was done at 100°C for one minute with just the standard RuBisCO and then the pigment was added, here only riboflavin, and again heated for one minute (100°C). Then the samples went through two freeze thaw cycles, following the methods of Paulson et al. (1990). The samples were frozen for 20 minutes

at -40°C and thawed for 20 minutes, with vortexing in between to ensure mixing. Repeatedly freezing and thawing of pigments with lipid-extracted proteins in lithium dodecyl sulfate resulted in the formation of a protein-pigment complex that is similar to that found in plants, but it is unclear how the binding occurs and what factors need to be present to promote binding (Paulsen et al., 1990) and if this method will promote formation of protein pigment complexes between RuBisCO and the pigments chosen here.

All of the pigments were then tested under heating and freeze thaw cycles with UV-Vis as a final study. For this portion, the pigments were added directly to the standard RuBisCO in PBS at pH 7.9 (1mg/mL, stock). The goal was to overcome solubility issues with heating and freeze thaw cycles, so the pigments were not previously dissolved in solution and instead were directly added to RuBisCO in solution. Table 6 shows the variety of solutions used. MgCl₂ was also added to each pigment in order to possibly promote binding since Mg²⁺ is needed in order to activate RuBisCO in plants (Reinhard and Höcker, 2005).

Table 6: Standard RuBisCO and pigment solutions used for heating and freeze thaw cycles in protein-pigment complex formation for UV-Vis study.

Standard RuBisCO	Solution	Pigment	MgCl ₂
500µL stock	500µL PBS at pH 7.9	None	None
500µL stock	500µL PBS at pH 7.9	Riboflavin, 0.034 mg	None
500µL stock	500µL PBS at pH 7.9	Beta-carotene, 0.048 mg	None
500µL stock	500µL PBS at pH 7.9	Bixin, 0.035 mg	None
500µL stock	500µL PBS at pH 7.9	Riboflavin, 0.034 mg	2 mg
500µL stock	500µL PBS at pH 7.9	Beta-carotene, 0.048 mg	2 mg
500µL stock	500µL PBS at pH 7.9	Bixin, 0.035 mg	2 mg

The first heating of the standard RuBisCO was with no pigments or MgCl₂ added. The solutions were heated at 90°C for two to four minutes. The solutions were vortexed, and the pigments along with MgCl₂ (for particular treatments) were added directly to the standard RuBisCO solution. Again, each sample was heated at 90°C for two to four minutes and vortexed. Next three freeze thaw cycles were completed with freezing for ten minutes at -80°C and thawing at room temperature for 20 minutes. Then the NanoDrop was used to measure each sample.

4.2.2 Extraction

Freezing Tobacco Tissues

Approximately 10g of finely minced tobacco leaves was placed into a 50mL centrifuge tube and 10mL of freezing buffer with PIC was added. All samples were kept on ice throughout processing. The tissue was homogenized with buffer using a Polytron (Kinematic AG, system Polytron® PT-K/PT-G, dispersing aggregate \varnothing 12 mm, coupling type A, 9110024, PT A 10S) to break down cell walls, until the sample reached a soupy texture. Next, a labeled centrifuge tube was secured with a Styrofoam rack in an insulated container, and then liquid nitrogen was poured into the container.

The minced tobacco tissue in buffer was filtered with cheese cloth, and the left over tissue was saved in a labeled tube. Next, the filtered liquid was transferred into a chilled 50mL centrifuge tube with syringe needle attached (See Figure 10 for set up). The tobacco juice was allowed to drip into the liquid nitrogen filled centrifuge tube. If drops slowed down, a higher gauge needle was used. It was important to make sure that the tobacco juice did not clump together in large beads, but rather formed 0.5 – 1.0 cm diameter pellets, so that the pellets can later fit into the mortar and be ground down into a powder. The liquid nitrogen in the centrifuge tube was refilled as necessary. Once the tube was filled with pellets, the tube was carefully removed from liquid nitrogen and capped off with the ventilated cap (Figure 10). The tube

was inverted to expel liquid nitrogen, then recapped with a non-ventilated cap before immediate storage of the pellets at -80°C (Figure 11).



Figure 11: Final Tobacco Extract Pellets to be stored at -80°C .

4.2.3 Purification of Protein

Sample Preparation

Liquid nitrogen was poured into the Cryo Cooler container at a level just below the top of the mortar. It was critical to ensure that everything was cold at all times to avoid liquefaction of the frozen pellets and maintain formation of a powder; therefore all supplies were placed in liquid nitrogen. The pellets of previously extracted tobacco tissue were taken out and 1 or 2 pellets were placed into the mortar. Tongs were used to hold the mortar in place. The pellet

was ground with the pestle attached to a drill for approximately 30 seconds, and the pestle was placed back into liquid nitrogen (Figure 12).



Figure 12: Setup for grinding of tobacco pellets into fine powder for further use in extraction.

By using a spatula, the inside of the mortar was scraped to loosen the powder formed. The grinding and scraping were repeated two more times to create a well homogenized powder. The powder was stored in a 50mL polystyrene tube filled with liquid nitrogen at all times. The grinding process continued until about 20mL of powder had been formed. Again, liquid nitrogen was

removed by using a cap with holes and then inverting the tube before placing the original cap back on the tube.

Preparation of Antibody Paramagnetic Beads

In order to conjugate the antibody to the beads the following procedures were used. Three mg of beads were weighed into a small vial with screw cap (1.5mL). The beads were rinsed with 200 μ L PBS, vortexed, and then placed in the magnetic rack. All used wash solutions were placed into a waste container. The beads were left in PBS while preparing the rest of the solutions. The PBS was removed while the beads were being held in place by the magnetic rack. The beads were then washed with 0.1M sodium phosphate and then vortexed for 30 seconds. The wash solution was removed as indicated above with the magnet. This wash was repeated and the beads shook for 15 minutes on a vortex at level 12 (VELP Scientifica Vortex Mixer). Figure 13 shows how the magnet can pull the beads out of solution so that the supernatant can be removed and washing can be accomplished.

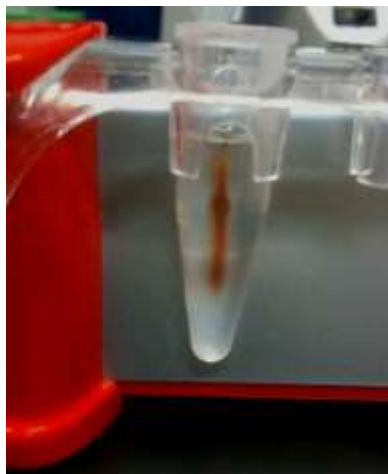


Figure 13: Example of beads on magnetic rack to aid in washing and removal of solution.

In order to conjugate the antibodies to the beads, the total volume of solution was set to be 60 μ L. To reach this volume, a total of 20 μ L 0.1M sodium phosphate (Sigma, dibasic, pH 7.4) was added to the beads. Initially 10 μ L 0.1M sodium phosphate was added and the volume was determined by the pipette method in order to take into account the volume of the beads. Then the rest of the 0.1M sodium phosphate was added in order to reach a total volume of 20 μ L. The solution was vortexed with 15 μ g of 1mg/mL antibody. Next, 5 μ L of 0.1M sodium phosphate was added to reach a total final volume of 40 μ L before adding 20 μ L of 3M ammonium sulfate. After this, 1 μ L of solution with beads was removed for “Before Western”, and then placed in 19 μ L of loading buffer (1X) and stored in the fridge until use. The beads were placed on the shaker at level 12 overnight.

The supernatant was removed with the magnetic rack and washing method. The beads were washed with 200 μ L of the stripping solution (glycine at pH 2.5), which was removed as quickly as possible in order to reduce the possibility of denaturing the protein due to the low pH. Then 200 μ L 10mM Tris at pH 8.8 was used to wash the beads and vortexed before removing the solution. Next 200 μ L of the triethylamine was used to wash the beads. Then the beads were washed four times with 200 μ L of PBS buffer followed by one wash with 200 μ L of PBS plus 0.5% Triton to reduce non-specific binding. The beads were shook again for 15 minutes at setting 12 before being rinsed with 200 μ L PBS. The actual volume was measured by pipette method and recorded. For this extraction a concentration of 1000 μ g/ μ L beads and the appropriate volume of PBS were used to achieve this concentration. One μ L of “After Western” was removed and placed in 19 μ L of loading buffer (1X) for SDS-PAGE. Both the “After Western” and the beads were stored in 30 μ L of PBS in the refrigerator until use.

The second method to conjugate the antibody to beads was to use the Dynabeads® Antibody Coupling Kit. On the first day 100 μ L of beads (3mg) were taken out and washed once with 1mL of C1. The tube was placed on the magnetic rack and the beads allowed to collect so that the supernatant could be easily removed. Then 140 μ L C1 was added with 10 μ L of antibody and the solutions mixed by pipetting. Next, C2 (150 μ L) was added to reach a total volume of 300 μ L. The solution was incubated overnight at 37°C while

mixing. On day two the tube was placed on a magnetic rack and the beads allowed to collect. The supernatant was removed and washed with 800 μ L each of HB, LB, and SB. Incubation in SB was conducted for 15 minutes at room temperature and then the solution removed and stored under refrigeration in 300 μ L of SB for a final amount of 10mg/mL of beads coupled to antibody.

Antibody Paramagnetic Beads with Protein Extraction

The initial trials with the antibody coated beads used standard RuBisCO (95% purity, Sigma). Fifty μ L of extraction buffer with 10 μ g of 1mg/mL standard RuBisCO in PBS was added to the beads. The appropriate volume of beads for 1000 μ g/ μ L was placed in a new tube. The beads were resuspended in 50 μ L of standard RuBisCO in extraction buffer. Then 1 μ L of beads with RuBisCO were taken out for “Before Western RuBisCO” and put in 19 μ L of loading buffer (1X), and stored in the refrigerator until use. Incubation at room temperature was conducted while shaking at setting 12 for 15 minutes. The beads were washed with 50 μ L of dilution buffer four times with the magnetic rack as well as with one wash of 0.01 M PBS + 0.05% Tween 20 in between each dilution buffer rinse to reduce non-specific binding. For standard RuBisCO samples, 20 μ L of loading buffer (1X) was added for SDS-PAGE.

Two different extraction buffers (Table 2) were used with the tobacco powder to optimize the protocol of extraction with beads. Five mL of extraction buffers were added to tobacco RuBisCO powder (1g) and the extraction samples were homogenized with the Polytron on ice, at setting five for five minutes at one minute intervals. Centrifugation was conducted at 9,500 RPM for 30 minutes at 4°C. The pellet was stored in LDS loading buffer (1X) to be run on the gel. This was completed for each pellet from buffers A and B. To the supernatant for both A and B, the determined amount of beads was added after conjugation (1000 µg/µL). The supernatant was incubated for 15 minutes on a 50mL tube rotator. The beads were transferred with supernatant to smaller Eppendorf tubes that can be used on the magnetic rack and washed with 200µL of dilution buffer, followed by a 0.01M PBS + 0.05% Tween 20 wash. This procedure was repeated four times. To run on the gel, 20µL of loading buffer (1X) to dry final beads (this will be supernatant “After A and After B”) was added. A control of standard RuBisCO was also used. The stock was made up at 1mg/mL PBS at pH 7.9. Then 0.5µL with 20µL of loading buffer (1X) were added and run with 1µL of stock in 19µL of loading buffer (1X).

After initial trials with standard RuBisCO and extraction buffers the protocol was optimized and methanol precipitation was used to understand how much protein was present so that RuBisCO could be successfully and efficiently extracted from the tobacco leaves. The final procedure used 10mL of

extraction buffer plus the ground tobacco powder (1g) in a 50mL centrifuge tube (on ice). Both extraction buffer A and B were used to provide two different samples. Each mixture was homogenized with the Polytron, to break up the plant components further and release the protein (six to seven setting for five minutes at one minute intervals on ice). Then the samples were centrifuged at 4,700 RPM for 30 minutes at 4°C. The supernatant was removed and 40mL of methanol were added, followed by centrifugation at 4,700 RPM for one hour at 4°C. The pellets from the original spin were saved and stored in 1mL of loading buffer (1X) in the refrigerator for further use. After the second spin the supernatant was removed and 5mL of 90% methanol were added to each pellet, and the mixture was vortexed. The samples were again centrifuged at 4,700 RPM for 30 minutes at 4°C. The supernatant was decanted and the final pellet was stored in 1mL of loading buffer (1X). The final pellet was called either supernatant A or B since it began as the supernatant after the initial spin before methanol extract. In order to run the pellet from the original spin and the supernatant after methanol precipitation that were stored in 1mL of loading buffer (1X), 10 μ L of the pellet or supernatant in loading buffer were added to 10 μ L of loading buffer (1X) to create a final volume of 20 μ L. The stock standard RuBisCO was run with the supernatant and pellet samples. For standard RuBisCO 1 μ L of stock (standard RuBisCO at 1mg/mL in PBS at pH 7.9) in 19 μ L of loading buffer (1X) was prepared. The results from this methanol precipitation with the pellet and

supernatant for extraction buffers A and B were developed with Ponceau stain.

Standard RuBisCO was created as a final stock solution in loading buffer to be used for further experiments: 30 μ L of stock (standard RuBisCO at 1mg/mL in PBS at pH 7.9) plus 570 μ L of loading buffer (4X) and stored at - 40°C. The supernatant from extraction buffer B, Polytroned at level 6 to 7 and centrifuged, was also stored in aliquots for further use.

Next, the supernatant from extraction buffer B was compared to methanol precipitation of supernatant with dilutions. The stored supernatant (15 μ L) was added to loading buffer (4X, 5 μ L) to prepare for the gel run. The final stock solution of standard RuBisCO in loading buffer was used, and the supernatant was run through the methanol precipitation procedure as described previously, this time starting with only 500 μ L of supernatant. The final pellet was resuspended in 100 μ L of loading buffer (1X) and dilutions were created starting at 20 μ L serially to 1 μ L of resuspended pellet in 19 μ L of loading buffer (1X) with a total volume always of 20 μ L.

The final selected antibody, RbcL, anti-rabbit polyclonal (Agrisera) needed to be confirmed for specificity to the tobacco RuBisCO. In order for this to be accomplished the standard RuBisCO final stock solution in loading buffer was compared to dilutions of the supernatant (previously homogenized and

centrifuged) with reducing agent added to help promote migration. The dilutions were used to establish the correct amount of supernatant to not overload lanes. The reducing agent was 10X, so 2 μ L were needed for each total 20 μ L loading sample.

The final step was to incubate the supernatant with the conjugated beads. For this 1mL of supernatant (previously homogenized and centrifuged) was incubated with 25 μ L of beads at 10mg/mL RbcL anti-rabbit polyclonal antibody for RuBisCO for 30 minutes while shaking at level 12 (VELP Scientifica Vortex Mixer). Next, the supernatant was removed (saved and run on gel at 10 μ L with 10 μ L loading buffer, 1X), and the beads were washed three times with 1mL of 0.01 M PBS with 0.05% Tween 20 to reduce nonspecific binding. To the final beads, 50 μ L of loading buffer (1X) was added in order to run on the gel at dilutions.

The beads were interrogated to ensure the antibody was conjugated to the surface. This was completed by comparing three different sets of beads. The first was 500 μ L of supernatant, previously homogenized and centrifuged, incubated with 25 μ L of beads at 10mg/mL (RbcL, anti-rabbit polyclonal for RuBisCO). The second bead set was 500 μ L of PBS at pH 7.9 with 25 μ L of beads at 10mg/mL (RbcL, anti-rabbit, polyclonal for RuBisCO). The final set was again 500 μ L of PBS at pH 7.9, but this time with 25 μ L of beads that had not been conjugated. All were incubated for 30 minutes while shaking on

setting 12 (VELP Scientifica Vortex Mixer). Each set of beads were washed three times with 1mL of 0.01M PBS with 0.05% Tween 20 to reduce nonspecific binding. The final beads were prepared in 23 μ L of loading buffer (1X) with 2 μ L of reducing agent.

After confirmation of bead conjugation, the final samples to be run in several sets were the standard RuBisCO, the beads with and without conjugation and incubation in supernatant, along with supernatant dilutions. For this the beads sets mentioned above were used but instead of a final volume of 23 μ L of loading buffer (1X) the beads were placed in 6.25 μ L of loading buffer (4X) with 2.5 μ L reducing agent and 16.25 μ L of water. The standard RuBisCO had reducing agent added with a final volume of 20 μ L. Supernatant with no dilutions was run with 5 μ L of supernatant and 5 μ L loading buffer (4X) with 2 μ L reducing agent and 8 μ L water. The dilutions created were 1:10, 1:100, and 1:1000 in PBS at pH 7.9 and then the same amount of each was used to create the running solution in loading buffer as listed for supernatant with no dilutions.

SDS-PAGE

The purpose of SDS-PAGE was to separate out proteins based on size and charge. This process was completed using NuPAGE Novex Tris-Acetate Mini Gels system. First the samples were prepared with NuPage LDS Sample Buffer, Tris-Glycine Native Sample Buffer and deionized water. The total

volume for these amounts can be found in the NuPage Novex Instructions and should have a total volume of 20 μ L. Next the sample with buffers was heated at 90°C for ten minutes. A hard spin was added for final trials at 16,000 \times g for 2 minutes. The 1X running buffer was then prepared by adding 50mL 20X NuPage Tris-Acetate SDS Running Buffer to 950mL deionized water. The sample was then loaded onto the gel, and the upper and lower buffer chambers were filled with the 1X running buffer. The protocol used a programmed method for approximately 30 minutes. It was also important to include a ladder with standard protein sizes to measure and find the protein of interest, in this case RuBisCO at 56 kDa.

Western Blot

The procedures from the Fast Western Kit were followed (iBlot). First the wash buffer was prepared so that it was available when the membrane was complete done. The filter paper was placed in distilled water to soak. The bottom attachment was placed in the iBlot, then gel with filter paper on top. The top portion was added and all air was removed with a roller before the sponge was placed in the lid. The lid was closed to the iBlot, and the 6 minute transfer started. Once the transfer was done the membrane was quickly removed and placed into the wash buffer. The membrane was then placed into the primary antibody solution and shook for 30 minutes. Next, the membrane was rinsed in the wash solution and then placed into the secondary antibody solution for 10 minutes. It was rinsed again with the wash solution and finally

put into the exposure solution. The image was acquired using the Kodak Image Station 2000R (Carestream Health, Inc., Rochester, NY) and Carestream MI image software (Carestream Health, Inc., Rochester, NY).

Silver Stain

For silver staining, the gel was washed for five minutes with MilliQ water after SDS-PAGE. The gel was washed for another five minutes after replacing the water. Next, the water was decanted before adding the fixing solution. The gel was incubated in this solution for 15 minutes at room temperature. The fixing solution was replaced and again the gel incubated in new fixing solution for 15 minutes. The gel was then washed twice with ethanol for five minutes. The next step was to rinse the gel in ultrapure water for five minutes (2x). Just before use, the sensitizer working solution, which is 1 part SilverSNAP® Sensitizer with 500 parts ultrapure water, was prepared. Incubation of the gel in sensitizer working solution for exactly one minute was conducted before it was washed with two changes of ultrapure water for one minute each. Next, incubation for five minutes in one part SilverSNAP® Enhance with 100 parts SilverSNAP® Stain was performed. The developer working solution was created with one part SilverSNAP® Enhancer and 100 parts SilverSNAP® Developer. The gel was washed with two changes of ultrapure water for 20 seconds after the gel had been in the stain for five minutes. Then the developer working solution was immediately added and the gel was incubated until protein bands appeared (approximately 2-3 minutes).

When the necessary band intensity was reached, the stop solution was added before obtaining the gel image.

Chapter 5: Results and Discussion

Overall, the scope of this project encompassed two aspects, the first being the possibility of binding the chosen pigments to a RuBisCO standard; the second creating an efficient extraction and purification of RuBisCO from tobacco leaves using paramagnetic antibody coated beads. Both objectives were developed in order to promote the use of alternative products of the tobacco crop. The research on binding used a RuBisCO standard instead of tobacco-isolated RuBisCO due to several challenges in optimizing the extraction and purification steps which overlapped with the binding studies. The results of each aspect of the project are discussed in full below.

5.1 Binding Effectiveness

5.1.1 Raman Spectroscopy

While it was initially anticipated that Raman spectroscopy would provide useful and relevant data for evaluating whether pigment binding had occurred, it was seen that the standard RuBisCO powder sample was too fluorescent to provide useful information, meaning no identifying peaks are measured. The fluorescence of the standard RuBisCO powder was seen as a large sweeping arch (Figure 14).

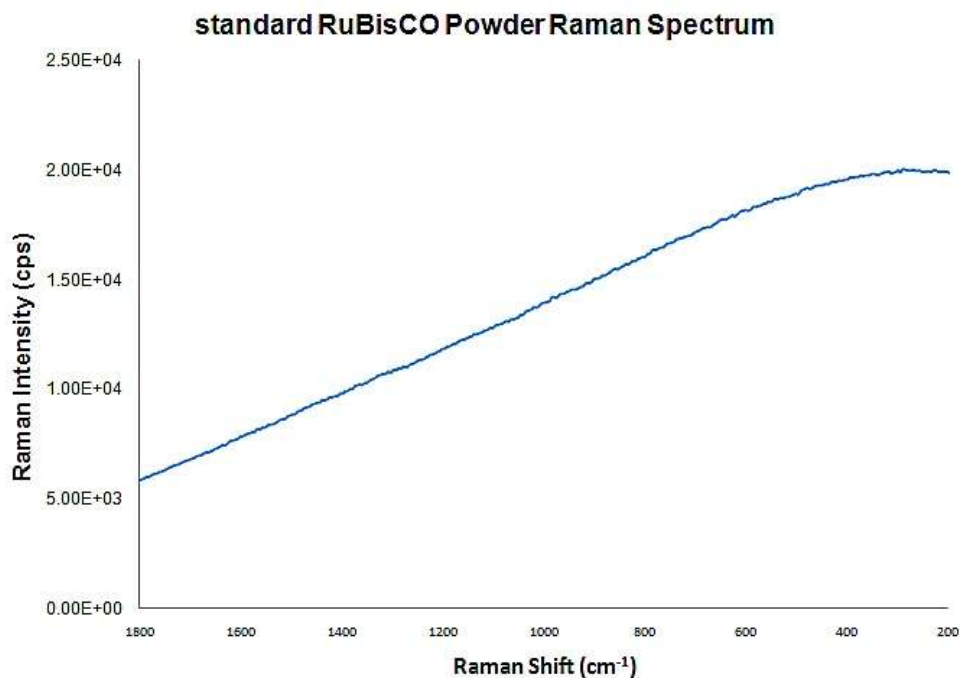


Figure 14: RuBisCO spectrum with no baseline adjustment and an exposure time of 1 second with 3 total exposures and following experiment setup seen in Table 5, value A (780nm).

While Raman spectroscopy could potentially be used to understand if there were any peak shifts or the development of new peaks due to binding as compared to original peaks of pigments and RuBisCO, the fact that the RuBisCO spectrum does not offer information means that Raman cannot be used to understand binding. The fluorescence overwhelmed any Raman bands that could be seen in the RuBisCO sample. However, the spectra of the individual pigments were measured with ease and compared well to literature.

An image using the Raman microscope was taken of each sample (Figures 15 through 18). These images show the various color of each sample. While all

three pigments offer yellow to orange color in solution and food products, they are very different in powder and liquid forms. Beta-carotene is a reddish color in powder form, while riboflavin is most similar to the color it produces in solution. The annatto extract, in liquid form, dried on the slide, and as a result shows cracking and little color. The RuBisCO powder is crystalline and not as dense as the pigment powders.

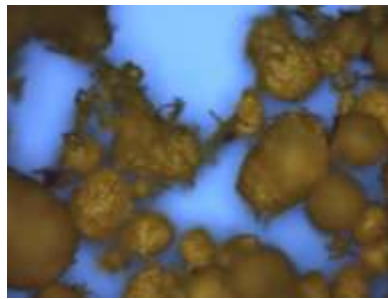


Figure 15: Riboflavin image, Raman microscope (10X, light field).

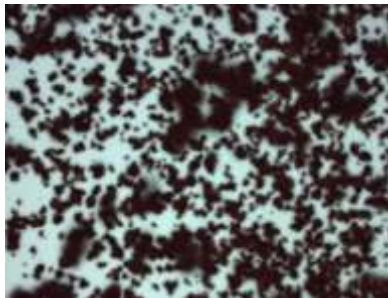


Figure 16: Beta carotene image, Raman microscope (10X, light field).



Figure 17: Annatto Extract image, Raman microscope (10X, light field).



Figure 18: Standard RuBisCO image, Raman microscope (10X, dark field).

The spectrum for each pigment was also measured. Spectra measured for riboflavin (Figure 19) and beta-carotene (Figure 19) match well with literature (Sigma Aldrich). The sample for annatto extract (Figure 21) was very similar to beta-carotene which was expected due to their similar structure (long hydrocarbon chain with alternating single/ double bounds) (Figures 2 and 3). The main peak in riboflavin ($\sim 1380\text{cm}^{-1}$) show the numerous hydroxyl groups present off of the nitrogen ring. The peak in both beta-carotene and annatto extract at $\sim 1500\text{cm}^{-1}$ represents the long hydrocarbon chain seen in both pigments.

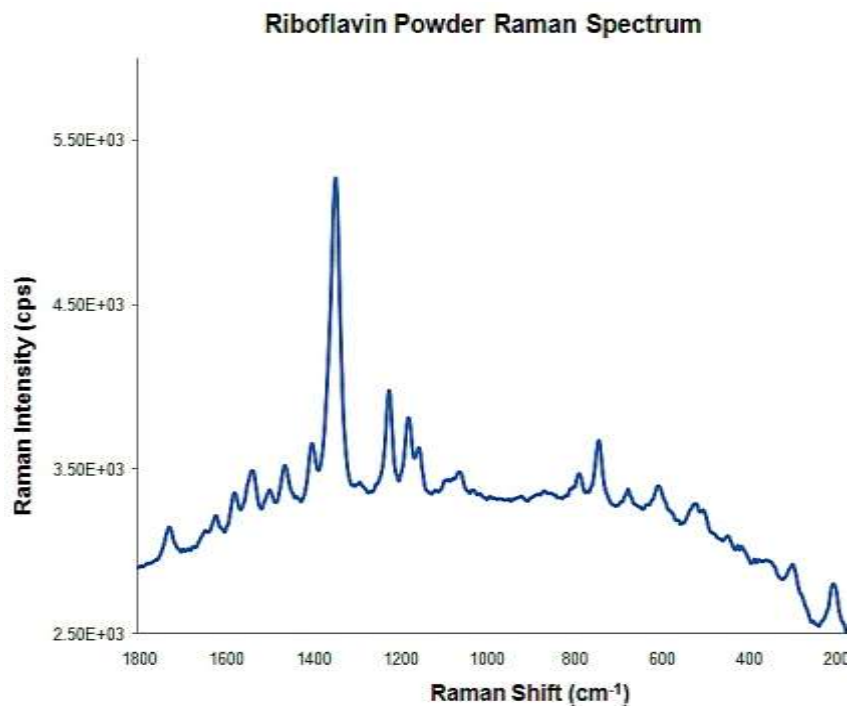


Figure 19: Riboflavin spectrum with baseline adjustment and an exposure time of 5 seconds with 3 total exposures and following experiment setup seen in Table 4 (780nm).

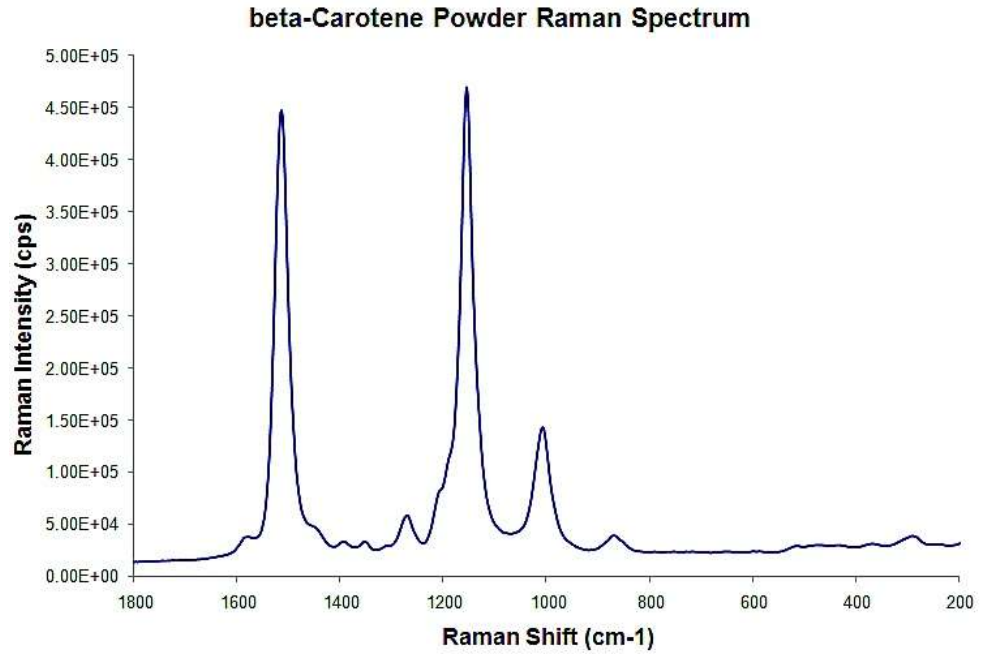


Figure 20: Beta-carotene spectrum with no baseline adjustment and an exposure time of 0.1 seconds with 3 total exposures and following experiment setup seen in Table 4 (780nm).

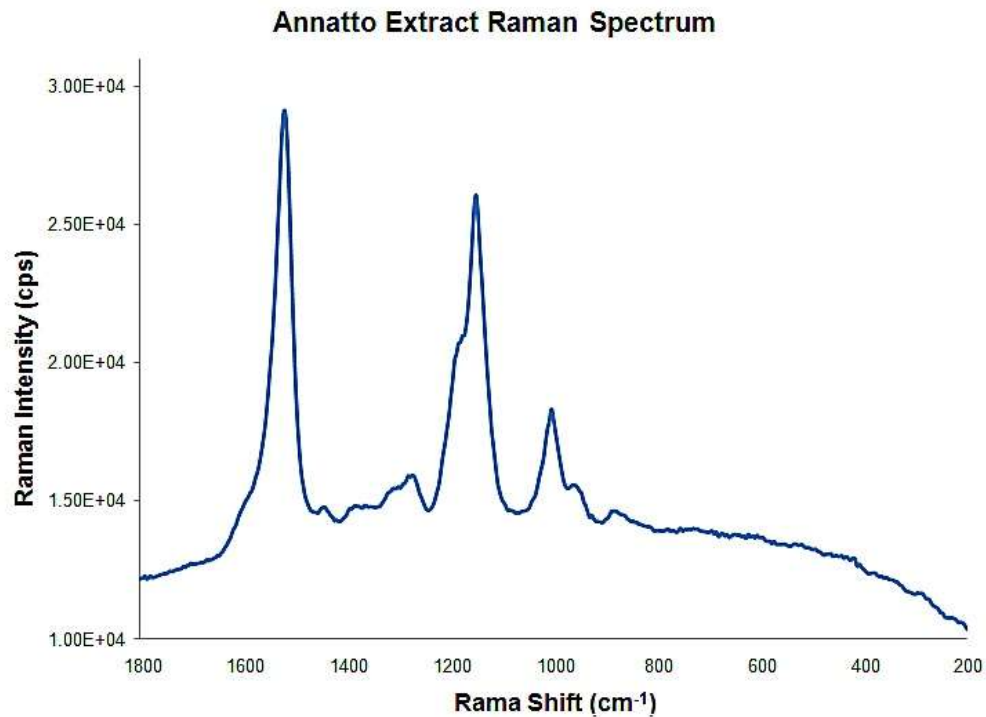


Figure 21: Annatto Extract spectrum with baseline adjustment and an exposure time of 1 second with 3 total exposures and following experiment setup seen in Table 4 (780nm).

Unfortunately, the pigments with RuBisCO were not studied due to the fact that no distinct peaks were observed in the RuBisCO powder spectrum because of fluorescence. Even though the pigments offer useful spectra, the fact that RuBisCO does not show any peaks means that binding cannot be understood or evaluated with Raman spectroscopy.

5.1.2 Surface Plasmon Resonance

SPR was used to study the kinetics of standard RuBisCO as it binds to the antibody (anti-RuBisCO, spinach, monoclonal) on the gold substrate. The

preliminary studies for standard RuBisCO used several different buffers including: 1M Tris HCl buffer pH 8.0, HBS-EP+, HBS-N, and PBS at pH 7.4. However, these buffer systems resulted in large amounts of protein aggregation which caused the kinetic data to be difficult to interpret. Even when solubilized, RuBisCO is a large protein and causes a high change in RU without surface binding due to refractive index change. This “solution matching” also caused challenges when fitting data, as the algorithm does not account fully for this refractive index change seen at the injection of RuBisCO analyte.

To overcome the challenge of protein aggregation and therefore loss of useful kinetic information, the standard RuBisCO was solubilized in PBS with a pH of 7.9. At this pH the standard RuBisCO completely dissolved into solution and there was no aggregation seen overnight.

The following figure provides general information on the shape of all sensorgrams to follow, as well as key points during the assay.

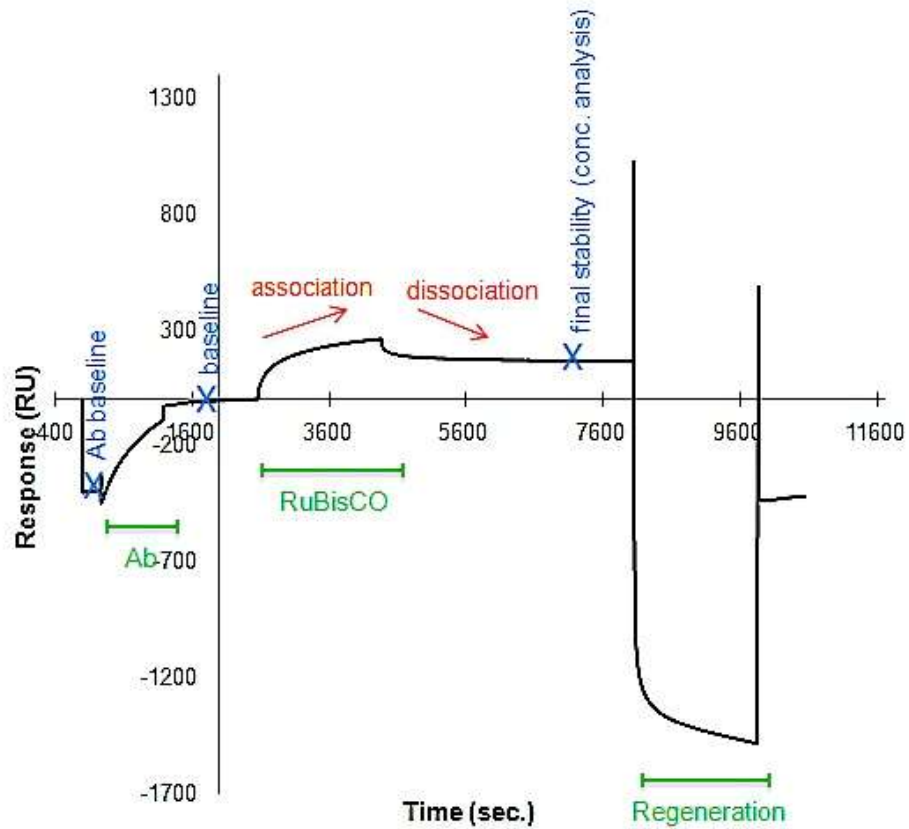


Figure 22: General sensorgram information with antibody binding, RuBisCO injection for association and dissociation measurements, followed by regeneration to establish baseline to allow chip to be reused. Data shown is from 0.5mg/mL standard RuBisCO in PBS at pH 7.9 for initial trials with antibody binding.

The following explanation shows how to understand the data seen in Figure 23 for kinetics of standard RuBisCO.

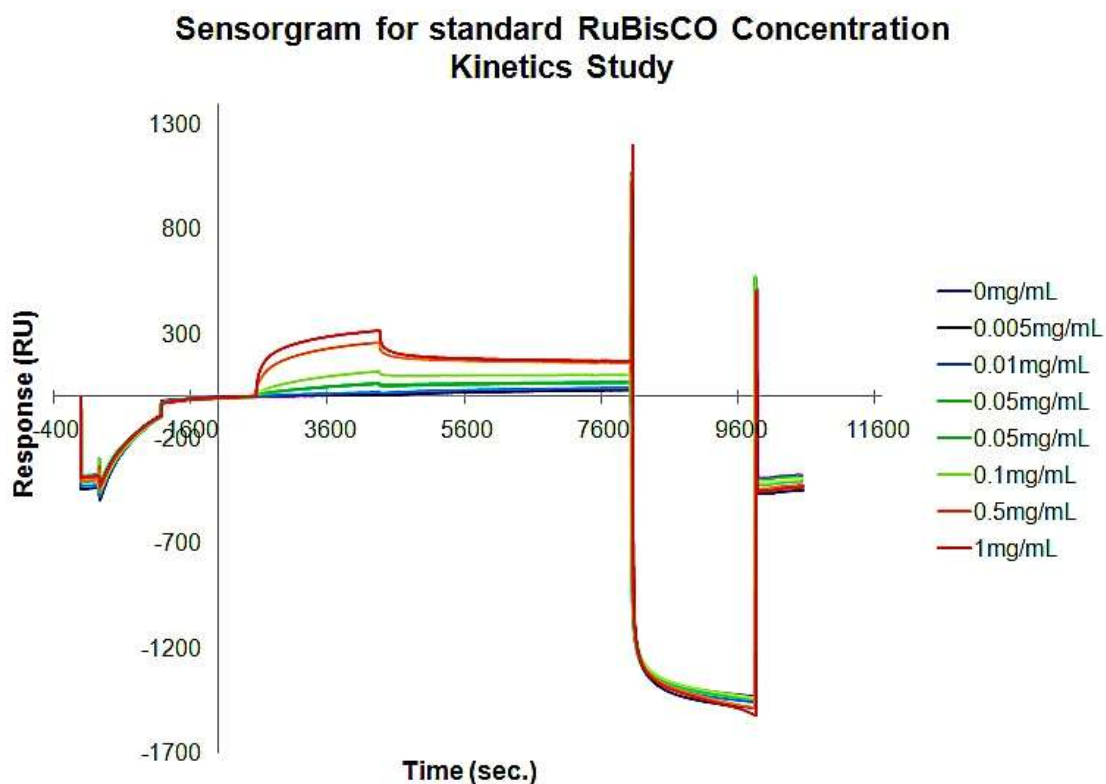


Figure 23: Sensorgram for RuBisCO Kinetics with anti-RuBisCO antibody (mouse monoclonal) and standard RuBisCO in PBS solution at pH 7.9.

First it was important to color the sensorgram by concentration and then add the report point markers so that was easy to understand the different sections of the sensorgram. Next antibody capture was checked to ensure that it was sufficient. To do this, adjust the sensorgram to “capture baseline” for both report points X and Y (axis). Then evaluate Ab (antibody) curve overlap. In Figure 23 the Ab all overlap and give 425 RU which indicate efficient capture. It was seen here that for cycle 2 the RU was 425 and for cycle 9 the RU was 365 a difference of 60 RU. The difference in antibody capture level usually is within 10% or less of the total change in RU to be acceptable with respect to

chip degradation. Here, the difference is not within 10%, as it would need to be less than 42.5 RU. The data was still used for these studies; however, as the kinetics were found statistically relevant and the repeat measurement (0.05mg/mL) was the identical during each cycle.

The next step was to check the binding of standard RuBisCO to the antibody. Again adjust the sensorgram, but this time to “baseline” for both X and Y axis. It can be seen here that there was a concentration close to zero and there was a concentration that reached saturation and leveled out (1mg/mL). Also, there are a good variety of concentrations between, and the repeat concentrations were comparable. This indicates the data can be used for modeling.

It was also important to make sure the regeneration occurred normally for each run. This is seen in Figure 23 by the return to a similar baseline after each cycle, and a smooth regeneration cycle curve.

The concentrations provided in the sensorgram can be used to establish a concentration curve (Figure 24). The expected sigmoidal curve is obtained, further validating the results.

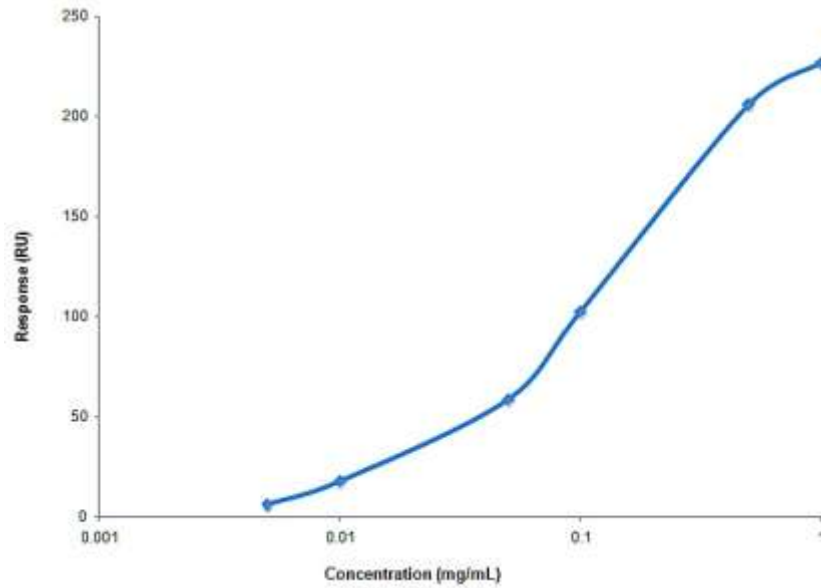


Figure 24: Standard curve for RuBisCO samples.

Next the system kinetics were analyzed using the Biacore Software. The first kinetics study was 1:1 binding. This represents that one protein molecule bound to one antibody arm at a time; that is to say, one epitope binds to one ligand site. The parameters followed were a global fit except the refractive index, which fit locally. Figure 25 shows the results from the 1:1 binding kinetics.

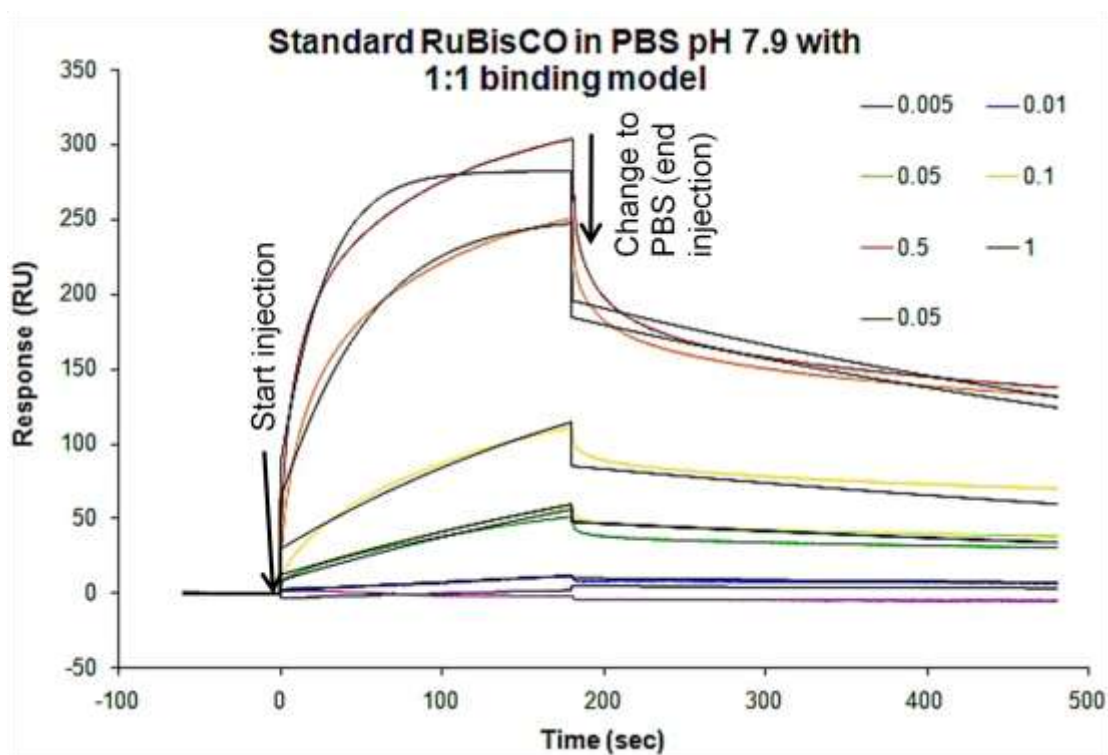


Figure 25: Kinetics results for standard RuBisCO using a 1:1 binding model. Colored lines are experimental; black lines are fit.

The 1:1 binding showed good fit in that the black lines follow the colored sensogram curves well. The residuals (a measure of how far fit is from experimental data) found for this set of data were between 20 and -20, whereas a good fit is usually between 10 and -10. The residuals were large, but this is to be expected as RuBisCO is a large molecule with large refractive index change that hinders proper fit at the start and end of the injection as seen in Figure 25. Table 7 shows the results from the kinetic study for 1:1 binding.

Table 7: Results for Kinetics 1:1 Binding for standard RuBisCO.

Value	Result	General Guidelines	Explanation
Uniqueness	3	Under 10	Means the data is relevant
R_{max}	202.3 RU	Between 100-500 RU	Within the limits of the instrument
χ^2	39.9	Under 1% of R_{max} , here <2.023	How well does theoretical curve (black) fit experimental curve (colors)
Standard Error	$SE_{k_a} = 1.9E2$ $SE_{k_d} = 7.5E-6$	Standard Error values should be 10% or less of their k_a or k_d value to indicate significance of fit	Reasonable response
Tc (Mass Transfer Coefficient)	7.16E6	No mass transport at 10^9 to 10^{12} , $>10^7$ may have mass transport	Mass transport expected with RuBisCO due to large size and aggregation
Kinetic Values	$k_a = 2.368E+4$ (1/Ms) $k_d = 0.001422$ (1/s) $K_D = 6.002E-8$ M	Monoclonal antibodies show values between 10^7 to 10^{-10}	K_D provides an appropriate value for a monoclonal antibody

There were two values given that need to be discussed further: χ^2 and the Mass Transfer value. The χ^2 value tells how well the theoretical data matches your experimental results. In general, if the residual values are high, which they are here, then the χ^2 value will be high as well. The χ^2 value was high as compared to the target, but this was acceptable due to the high residuals found, and the large refractive index produced from RuBisCO. The Mass Transfer Coefficient measured the possibility of mass transport, which is how well an analyte can reach the surface to bind the ligand. Having mass transport limitations means that the analyte has difficulty in penetrating the diffuse layer, thus not efficiently reaching the surface. This can result in decreased binding. For SPR no mass transport limitations are better, but it was acceptable here if there were some mass transport limitations. Mass transport

was expected in these experiments as RuBisCO is quite large and prone to aggregation.

The kinetics software was also used to run two other binding models, Bivalent and Heterogeneous Analyte. Bivalent binding means that the analyte binds twice and therefore does not provide a K_D since it cannot be determined which k_a of the two values is associated with a single (or dual) k_d value. This model is only relevant if there is a biological explanation for binding and here the RuBisCO was not assumed to bind twice to the antibody. The Heterogeneous Analyte Binding model occurs when there are two different size or two different affinity binders in the analyte solution and each has different kinetic values. For Heterogeneous Analyte Binding the values for a second concentration and molecular weight are used (Table 8). The 557,000 molecular weight is for the intact RuBisCO and the 55,000 represents the large subunit molecular weight. The concentrations are stated as entire solution concentrations.

Table 8: Heterogeneous Analyte Binding values for molecular weight and concentration.

Cycle	Concentration (mg/mL)	Concentration 1	Molecular Weight 1	Concentration 2	Molecular Weight 2
2	0.005	8.98×10^{-9}	557000	8.98×10^{-9}	55000
3	0.01	1.8×10^{-8}	557000	1.8×10^{-8}	55000
4	0.05	8.98×10^{-8}	557000	8.98×10^{-8}	55000
5	0.1	1.8×10^{-7}	557000	1.8×10^{-7}	55000
6	0.5	8.98×10^{-7}	557000	8.98×10^{-7}	55000
7	1	1.8×10^{-6}	557000	1.8×10^{-6}	55000
8	0.05	8.98×10^{-8}	557000	8.98×10^{-8}	55000

In Heterogeneous Analyte Binding the values added are those of the RuBisCO molecule as a whole as well as the small subunit broken off since the antibody is specific to the large subunit. However, it is difficult to know if this was actually occurring in solution. The small subunit was not taken into account if was was broken off because the antibody does not bind to the small subunit. This kind of binding is highly prone to error, as the molecular weights as a whole and as individual component are needed along with the concentrations of each. In this case the concentrations were not known for the large subunit or RuBisCO as a whole, so it was a less likely fit for the data and not used for further studies.

The next step for studies with SPR were to combine the various pigments with the standard RuBiSCO (Table 3). For all of the SPR studies these solutions were solely mixed together by votexing and pipetting.

The first pigment study was with riboflavin, and Figure 26 shows the results from the various concentrations.

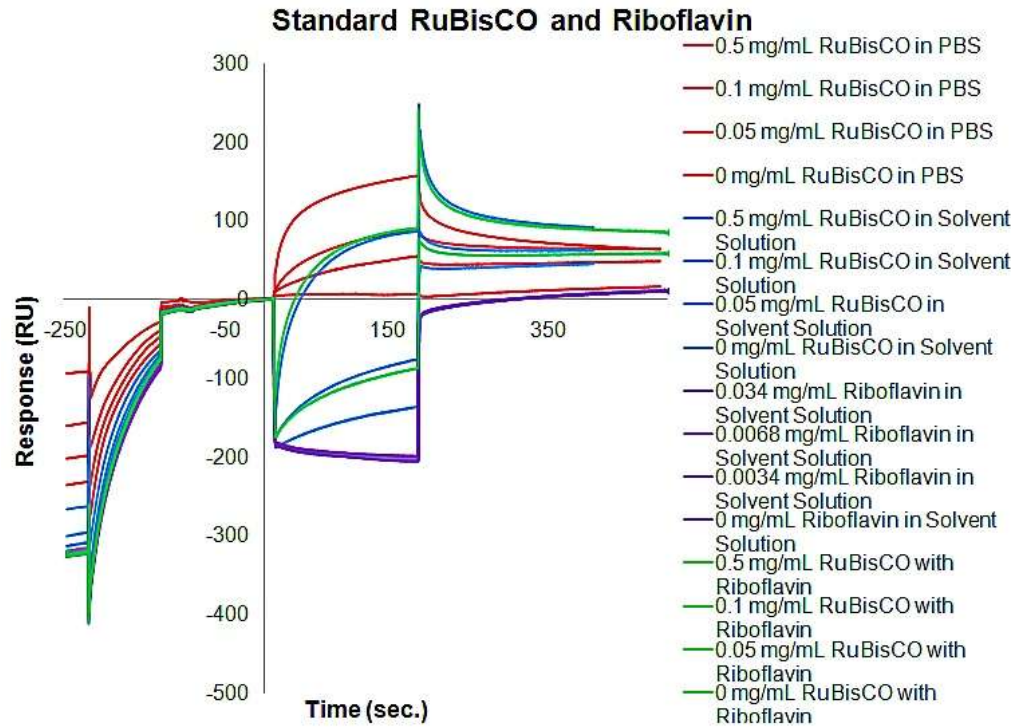


Figure 26: Standard RuBisCO with Riboflavin.

This graph shows general trends in binding with first, antibody binding to reach a baseline followed by second, RuBisCO and/or pigment binding. The RuBisCO and pigment solutions show association and dissociation and the regeneration is not shown. The large changes in RU were due to the different solutions used with varying refractive indexes created.

This data set goes through the same analysis as the original sensorgram (Figure 23). The antibody capture was evaluated and for cycle 12 the RU was

310 and for cycle 1 the RU was 90 for a difference of 220 RU. The difference in antibody capture level needed to be within 10% or less of the total change in RU (310). Here the difference (220) was much higher than the 10% of the total change in RU. Despite this degradation, the data was evaluated for general trends and comparison purposes.

Before taking a direct look at the kinetics of the assay the control and sample runs were compared in Figure 27.

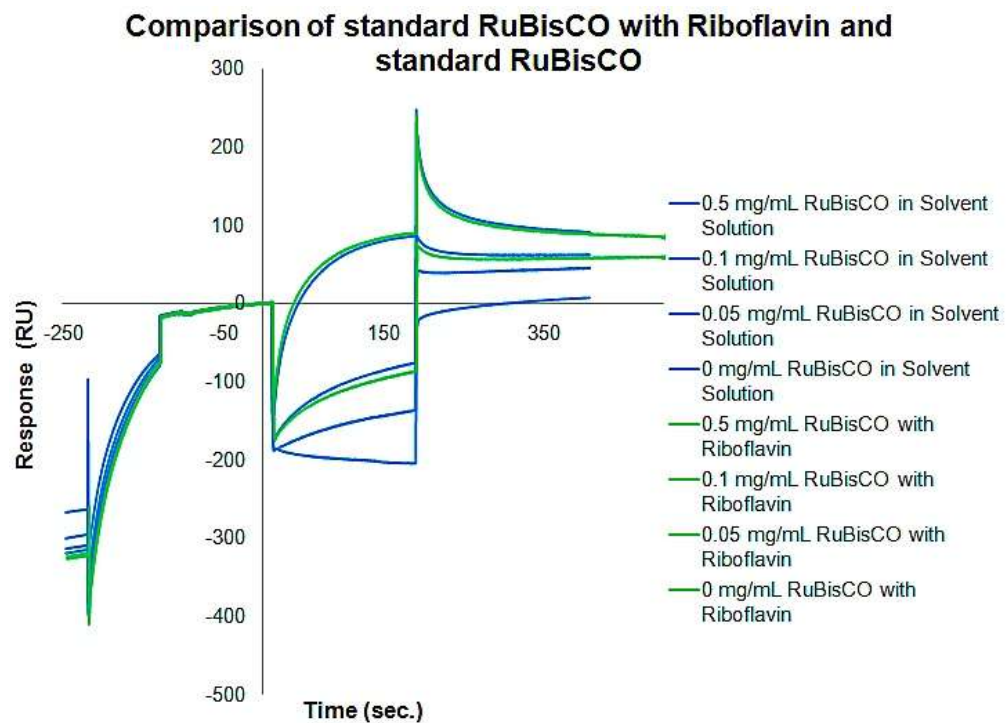


Figure 27: Comparison of standard RuBisCO/riboflavin complex and standard RuBisCO.

This sensorgram shows that there was no difference between the standard RuBisCO alone and the standard RuBisCO with the pigment in the solvent solution. The curve shapes for binding provided information even before further analysis. There was no significant change in the curve shapes, meaning that the kinetic results will be similar. Due to these findings it was seen that SPR was not helpful in determining if the pigment was bound or not to the standard RuBisCO. Either there was no binding and thus no change in kinetic values or there was binding, but no change to kinetics. In addition, if there was binding, the pigment does not change the inherent binding of the standard RuBisCO, and therefore there is no structural stability lost.

The RuBisCO and riboflavin trial was completed with 1:1 binding as seen in Figure 28.

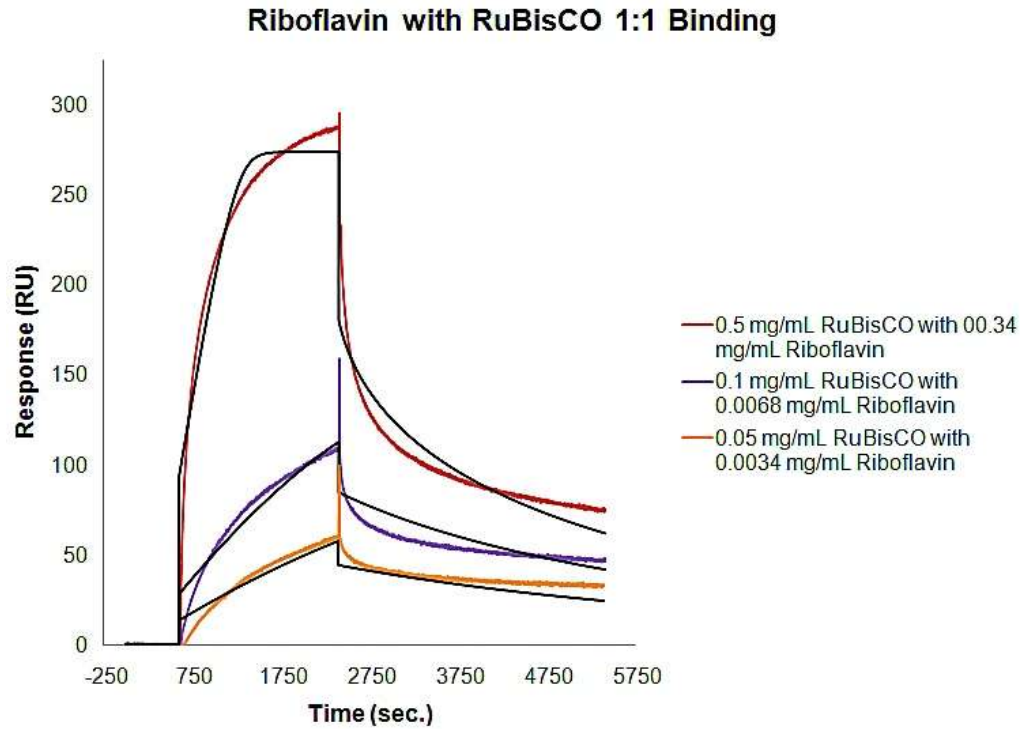


Figure 28: Kinetics for standard RuBisCO with riboflavin using a 1:1 binding model.

Colored lines are experimental; black lines are fit.

It was determined previously that 1:1 binding provides the most useful analysis of data. The 1:1 binding showed good fit with the black lines fitting the color sensorgram curves closely. The residuals found for the standard RuBisCO with riboflavin were between 25 and -25, which is large compared to the goal. The residuals were accepted as explained previously. Table 9 shows the results from the kinetic study for 1:1 binding for the standard RuBisCO with riboflavin.

Table 9: Results for Kinetics 1:1 Binding for standard RuBisCO with riboflavin.

Value	Result
Uniqueness	3
R_{\max}	200.5 RU
χ^2	77.7
Standard Error	$SE_{k_a} = 2.9E4$ $SE_{k_d} = 0.0029$
Tc (Mass Transfer Coefficient)	1.576E+6
Kinetic Values	$k_a = 4.197E5(1/Ms)$ $k_d = 0.04315 (1/s)$ $K_D = 1.028E-7 M$

The standard RuBisCO with riboflavin have similar values to the standard RuBisCO alone (Table 7). The K_D value is $1.028E-7 M$. This value was not significantly different, based on the standard error, from the original K_D value for standard RuBisCO alone ($6.002E-8 M$). As such, the kinetic data indicates binding for standard RuBisCO to the antibody has not changed, and either pigment did not bind to RuBisCO or the pigment binding does not change the kinetic values.

Annatto extract was run on SPR with standard RuBisCO in order to understand possible kinetic changes using solutions previously described (Table 3). Figure 29 shows the sensorgram for annatto extract and standard RuBisCO.

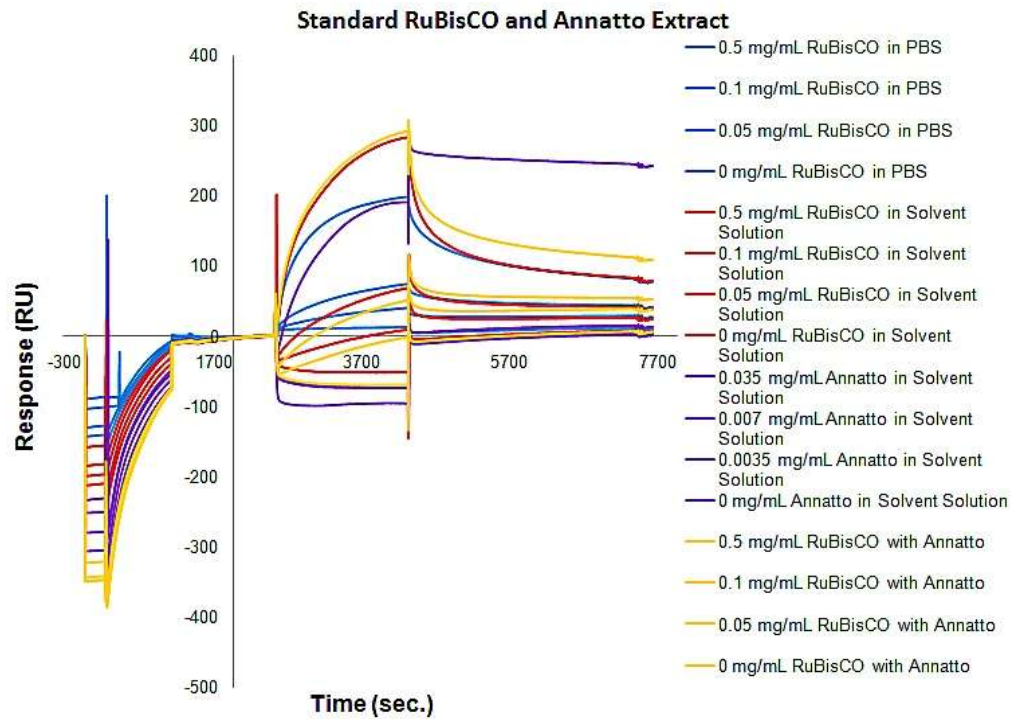


Figure 29: Standard RuBisCO with annatto extract.

The data set goes through the same analysis as the original sensorgram for standard RuBisCO (Figure 23). This graph shows general trends in binding as seen with both RuBisCO alone and the riboflavin trials. First, antibody binding reaches a baseline followed by second, RuBisCO and/or pigment binding with association and dissociation. Again, regeneration is not shown. The large changes in RU were due to the different solutions used with varying refractive indexes created.

Before taking a direct look at the kinetics, the control and sample runs are compared in Figure 30 and the control and calibration 2 are compared in Figure 31.

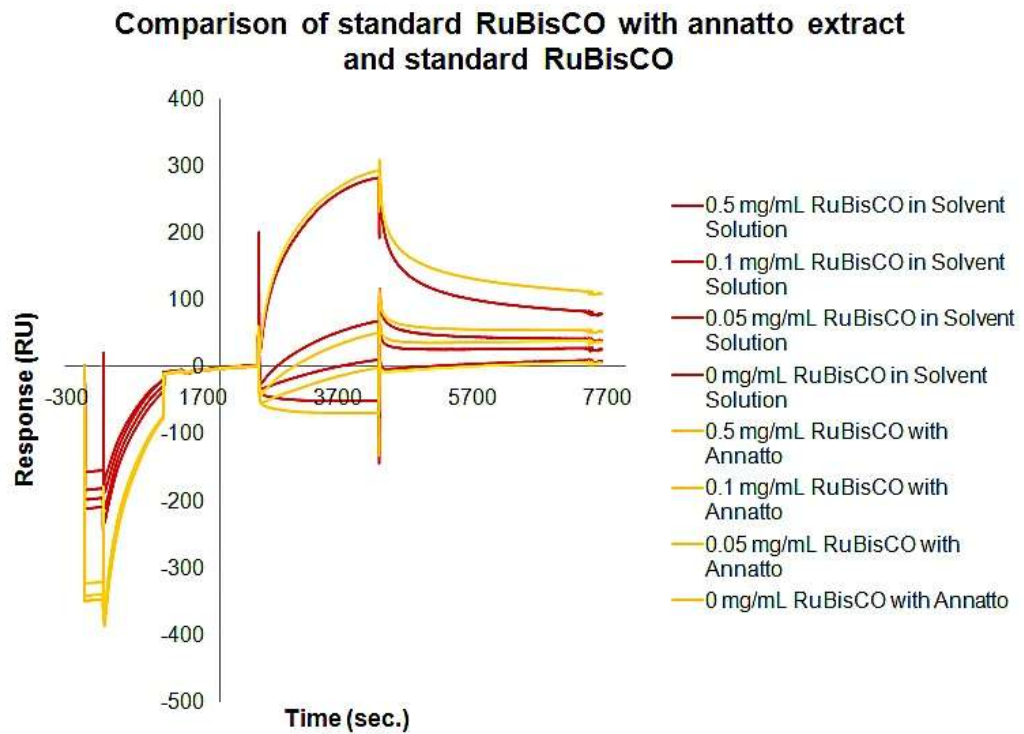


Figure 30: Comparison of standard RuBisCO to standard RuBisCO with annatto extract.

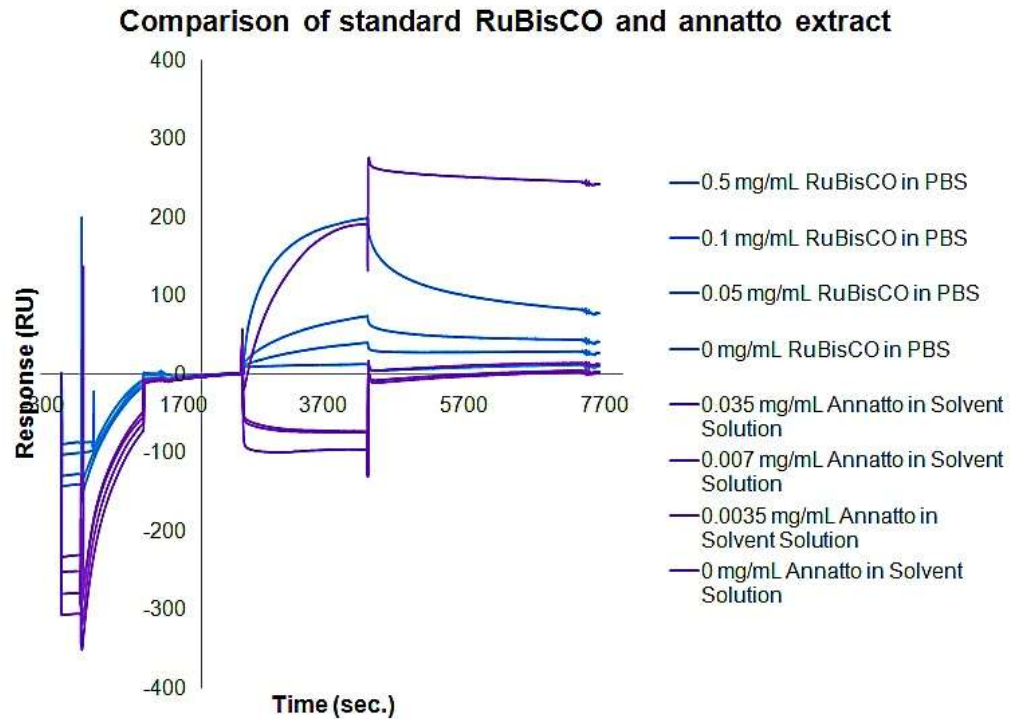


Figure 31: Comparison of standard RuBisCO to annatto extract in solvent solution (calibration 2).

In Figure 30 there was no significant change in the curves for binding of standard RuBisCO (control) when compared to the standard RuBisCO with annatto extract. In Figure 31 there was an interesting curve shape for the highest concentration of annatto extract (0.035mg/mL). This curve has an increase RU which could indicate non-specific binding of the annatto to the surface. Note that this trial was completed twice (data not shown) to ensure that the varying curve shape was a realistic factor of the data and not an anomaly. The high concentration for annatto extract showed the same curve shape each time. A factor that might be involved in the curve shape is that the annatto sample provided was in an unknown liquid and this might cause non-

specific binding at higher concentrations. Furthermore, the concentration of annatto extract may be incorrect due to the liquid evaporating during weighing and so accurately weighing out the annatto extract proved challenging.

The RuBisCO and annatto extract trial was completed with 1:1 kinetic modeling (Figure 32).

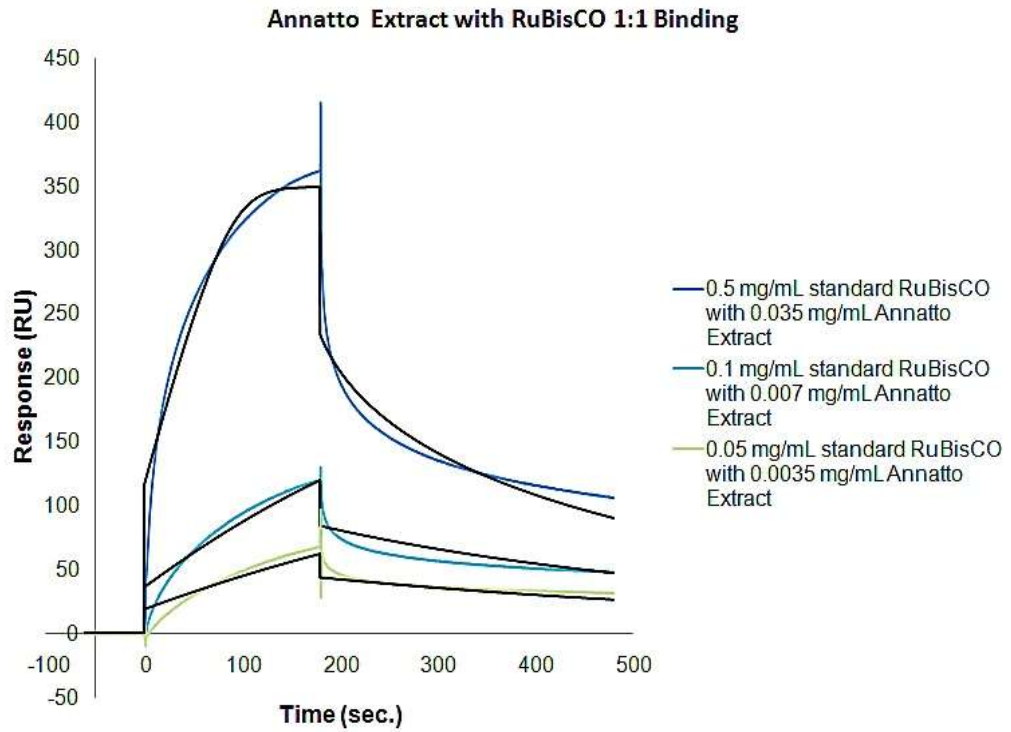


Figure 32: Kinetics for standard RuBisCO with annatto extract using a 1:1 binding model. Colored lines are experimental; black lines are fit.

For analysis 1:1 binding was used and shows good fit. Table 10 shows the results from the kinetic study for 1:1 binding for the standard RuBisCO with annatto extract.

Table 10: Results for Kinetics 1:1 Binding for standard RuBisCO with annatto extract.

Value	Result
Uniqueness	3
R_{\max}	267 RU
Chi^2	97.5
Standard Error	$\text{SE}_{k_a} = 1.3\text{E}4$ $\text{SE}_{k_d} = 0.0016$
Tc (Mass Transfer Coefficient)	1.551E+6
Kinetic Values	$k_a = 1.835\text{E} +5$ (1/Ms) $k_d = 0.02355$ (1/s) $K_D = 1.284\text{E} -7$ M

The kinetic values found for the standard RuBisCO with annatto extract matched well with the previous data from the original kinetic study and the riboflavin study (Table 7 and 9). The K_D value for standard RuBisCO and annatto extract was $1.284\text{E}-7$ M. This value was not significantly different from the original RuBisCO K_D value of $6.002\text{E}-8$ M based on standard error.

The overall goal of SPR was to determine if the kinetics changed when the pigment bound to protein. The kinetics do not change significantly meaning there was no evidence of RuBisCO binding to the pigments or the bound

pigments does not change the kinetics of RuBisCO and antibody binding. The K_D values for each assay, standard RuBisCO ($6.002E-8$ M), standard RuBisCO with riboflavin ($1.028E-7$ M), and standard RuBisCO with annatto extract ($1.284E-7$ M) were all similar within standard error. This was also exemplified in the fact that the curve shapes were similar when comparing the standard RuBisCO control to the samples with each pigment added.

Since SPR cannot provide confirmation of binding, UV-VIS was also used, as an independent means for assessment, to understand if binding to pigments has or has not occurred with standard RuBisCO to each pigment.

5.1.3 UV-Vis

The goal of UV-Vis was to determine if binding occurred between the standard RuBisCO and the pigments. The solutions used are expressed in Table 3. For the heating and freeze thaw cycles the pigments were added directly to standard RuBisCO in PBS at pH 7.9 after the first heating and in the same 1:100 mole ratio. This means that no solubilizing solutions were needed during those experiments. UV-Vis provides a spectrum for each compound studied here and if a protein-pigment complex is formed there may be a shift in spectra or addition/subtraction of a peak, which could represent the binding of protein with pigment. In all of the results presented there was no change in spectra shape, further evidence that binding was not confirmed.

Figure 33 shows standard RuBisCO in PBS at pH 7.9 at various concentrations. Before each trial the standard RuBisCO was run in order to make sure that the stock did not degrade over time as well as ensure that the instrument was working properly and provided consistent results.

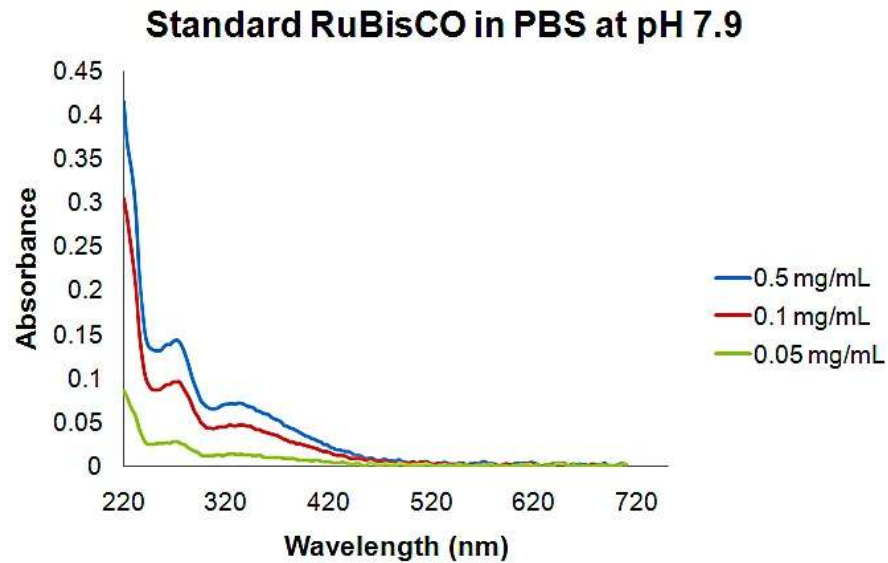


Figure 33: UV-Vis spectra for standard RuBisCO in PBS at pH 7.9 at varying concentrations.

The spectrum found for standard RuBisCO were normalized to assure that peaks did not change position at different concentrations; movement of peaks could indicate aggregation or denaturation of the protein. Figure 34 shows the normalization for standard RuBisCO at the various concentrations, and all spectra align well.

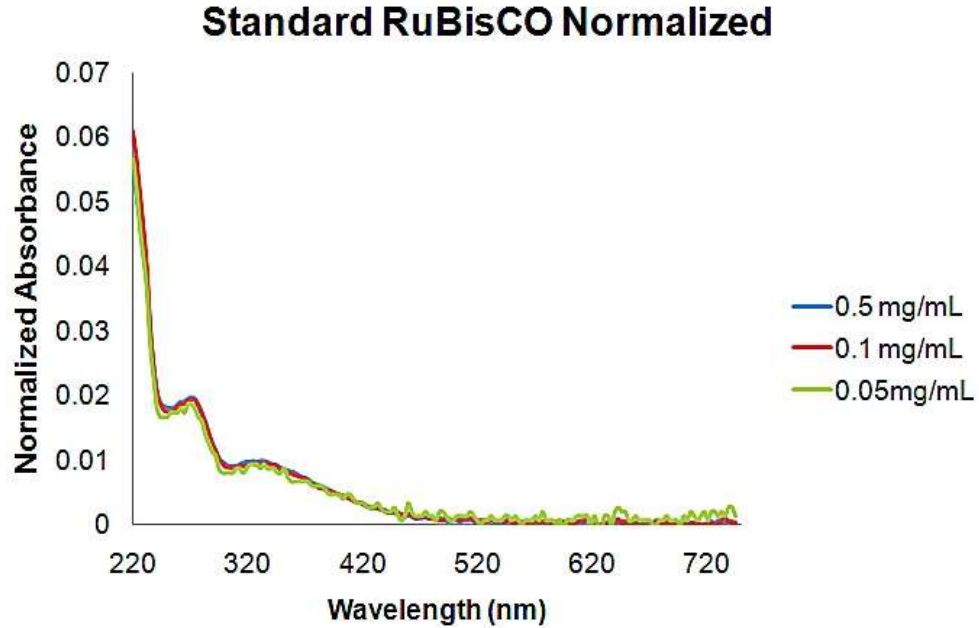


Figure 34: UV-Vis spectra normalized for standard RuBisCO in PBS at pH 7.9.

The first trial was that of riboflavin following samples from Table 3 with no heating or sonication. Calibration one (Figure 35), which was standard RuBisCO in solvent solution (Table 3), shows that the standard RuBisCO was not affected by the solubilizing solution for riboflavin, water. The peak heights match and the position of the peak compared to the wavelength was the same whether in the PBS or in the solvent solution. This was expected since RuBisCO was a water soluble protein as previously mentioned.

Standard RuBisCO in PBS at pH 7.9 and Solvent Solution with Water

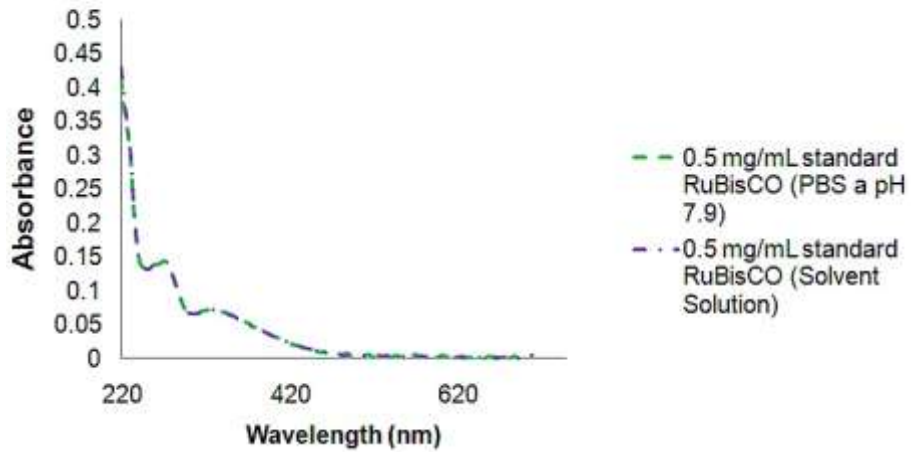


Figure 35: UV-Vis spectra for standard RuBisCO in PBS at pH 7.9 and solvent solution for riboflavin (water).

A comparison of standard RuBisCO with riboflavin in solvent solution to the additive values of standard RuBisCO in PBS at pH 7.9 plus riboflavin in solvent solution (Figure 36 and 37) shows no significant difference in spectra; results were additive.

Comparison of Riboflavin Solutions

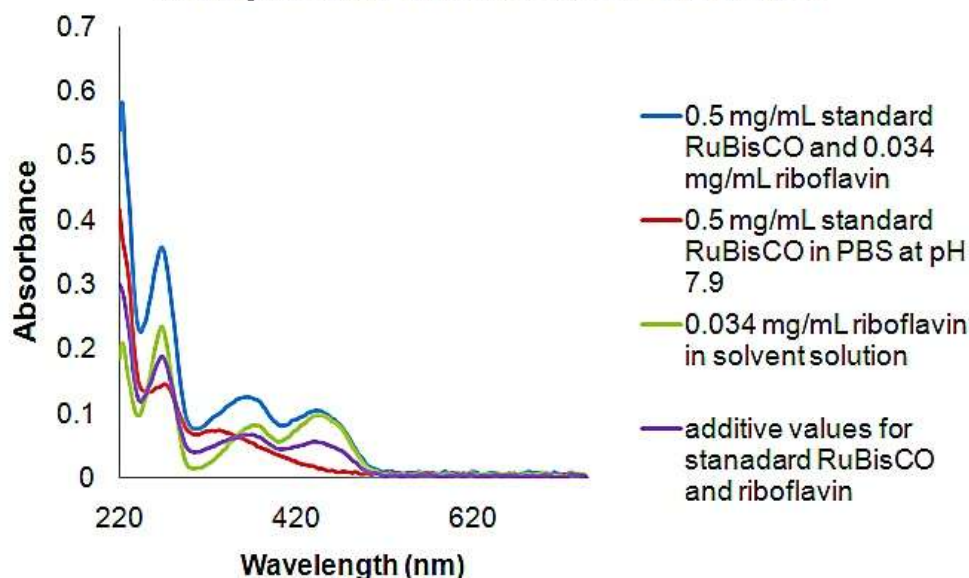


Figure 36: UV-Vis spectra comparing standard RuBisCO in PBS at pH 7.9, riboflavin in solvent solution, standard RuBisCO with riboflavin, and the additive values of standard RuBisCO in PBS at pH 7.9 and riboflavin in solvent solution.

In Figure 36 the resulting spectrum from standard RuBisCO and riboflavin in solvent solution is seen, with a mole ratio of 1:100 (Table 3). The spectrum of standard RuBisCO in PBS at pH 7.9 (red) was added to the spectrum of riboflavin in solvent solution (green) to produce the additive value (purple). The purpose of creating the additive value spectrum was to understand if there was a shift in spectrum produced by binding or if the solutions are both being measured in solution with no binding. The additive values and the spectrum values of standard RuBisCO and riboflavin in solvent solution (complex) were normalized for comparison (Figure 37).

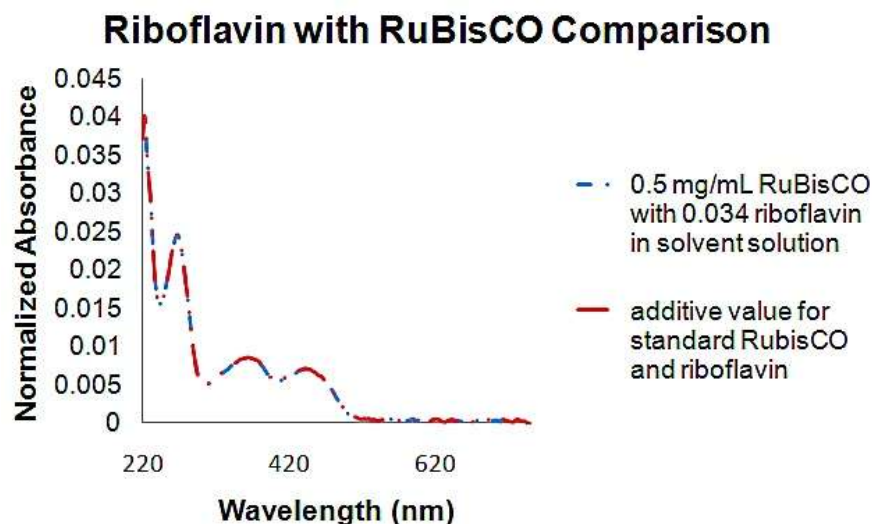


Figure 37: UV-Vis spectra comparing the normalization of standard RuBisCO with riboflavin and the additive values of standard RuBisCO in PBS at pH 7.9 with riboflavin in solvent solution.

When comparing the normalized values for the standard RuBisCO and riboflavin at the 1:100 mole ratio with the additive values it was seen that there was no difference in spectra. This means that binding was not proven or that upon binding no change in spectra resulted. By adding the pigment to standard RuBisCO in solution the results are additive.

The second trial was of annatto extract, which again follows Table 3. Figure 38 shows annatto extract in solvent solution.

Annatto Extract in Solvent Solution (Calibration Two)

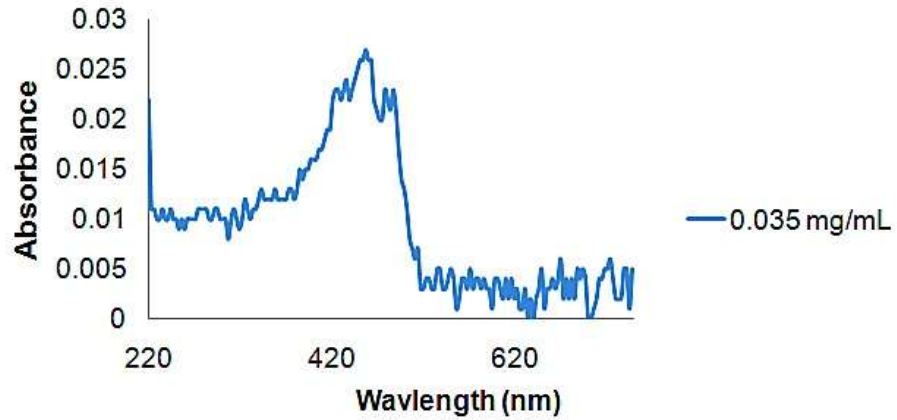


Figure 38: UV-Vis spectra for annatto extract in solvent solution.

The spectra for annatto extract in solvent solution shows extremely low absorbance values. This may be due to the difficulty when measuring the volume of extract, as the solution evaporated quickly. The main peak for annatto extract, while with a low absorbance value, is at the expected wavelength for carotenoids (400 to 500 nm (Britton et al., 2004)).

Figures 39 and 40 show a comparison of standard RuBisCO (0.5mg/mL) with annatto extract (0.035mg/mL) in solvent solution to the additive values of standard RuBisCO in PBS at pH 7.9 (0.5mg/mL) and annatto extract in solvent solution (0.035mg/mL).

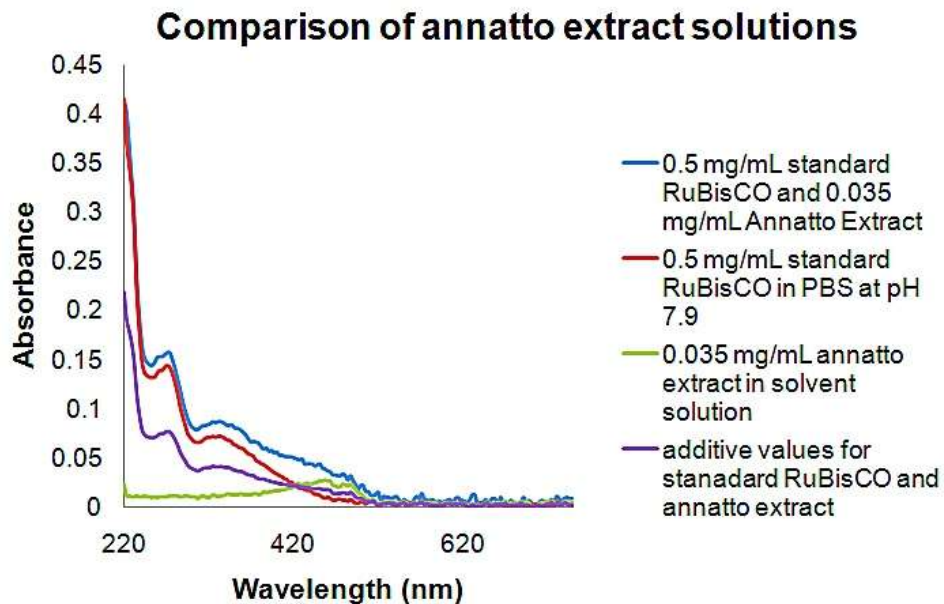


Figure 39: UV-Vis spectra comparing standard RuBisCO in PBS at pH 7.9, annatto extract in solvent solution, standard RuBisCO with annatto extract, and the additive values of standard RuBisCO in PBS at pH 7.9 and annatto extract in solvent solution.

Annatto extract with RuBisCO comparison normalized

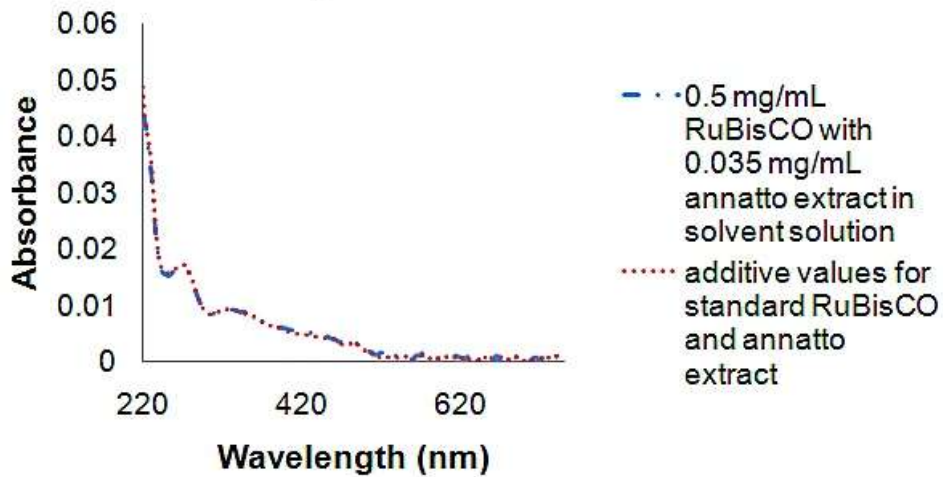


Figure 40: UV-Vis spectra comparing the normalization of standard RuBisCO with annatto extract and the additive values of standard RuBisCO in PBS at pH 7.9 with annatto extract in solvent solution.

There was no difference found when comparing the normalized values for the standard RuBisCO and annatto extract at the 1:100 mole ratio with the additive values of standard RuBisCO in PBS at pH 7.9 and annatto extract in solvent solution. This shows that binding was not proven or upon binding no change in spectra is obtained and that when adding the pigment to standard RuBisCO the results are additive.

Figure 41 shows inconsistent absorbance values for beta-carotene at the same concentration as a result of solubility properties. The spectra provided variable results due to aggregation of beta-carotene in solution which contributed to unreliable readings. Calibration two is beta-carotene in solvent solution which

contains PBS; however, beta-carotene is not water soluble and aggregated in solution. As such, no further studies were performed on this system.

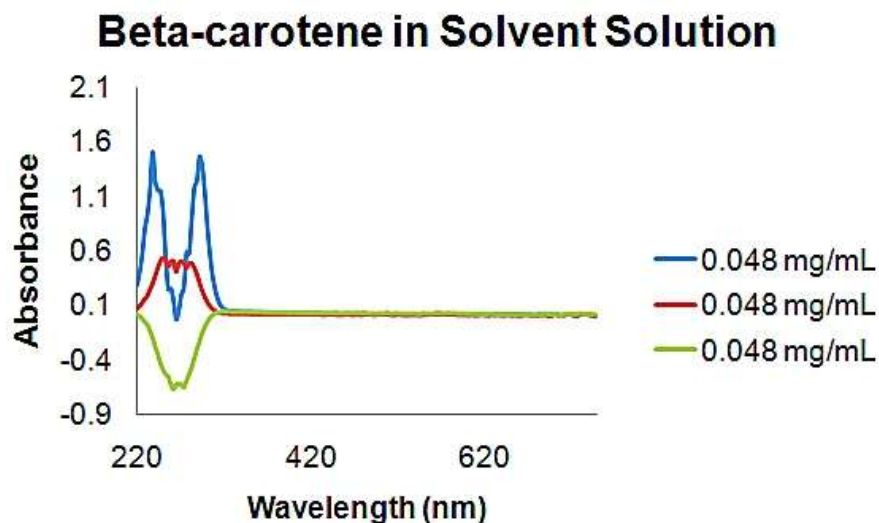


Figure 41: UV-Vis spectra for beta-carotene in solvent solution.

The next studies involving riboflavin were performed with sonication and then heating and freeze thaw cycles. Overall, the sonication and heating with freeze thaw cycles did not change the conclusion that binding was not confirmed. All of the following trials used a concentration of 0.5mg/mL for standard RuBisCO in PBS at pH 7.9 and 0.034mg/mL riboflavin in solvent solution as these values provided appropriate absorbance values.

Figures 42 and 43 show that sonication of standard RuBisCO in PBS at pH 7.9 and riboflavin in solvent solution do not change the spectra produced.

Standard RuBisCO in PBS at pH 7.9

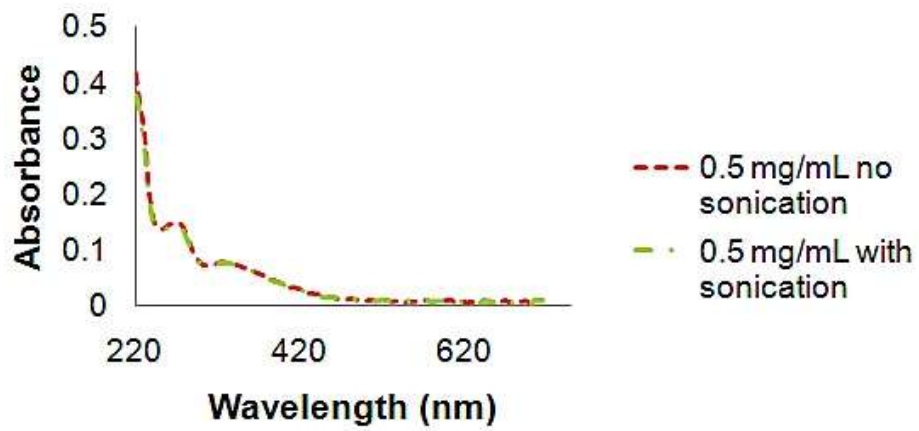


Figure 42: UV-Vis spectra for standard RuBisCO in PBS at pH 7.9 with and without sonication.

Riboflavin in solvent solution comparison with sonication

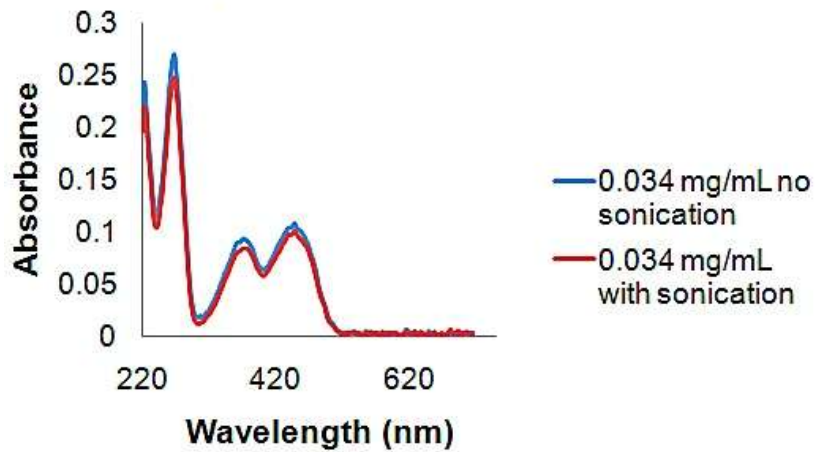


Figure 43: UV-Vis spectra for riboflavin in solvent solution with and without sonication.

Once it was established that sonication would not degrade the signals produced by both standard RuBisCO and riboflavin, the next step was to look at the standard RuBisCO with riboflavin in solvent solution and again compare the results this to see if they were additive or if there was a shift/change in spectra due to sonication potentially promoting binding. Figure 44 shows the comparison between standard RuBisCO with riboflavin in solvent solution with sonication and the additive values of standard RuBisCO in PBS at pH 7.9 with sonication plus riboflavin in solvent solution with sonication.

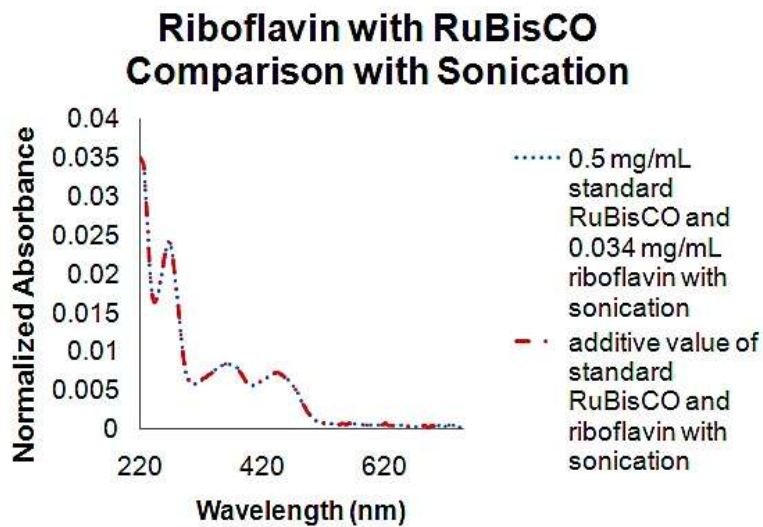


Figure 44: UV-Vis spectra comparing standard RuBisCO and riboflavin with sonication (normalized) to the additive value of standard RuBisCO in PBS at pH 7.9 with sonication plus riboflavin in solvent solution with sonication (normalized).

Sonication did not provide a change in spectra so again binding was not proven or if binding did occur there was no visible change in spectra (Figure 44). The total sonication time was twenty minutes, and it might be that this process was not long enough to promote binding; however, in Booth and Paulsen (1996) sonication only involved 15 minutes of protein sonication prior to adding pigments in order to create a protein-pigment complex of light harvesting pigments.

The heating of riboflavin with standard RuBisCO in PBS at pH 7.9 was experimented with prior to other pigments. The goal was that with heating and freezing the solubility differences would be overcome to help promote binding of pigment with protein (Paulsen et al. 1990). Figure 45 shows the comparison of standard RuBisCO and riboflavin in solvent solution with heating to the additive values of standard RuBisCO in PBS at pH 7.9 plus riboflavin in solvent solution, both with heating.

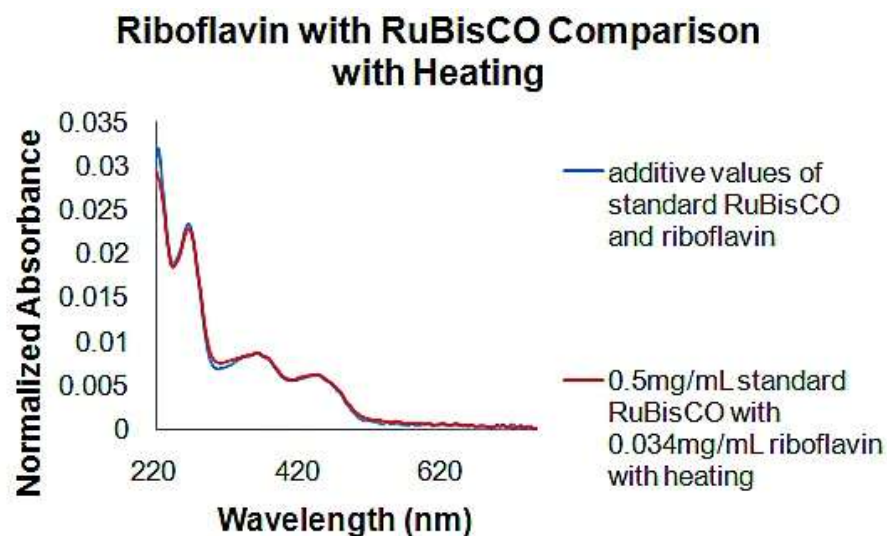


Figure 45: UV-Vis spectra comparing normalization values of standard RuBisCO with riboflavin with heating to additive values of standard RuBisCO in PBS at pH 7.9 and riboflavin in solvent solution both with heating.

Figure 45 shows that heating followed by freeze thaw cycles for initial trials of riboflavin did not provide any variation in spectra peaks; binding is not confirmed in this method.

The final trial using UV-Vis provides the addition of pigments directly to standard RuBisCO in PBS at pH of 7.9. The same concentrations were used to maintain the 1:100 mole ratio. Also, $MgCl_2$ was added in attempts to promote binding, as a metal ion is needed to activate RuBisCO (Reinhard and Höcker, 2005). The pigments were added directly to the standard RuBisCO in PBS at pH 7.9 to avoid variations in solvents and reduce aggregation or RuBisCO. Also, for this study bixin was used in powder form instead of the fast evaporating annatto extract to ensure the correct amount was used.

The RuBisCO was heated before the addition of pigments and then heated once again once the pigments were added. After heating with the pigments in solution, both riboflavin and bixin yielded a solution that did not show aggregation. The beta-carotene mixture did show minimal aggregation, but the aggregation was dispersed throughout the solution and not settling at the bottom. The $MgCl_2$ was challenging to measure because the crystals melted upon exposure to air and after heating it created white clumps at the bottom of the tube. After the three freeze thaw cycles, beta-carotene was not well solubilized, and the $MgCl_2$ samples had white clumps throughout. Figure 46 shows each solution after the heating and freeze thaw cycles.



Figure 46: Solutions for final trial of heating and freeze thaw cycles with pigments added directly to standard RuBisCO in PBS at pH 7.9 for a final concentration of 1:100 mole ratio (protein: pigment), with (1) beta-carotene, (2) beta-carotene with $MgCl_2$, (3) bixin, (4) bixin with $MgCl_2$, (5) riboflavin, (6) riboflavin with $MgCl_2$, and (7) standard RuBisCO .

Beta-carotene is not solubilized in solution (Figure 46 (1)) and as such it does not provide an intense color similar to riboflavin (Figure 46 (5)) since most of the beta-carotene powder aggregated to the bottom. The bixin solution with $MgCl_2$ shows color that was not as bright yellow as without the metal. Riboflavin appears to have the brightest color, and this was due to the fact that it was water soluble and went into solution easily. The heating and freeze thaw cycles did not appreciably help to overcome the solubility issues.

The final heating and freeze thaw cycles did not show any significant change in UV-Vis spectra for any of the samples, meaning that binding was not confirmed. Figure 47 shows the final values normalized to more clearly show shifts or changes in spectra.

Comparison of Standard RuBisCO with Riboflavin after Heating and Freeze Thaw with the Additive Absorbance of Standard RuBisCO and Riboflavin

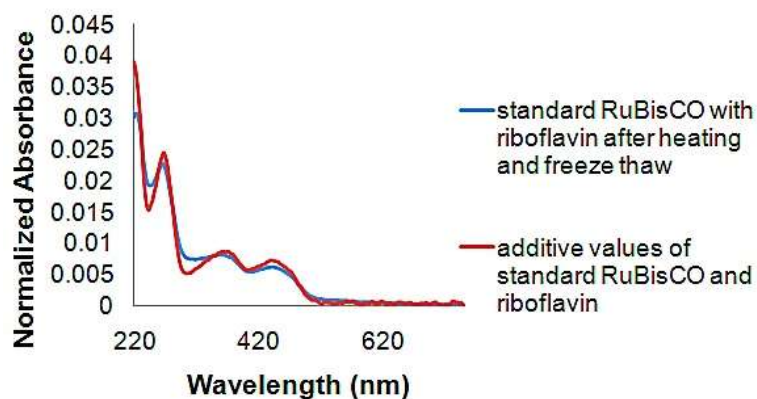


Figure 47: UV-Vis spectra comparing normalized values of standard RuBisCO with riboflavin after heating and freeze thaw cycles to additive values of standard RuBisCO in PBS at pH 7.9 plus riboflavin in solvent solution.

After the heating and freeze thaw cycles for standard RuBisCO and riboflavin there is no significant shift or change in spectra showing again that UV-Vis cannot confirm binding or that if binding did occur it did not result in any change to the spectra produced.

Next beta-carotene along with bixin samples are shown in Figures 48 through 49, with a comparison of the normalized spectra.

**Comparison Standard RuBisCO with
Beta-Carotene After Heating and
Freeze Thaw with the Additive
Absorbance of Standard RuBisCO and
Beta-Carotene**

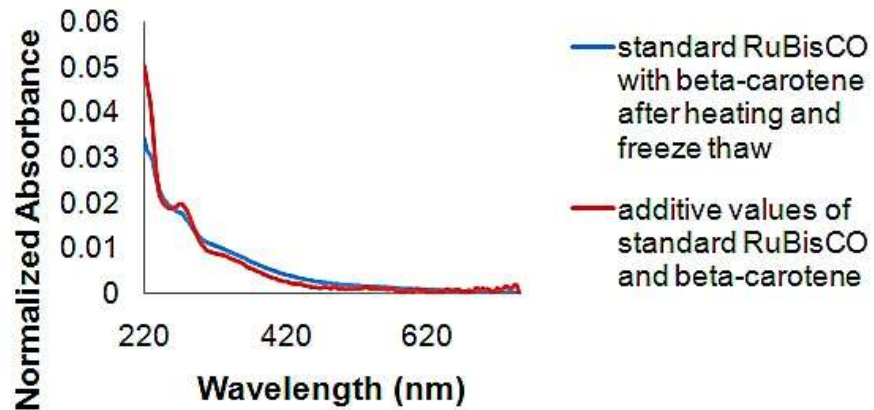


Figure 48: UV-Vis spectra comparing normalized values of standard RuBisCO with beta-carotene after heating and freeze thaw cycles to additive values of standard RuBisCO plus beta-carotene in PBS at pH 7.9.

Comparison of Standard RuBisCO with Bixin After Heating and Freeze Thaw with the Additive Absorbance of Standard RuBisCO and Bixin

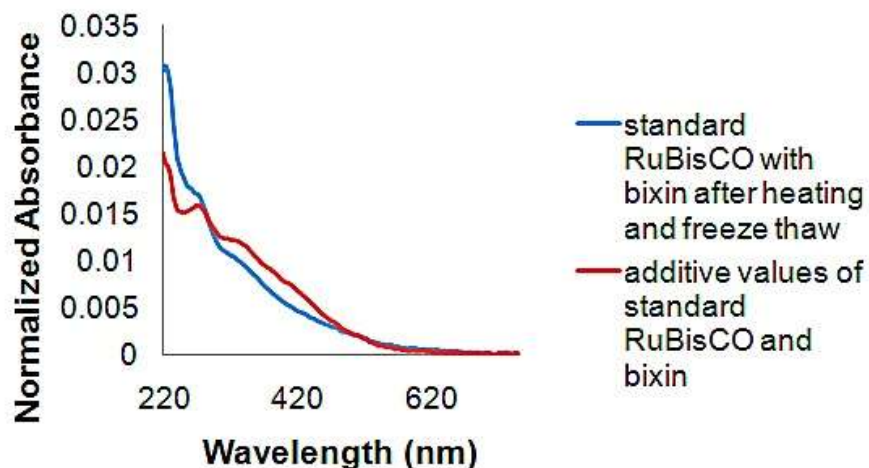


Figure 49: UV-Vis spectra comparing normalized values of standard RuBisCO with bixin after heating and freeze thaw cycles to additive values of standard RuBisCO plus bixin in PBS at pH 7.9.

For this data both the bixin and beta-carotene spectra shapes were measured in PBS at pH 7.9; however, the results do not show that the pigments were measured in solution due to the lack of peaks around 400nm, which are specific for these two pigments. This was due to the fact that the two pigments were not solubilized in PBS and precipitation resulting in inaccurate readings. Figure 50 shows the pigments in both PBS at pH 7.9 as well as in ethanol. When each of these pigments are completely dissolved, they create a yellow color in solution.

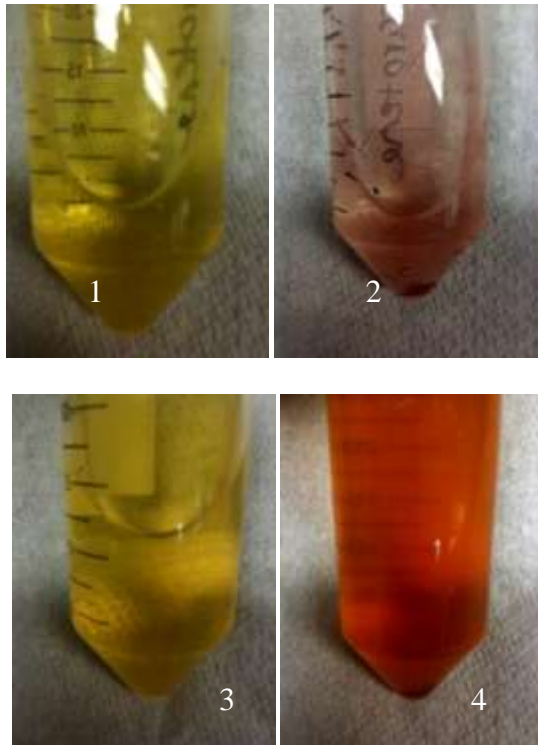
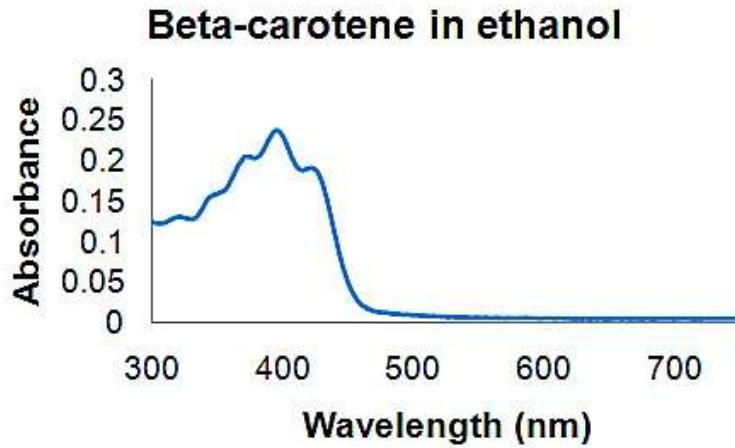
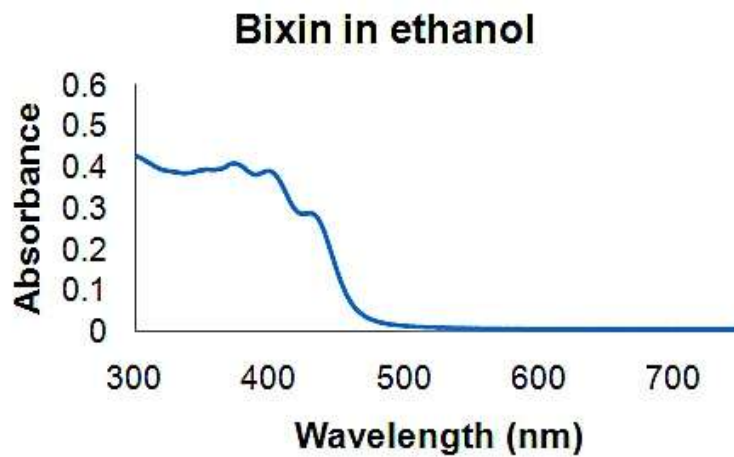


Figure 50: Comparison of bixin and beta-carotene in PBS at pH 7.9 and ethanol with (1) beta-carotene in ethanol, (2) beta-carotene in PBS, (3) bixin in ethanol, (4) bixin in PBS.

Both pigments are soluble in ethanol and so they produce the expected spectra with peaks for carotenoids between 400 and 500 nm (Britton et al., 2004) as seen in Figures 51(a) (beta-carotene) and 51(b) (bixin).



(a)



(b)

Figure 51: (a) UV-Vis results for beta-carotene in ethanol, (b) UV-Vis results for bixin in ethanol.

All data combined indicate that the heating and freeze thaw cycles did not help the pigment to overcome the solubility issues and therefore the results cannot prove or disprove binding.

The final results to review are the reactions with $MgCl_2$ added. $MgCl_2$ is added in solution because a metal ion is needed in order to enhance RubisCO's activity. The goal for this reaction was to possibly promote binding by the increased activity of RuBisCO. Since the results for bixin and beta-carotene without $MgCl_2$ show that they are not successfully solubilized in solution their results are not included. Riboflavin shows no difference when added to standard RuBisCO in PBS at pH 7.9 with or without $MgCl_2$ after heating and freeze thaw cycles (Figure 52).

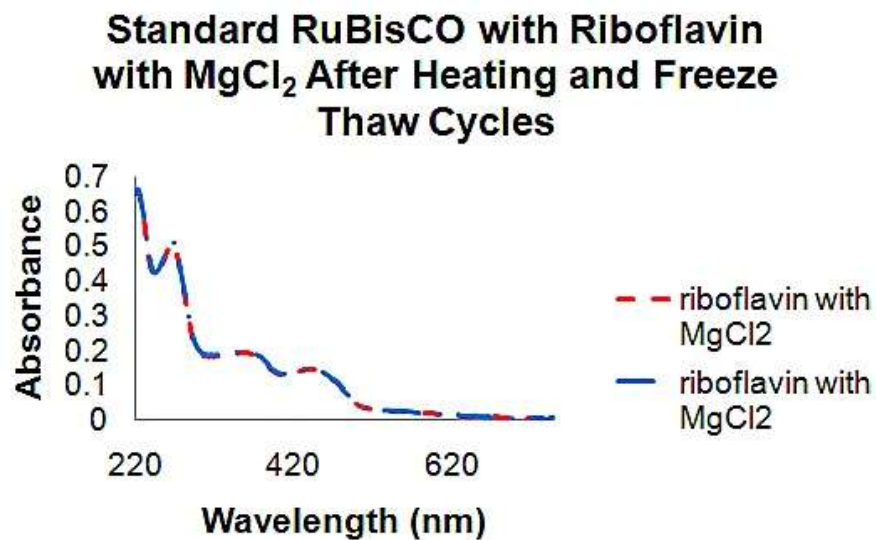


Figure 52: UV-Vis results comparing standard RuBisCO with riboflavin after heating and freeze thaw cycles with and without $MgCl_2$.

Overall, for binding interrogation Raman spectroscopy, SPR, and UV-Vis could not indicate that binding occurred between standard RuBisCO and each pigment. Raman was not able to be used with the standard RuBisCO due to

high fluoresces. SPR showed that standard RuBisCO kinetics could be determined for binding to anti-RuBisCO (mouse monoclonal) but that when the pigments were added in solution the kinetics did not change significantly. UV-Vis offered results that did not confirm or deny binding or creation of protein-pigment complex. The fact that the carotenoid pigments chosen could not be solubilized in solution offered an increased challenge and made it difficult to compare spectra. Riboflavin, which was soluble in water, did not offer any information that confirmed binding even with heating and freeze thaw trials or sonication.

5.2 Extraction

Freezing Tobacco Tissues

The tobacco plants were harvested in the August 2009 and then immediately and successfully frozen in liquid nitrogen stored at -80°C. It was imperative that the plant material be stored in a manner that would maintain the protein structure so that experiments could be run throughout the year, rather than limit research to the main harvesting time for the tobacco crop in the summer to early fall. The frozen pellets of tobacco extract in were then ground down to a fine powder as needed. This powder was then further used in assays to extract protein with the paramagnetic antibody beads.

5.3 Purification

5.3.1 Confirmation of Protein using Paramagnetic Antibody Beads

SDS-PAGE and Western Blot along with Silver Stain were used in order to confirm the presence of RuBisCO protein in the tobacco powder extraction and purification.

The first results were of the initial extraction using Extraction Buffer A (Figure 53).

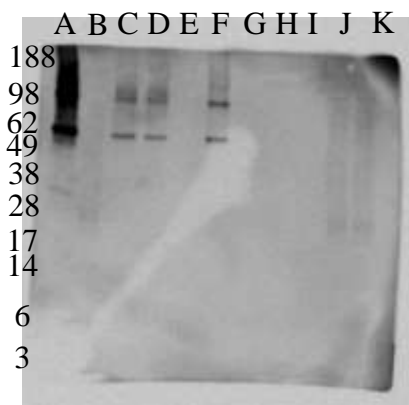


Figure 53: Results for Western Blot and stained membrane, (A) standard RuBisCO (1mg/mL); (B) molecular weight marker; (C) standard RuBisCO with beads before wash; (D) standard RuBisCO with beads after, no wash; (E) standard RuBisCO with beads after, with wash; (F) standard RuBisCO with beads, final; (G) tobacco supernatant with beads after, no wash; (H) tobacco supernatant with beads after, with wash; (I) tobacco supernatant with beads, final; (J) molecular weight marker; (K) molecular weight marker.

For this run it can be seen that the control, lane A (Figure 53), of 1mg/mL standard RuBisCO shows that the antibody (anti-RuBisCO, spinach, monoclonal) used binds well to the protein of interest. Lanes B, J, and K are the molecular weight markers. Lane F shows the final, after incubation and washing is complete, for the standard RuBisCO with the beads, and this provides an example that the beads do extract the standard RuBisCO protein. Lanes C and D show standard RuBisCO on the beads with no washes, so RuBisCO is expected to be present. Lane E shows the supernatant after washing which should contain no RuBisCO, as all the protein should be bound to the beads, which was accomplished. Rows G through I are the tobacco extraction lanes, and these do not show any RuBisCO present. At this point the Extraction Buffer B was developed in order to help optimize the extraction and obtain RuBisCO extraction from tobacco. Extraction Buffer B had more Triton, and more detergent can help protein solubilized into solution. Also, there was more NaCl added to provide a net negative environment that can make the proteins more likely to solubilized. The pH of each extraction buffer was adjusted to 7.9, as this was the most favorable pH to have RuBisCO in solution based on previous studies with aggregation as well as details provided when ordering standard RuBisCO (Sigma).

The next run involves the use of both Extraction Buffers A and B (Table 2). For this part of the experiment both the pellet and the supernatant from the extraction were used in order to understand where the RuBisCO protein may

be present from the tobacco powder. Figure 54 shows the results of the stained Western.

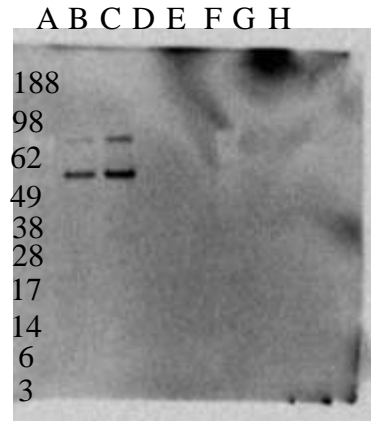


Figure 54: Results for Western Blot and stained membrane A molecular weight marker; (B) standard RuBisCO control (0.5 μ L); (C) standard RuBisCO control (1 μ L); (D) Pellet A; (E) Pellet B; (F) Molecular weight marker; (G) supernatant A; (H) supernatant B.

Figure 54 shows lanes B and C with standard RuBisCO, control, worked well with the antibody (anti-RuBisCO spinach, monoclonal) used to label the protein of interest. However in lanes D, E, G, and H there was no RuBisCO found in any part of the tobacco powder extraction.

The standard RuBisCO was working well with the beads; however, the tobacco powder extraction was not showing binding to the beads after being homogenized with the Polytron to break up as much of the cell as possible to release the RuBisCO. The antibody initially used was a spinach mouse

monoclonal antibody for the large subunit of RuBisCO. This antibody was used for SPR and there was hope of it also working for tobacco protein; however no cross reactivity of this antibody between species was seen due to a in the lack of any protein bands from tobacco samples when incubated with beads on the gel (Figure 54 (D-H)). The standard RuBisCO (spinach) samples worked well with the beads and help to confirm the methodology chosen (Figure 53, (F)). Another antibody was chosen, RbcL polyclonal anti-rabbit because it was stated to be specific for all plant and algal samples (www.agreseria.com).

Before the RbcL polyclonal antibody was used, the tobacco extract was run through methanol precipitation to determine if there was in fact protein present for the paramagnetic antibody conjugated beads to capture. The ground tobacco powder was homogenized with the Polytron in both extraction buffers A or B and then run through a methanol precipitation procedure with results shown via poncaeu stain (dye electrostatically binds to protein) (Figure 55).

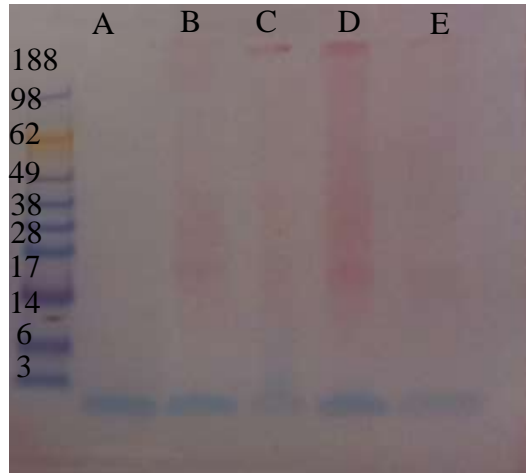


Figure 55: Poncaeu stain of samples from tobacco powder extraction with methanol extraction: (A) standard RuBiSCO; (B) supernatant A; (C) pellet A; (D) supernatant B; (E) pellet B.

The results from Figure 55 showed that protein was present in the ground tobacco powder after methanol precipitation. The final ground tobacco powder when used with the beads did not go through methanol extraction, this method was solely used to check the protein content to ensure that the extraction buffer with ground tobacco powder did contain protein. In lane D it can be seen that extraction buffer B provides a higher level of overall protein, so for all future extractions from the ground tobacco powder, extraction buffer B was used. Also, the Polytron for these samples was used at the higher level of 6 to 7 to help break up all ground tobacco powder and release all protein present.

The supernatant from extraction buffer B was compared to methanol precipitation of supernatant with dilutions (Figure 56).

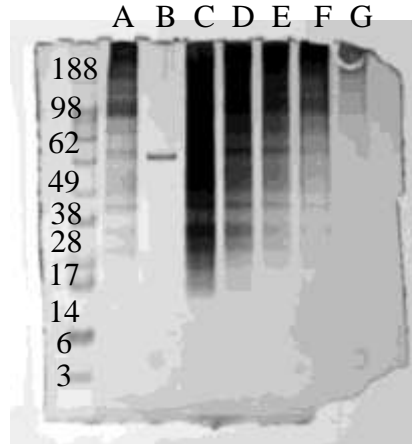


Figure 56: Silver stain comparison of supernatant from extraction buffer B with methanol extraction and dilutions, (A) supernatant from extraction with buffer B; (B) standard RubisCO; (C) supernatant with methanol extraction; (D) 15 μ L supernatant with methanol extraction in loading buffer (1X) plus 5 μ L loading buffer (1X); (E) 10 μ L supernatant with methanol extraction in loading buffer (1X) plus 10 μ L loading buffer (1X); (F) 5 μ L supernatant with methanol extraction in loading buffer (1X) plus 15 μ L loading buffer (1X); (G) 1 μ L supernatant with methanol extraction in loading buffer (1X) plus 19 μ L loading buffer (1X).

Figure 56 shows that there were bands in the supernatant that match the standard RuBisCO, 56 kDa (lane B), as rows A and C all have dark stains in a similar region as the standard. The methanol precipitation was no longer

needed because the supernatant without methanol precipitation contained sufficient protein.

It was confirmed that the supernatant contains the protein of interest. The goal was then to determine the amount of supernatant needed to not cause the gel to overload as well as ensure that the antibody selected (RbcL, anti-rabbit polyclonal) reacts with tobacco RuBisCO. Figure 57 shows the western blot results for standard RuBisCO followed by dilutions of supernatant in loading buffer (1X).

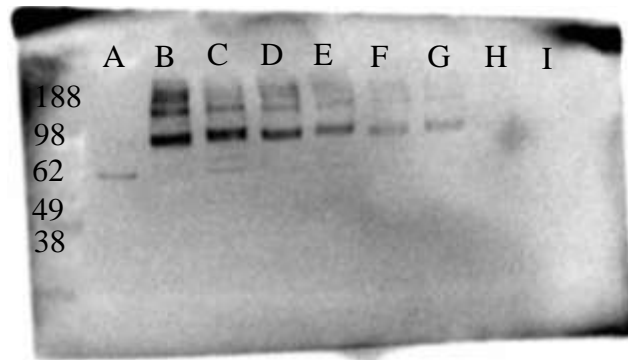
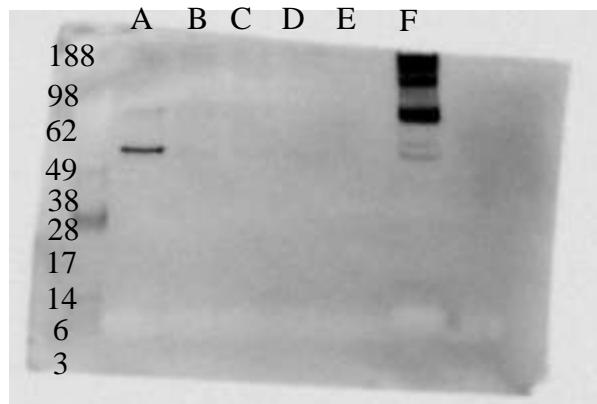


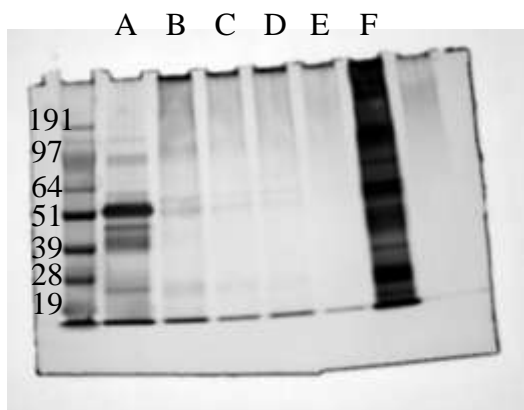
Figure 57: Western results for (A) standard RubisCO; (B) 15 μ L supernatant with 5 μ L loading buffer (1X); (C) 15 μ L supernatant with 3 μ L loading buffer (1X) and 2 μ L reducing agent (10X); (D) 10 μ L supernatant with 10 μ L loading buffer (1X); (E) 10 μ L supernatant with 8 μ L loading buffer (1X) and 2 μ L reducing agent (10X); (F) 5 μ L supernatant with 15 μ L loading buffer (1X); (G) 5 μ L supernatant with 13 μ L loading buffer (1X) and 2 μ L reducing agent (10X); (H) 1 μ L supernatant with 19 μ L loading buffer (1X); (I) 1 μ L supernatant with 17 μ L loading buffer (1X) and 2 μ L reducing agent (10X).

The results from Figure 57 show that the reducing agent does not affect the migration of the tobacco supernatant because there was no band shift. The reducing agent, which helps to break apart proteins further, was added in order to help migration because of all the debris present in the supernatant. Also, this shows that the antibody was not reacting with the RuBisCO present in tobacco, as none of the bands correspond with the standard RuBisCO band around 56 kDa (only faint bands in lane C). This may be because the tobacco supernatant had too much debris and other proteins present that it was not able to migrate as fast as the standard RuBisCO. So, the dark lower band in the dilutions could be tobacco RuBisCO, or the antibody may not be specific for tobacco RuBisCO.

The final step in using the beads was to determine if the conjugated beads can capture the tobacco RuBisCO, and this was determined with both Western blot results as well as silver staining. Figure 58 shows the results of incubating 1mL of the supernatant with 25 μ L of the conjugated beads (RbcL anti-rabbit, polyclonal for RuBisCO).



(a)



(b)

Figure 58: (a) Western blot results for standard RuBisCO followed by dilutions of beads and supernatant not incubated in beads and (b) Silver stain results. (A) standard RuBisCO; (B) 20 μ L beads incubated in supernatant; (C) 15 μ L beads incubated in supernatant with 5 μ L loading buffer, 1X; (D) 10 μ L beads incubated in supernatant with 10 μ L loading buffer, 1X; (E) 5 μ L beads incubated in supernatant with 15 μ L loading buffer 1X; (F) supernatant from ground tobacco powder.

In Figure 58 (a) and (b) the standard RuBisCO showed up with a clear band; however, the beads incubated in supernatant do not show any band. The supernatant (Figure 58 (b), F) showed again that there was protein present. Figure 58(b) for the silver stain showed a strong band for the standard RuBisCO and also showed in B through E that there was protein present in the supernatant with beads but that the antibody for the Western was not picking up the bands (faint bands in lane F, Figure 58(a)). This means that the antibody was most likely not specific for the tobacco RuBisCO.

The next step was to understand if the antibody had been conjugated to the beads since the Western did not show any bands from tobacco supernatant. Figure 59 shows that the beads were, in fact, conjugated with antibodies.

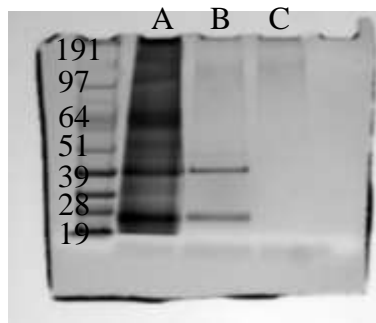
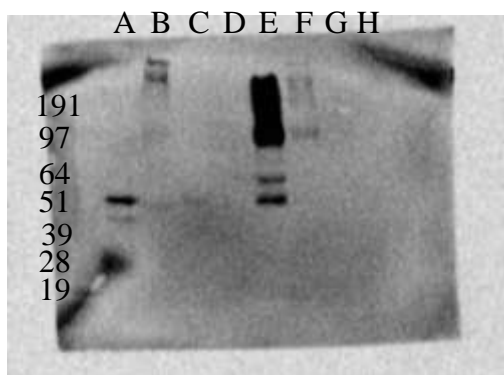


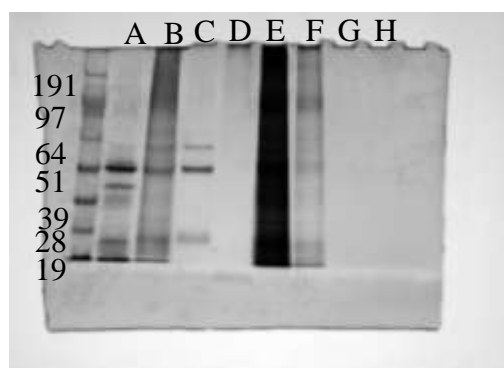
Figure 59: Silver stain results for bead conjugation study, (A) supernatant with beads conjugated (10mg/mL RbcL anti-rabbit, polyclonal for RuBisCO); (B) PBS at pH 7.9 with beads conjugated (10mg/mL RbcL anti-rabbit, polyclonal for RubisCO); (C) PBS at pH 7.9 with non-conjugated beads.

A main point from Figure 59 is that there was a difference between the conjugated beads and non-conjugated beads. In order to understand that the antibody had been conjugated this gel was used to show a difference between conjugated beads and non-conjugated beads. In lanes A and B the bands (39 kDa and 25 kDa) show protein was present (antibody) and lane C there was no protein present (no bands) meaning there was no antibody; confirming that the conjugation of the beads worked well. This means that the antibody was present on the beads when it was used with the supernatant from the ground tobacco powder. Also, the supernatant was proteinaceous and with silver staining does show a band matching with the standard RuBisCO, so it was possible that again the antibody was not specific for tobacco RuBisCO.

The final trial with the supernatant and beads shows unique results. Figure 60 (a) shows that the antibody (RbcL, anti-rabbit, polyclonal for RuBisCO) was not specific for tobacco RuBisCO before unfolding. Figure 60 (b) shows the silver stain of the final trial.



(a)



(b)

Figure 60: (a) Western blot results for final bead and supernatant trials and (b) silver stain results. (A) standard RuBisCO; (B) supernatant with conjugated beads (10mg/mL anti-rabbit, polyclonal for RuBisCO); (C) PBS at pH 7.9 with conjugated beads (10mg/mL anti-rabbit, polyclonal for RuBisCO); (D) PBS at pH 7.9 with non-conjugated beads; (E) supernatant; (F) supernatant 1:10; (G) supernatant 1:100; (H) supernatant 1:1000.

The western results for this study show the supernatant contains RuBisCO from tobacco (Figure 60(a),(E)) and has strong bands. The antibody used for the western showed RuBisCO present as the bands line up with the standard RuBisCO (56 kDA). The main challenge was that the beads with supernatant

do not show any bands matching with standard RuBisCO. This could be due to the fact that the supernatant was unfolded (during heating before SDS-PAGE) in lane E (Figure 60(a)) and then exposed to the antibody, but with the beads the protein is folded and exposed to the antibody. The antibody (RbcL) contains an epitope that was specific to a peptide that is buried inside the protein (J. Porankiewicz-Asplund, personal communication) before unfolding and thus heating and denaturation opens the tertiary structure allowing the antibody to bind. So, when the protein was folded in the supernatant it could not bind to the antibody on the beads because the peptide was not presented in a manner that it could reach; however, when the supernatant was denatured and then run on Western blot the antibody could clearly bind the peptide, and thus the bands for the protein are seen. The company (www.agrisera.com) that produces the antibody provides an image of Western blot results using the antibody RbcL, anti-rabbit, polyclonal for RuBisCO that shows a variety of affinity to different plants (Figure 61).

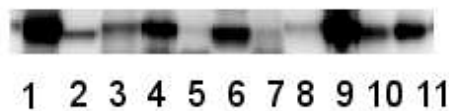


Figure 61: Western blot results from (1) *Spinacia oleracea*; (2) *Synechococcus* PCC 7942; (3) *Cyanophora paradoxz*; (4) *Heterosigma akashiwo*; (5) *Thalassiosira pseudonana*; (6) *Euglena gracilis*; (7) *Micromonas pusila* (8) *Chlamydomonas reinhardtii* (9) *Prophyra* sp; (10) *Gonyaulax polyedra*; (11) *Emiliana huxleyi*. Prepermission from www.agrisera.com.

The Western blot shown in Figure 61 showed that the antibody has varying affinity potentially due to the peptide sequence being buried inside of the RuBisCO molecule. In lanes 5, 7, and 8 it was difficult to make out the bands for RuBisCO.

The other main challenge was that there was increased background noise in the samples with supernatant as seen in Figure 56 lanes B and E through H. The noise (lipids, sugars, or other proteins) could result in interference with the beads conjugated with the antibody (RbcL) and preventing binding to the protein of interest. When the supernatant was diluted the background noise is reduced, but it also reduced the overall level of protein that could be seen (Figure 56 lanes E and F). This means that even if the noise is removed, it is unlikely that the tobacco RuBisCO will be left at a high enough concentration to detect and bind to the antibody conjugated beads.

The next step in research is to continue screening antibodies to find one that works well with tobacco RuBisCO, to provide strong darkly color bands of protein at 56 kDa similar to the standard RuBisCO, and can bind the protein to the conjugated beads to provide future purification and use of the protein.

5.4 Recommendations to Continue Research

5.4.1 Binding Promotion

Originally it was thought that since RuBisCO is present in the chloroplast and it is difficult to remove any green coloring completely that the protein was actively bound to the pigment; however, chlorophyll binds and helps to fold light harvesting proteins. In fact, denatured light harvesting protein, such as LHC II, does not refold unless the pigment [chlorophyll] are present (Booth et al. 2001). While RuBisCO does not bind chlorophyll itself, it may be possible to use this similar idea to promote the refolding of the protein in order to bind the pigments of interested by the use of a chaperone. A chaperone, while not necessarily a protein itself, helps to organize the protein structure that it is interacting with to provide function and correct or reorganized folding (Sadava, 2011). It was seen that with solely RuBisCO and each pigment in solution binding did not occur or the instruments used to measure the binding did not show that it occurred. Sonication did not help to increase binding and freezing and heat thaw cycles (used to create protein-pigment complexes with chlorophyll and LHCII (Paulsen et al. 1990)) did not help to form protein-pigment complexes with RuBisCO and the pigments chosen and overcome solubility differences. The major challenge that needs to be addressed is the fact that both beta-carotene and annatto extract are not water soluble, whereas RuBisCO is water soluble. This means that if the pigments are dissolved in solution the RuBisCO aggregates out and binding cannot occur.

If the issue of solubility was the only challenge then binding would have been achieved with water soluble riboflavin, but this was not the case. Help is needed to promote binding of these pigments. Apetri and Horwich (2008) show that a molecular chaperon (GroEL) is needed in order to increase the reactivity and folding of RuBisCO, and as seen before in Booth et al., (2001) the light harvesting proteins will not fold correctly without pigments present. Overall, the methods used of adding the pigments in solution with RuBisCO followed by mixing, sonication, or heating and freeze thaw cycles, do not result in binding or confirmation of binding with the instruments used and further trials are needed to understand how these pigments interact with the protein. By understanding how the proteins and pigments interact it might be possible to choose a chaperon that will help to promote binding.

5.4.2 Completion of Protein Purification

A secondary focus of the research was extracting the tobacco RuBisCO directly from tobacco leaves in a manner that provided purified protein that was not denatured in order to keep the stability of the protein and offer a pure sample to bind to the pigments of interest. A method to extract proteinaceous liquid from tobacco leaves was developed; however, removing RuBisCO from this solution was not accomplished due to a lack of cross reactivity among the antibodies chosen. The first antibody was specific only for spinach RuBisCO and demonstrated that the method of using paramagnetic antibody beads will be useful to single out tobacco RuBisCO if an appropriate antibody can be

chosen. The second antibody used was said to have a general specificity for plants and algae; however, this antibody also did not prove to be specific for tobacco. The peptide of interest for this second antibody is buried inside of the RuBisCO protein, so when the protein was unfolded it reacted well with the antibody. The next step will be to continue screening antibodies and to start with the antibody mentioned in Foyer et al., 1993. This article offers an antibody that is proven to work with tobacco RuBisCO. After the antibody is found to work with tobacco RuBisCO on the paramagnetic beads, a method to remove the protein will need to be optimized.

Chapter 6: Conclusion

The foci of the present studies include the feasibility of binding RuBisCO protein to the pigments chosen (riboflavin, beta-carotene, and annatto extract [bixin]) as well as extracting a pure protein from tobacco to provide alternative uses for the ill-imaged crop. The attempt to form RuBisCO-pigment complexes was not successful or not be confirmed with the tools used to measure the formation, due mainly to the limited sites available for binding, which could be attributed to the folding of protein during the extraction and purification of RuBisCO. A better understanding of how to expose the sites responsible for pigment binding as well as how each of the pigments interacts with RuBisCO is needed in order to promote and enhance binding. A method to extract RuBisCO protein from tobacco crops was developed with a highly proteinaceous solution from tobacco leaves. While such an approach was proven feasible; however, further research with antibody screening is needed in order to select the most effective antibody to optimize the extraction methods that could reach a final pure protein from the tobacco plant. The ability of RuBisCO to bind antioxidative pigments is of interest to the food industry, if effective binding can be established. Furthermore, the stability of the protein-pigment complex will need to be assessed to understand how it might be utilized in food products to provide enhanced color, antioxidants, and protein to the consumer.

Bibliography

- Biacore (2002) An Introduction to Biacore's SPR Technology. Web. 25 June 2010.
<http://www.rci.rutgers.edu/~longhu/Biacore/pdf_files/SPR_Technology_Brochure.pdf>
- Agte V, Kirtan T, Sangeeta M, Ashwini H, & Shashi C (2002) Vitamin profile of cooked foods: how health is the practice of ready-to-eat foods? *International Journal of Food Sciences and Nutrition*, 53, 197-208.
- Andersson I, Ann-Christin T, Eila CZ, & Branden CI (1983) Crystallization and Preliminary X-ray Studies of Spinach Ribulose 1, 5-Bisphosphate Carboxylase/Oxygenase Complexed with Activator and a Transition State Analogue. *The Journal of Biological Chemistry*, 258, 14088-4090.
- Apetri AC & Horwich AL (2008) Chaperonin Chamber Accelerates Protein Folding through Passive Action of Preventing Aggregation. *Proceedings of National Academy of Science*, 105.45, 17351-7355.
- Baker TS, Se WS, & Eisenberg D (1977) Structure of Ribulose-1, 5-bisphosphate Carboxylase-oxygenase. *Proceedings of National Academy of Sciences of the USA*, 74.3, 1037-041.
- Britton G, Liaaen-Jensen S, & Pfander H (2004) *Carotenoids Handbook*. Boston: Birkhäuser Verlag.
- Booth PJ & Paulsen H (1996) Assembly of Light-Harvesting Chlorophyll A/b Complex in Vitro. Time-Resolved Fluorescence Measurement. *Biochemistry*, 35.16, 5103-108.
- Booth PJ, Templer RH, Meijberg W, Allen SJ, Rachael C, & Mark L (2001) *In Vitro*

- Studies of Membrane Folding Proteins. *Critical Reviews in Biochemistry and Molecular Biology* 36.6, 501-603.
- Burri BJ (1997) Beta-Carotene and Human Health: A Review of Current Research. *Nutrition Research* 17.3, 547-80.
- Chang PH, Sakano K, Singh S, & Wildman SG (1972) Crystalline Fraction I Protein: Preparation in Large Yield. *Science*, 176.4039, 1145-146.
- Darago, Connie (2000) Maryland Tobacco Futures. *Bay Weekly Online* 8. Web 12 Jan. 2009 <http://www.bayweekly.com/year00/issue8_13/lead8_13.html>.
- De La Cruz-Cañizares J, Doménech-Carbó MT, Gimeno-Adelantado JV, Mateo-Castro R, & Bosch-Reig F (2004) Suppression of Pigment Interference in the Gas Chromatographic Analysis of Proteinaceous Binding Media in Paintings with EDTA. *Journal of Chromatography A*, 1025, 277-85.
- Delgado-Vargas F & Paredes-Lopez O (2003) *Natural colorants for Food and Nutraceutical Uses*. New York: CRC.
- Eitenmiller RR, Ye L, & Landen WO (2008) *Vitamin Analysis for the Health and Food Sciences*. Boca Raton: CRC.
- Fashui H, Chao L, Lei Z, Xuefeng W, Kang W, Weiping S, Shipeng L, Ye T, & Guiwen Z (2005) Formation of Complexes of Rubisco-Rubisco Activase from La^{3+} , Ce^{3+} Treatment Spinach. *Science in China Series B: Chemistry*, 48.1, 67-74.
- Fu H, Machado PA, Kratochvil RJ, Wei CI, & Lo YM (2010) Recovery of nicotine-free proteins from tobacco leaves using phosphate buffer system under controlled conditions. *Bioresource Technology*, 101(6), 2034-2042.

- Foyer CH, Nurmi A, Dulieu H, & Parry MJ (1993) Analysis of Two Rubisco-deficient Tobacco Mutants, H7 and Sp 25; Evidence for the Production of Rubisco Large Subunits in the Sp25 Mutant That Forms Clusters and Are Inactive. *Journal of Experimental Botany*, 44, 1445-452.
- Heras H, Dreon MS, Ituarte S, & Pollero RJ (2007) Review: Egg carotenoproteins in neotropical Ampullariidae (Gastropoda: Arquitaenioglossa). *Comparative Biochemistry and Physiology, Part C* 146, 158-67.
- Holler C & Zhang C (2008) Purification of an Acidic Recombinant Protein from Transgenic Tobacco. *Biotechnology and Bioengineering*, 99, 902-09.
- Ingle JD & Crouch SR (1988) *Spectrochemical Analysis*. Upper Saddle River, NJ: Prentice Hall.
- Johal S, Bourque DP, Smith WW, Suh SW, & Eisenberg D (1980) Crystallization and Characterization of Ribulose 1, 5-Bisphosphate Carboxylase/Oxygenase from Eight Plant Species. *The Journal of Biological Chemistry*, 255.18, 8873-880.
- Liu RH (2003) Health benefits of fruit and vegetables are from additive and synergistic combinations of phytochemicals. *American Journal of Clinical Nutrition*, 78(3), 517S-520.
- Kanjilal PB & Singh RS (1995) Agronomic evaluation of annatto (*Bixa orellana* L.). *Journal of Herbs, Spices, and Medicinal Plants*, 3(3), 13-17.
- Mimuro M & Tanaka A (2004) The in vivo and in vitro reconstitution of pigment-protein complexes, and its implication in acquiring a new system. *Photosynthesis Research*, 81, 129-37.

- Montanari L, Fantozzi P, & Pedone S (1993) Tobacco Fraction 1 Protein (F1P)
Utilization for Oral or Enteral Feeding of Patients. I: Heavy Metal Evaluation.
Journal of Food Science and Technology, 36.3, 259-63.
- Nienhaus GU (2005) Protein-ligand Interactions: Methods and Applications. Totowa,
N.J.: Humana.
- Nisha P, Singhal RS, & Pandit AB (2005) A study on degradation kinetics of
riboflavin in spinach (*Spinacea oleracea* L.). Journal of Food Engineering, 67,
407-12.
- Paulsen H, Rümmler U, & Rüdiger W (1990) Reconstitution of Pigment-containing
Complexes from Light-harvesting Chlorophyll A/b-binding Protein Over
expressed in *Escherichia Coli**. Planta, 181.2, 204-11.
- Pedone S, Selvaggini R, & Fantozzi P (1995) Leaf Protein Availability in Food:
Significance of the Binding of Phenolic Compounds to Ribulose-1, 5-
Diphosphate Carboxylase. Food Science and Technology, 28, 625-34.
- Petsko GA & Ringe D (2004) Protein Structure and Function. London: New Science.
- Ranhotra GS, Gelroth JA, Langemeier J, & Rogers DE (1995) Stability and \
Contribution of Beta Carotene Added to Whole Wheat Bread and Crackers.
Cereal Chemistry, 72.2, 139-41.
- Rao AV & Rao LA (2007) Carotenoids and human health. Pharmacological
Research, 55, 207-16.
- Sadava DE (2010) Life: the Science of Biology. Sunderland, MA: Sinauer Associates,
9th ed.

- Schasfoort RBM & Tudos AJ (2008) Handbook of Surface Plasmon Resonance.
Cambridge: Royal Society of Chemistry.
- Schneider G, Lindqvist Y, & Branden CI (1992) RUBISCO: Structure and
Mechanism. Annual Review of Biophysics and Biomolecular Structure, 21,
119-43.
- Skoog DA, Holler FJ, & Crouch SR (2007) Principles of Instrumental Analysis.
Belmont: Thomson, 6th ed.
- Socaciu C (ed) (2008) Food Colorants: Chemical and Functional Properties. Boca
Raton, Fla.: CRC.
- Sterner R & Höcker B (2005) Catalytic Versatility, Stability, and Evolution of the
(beta-alpha)₈- Barrel Enzyme Fold. Chemical Reviews, 105, 4038-055.
- United States Department of Agriculture (2007) Census of Agriculture: Economics.
National Agricultural Statistics Service Web. 14 June 2010.
<http://www.agcensus.usda.gov/Publications/2007/Online_Highlights/Fact_Sheets/economics.pdf>.
- Wang W, Liu QL, & Cui H (2007) Rapid desalting and protein recovery with phenol
after ammonium sulfate fractionation. Electrophoresis, 28, 2358-360.
- Wang W, Vignani R, Scali M, & Cresti M (2006) A universal and rapid protocol for
protein extraction from recalcitrant plant tissues for proteomic analysis.
Electrophoresis, 27, 2782-786.
- Wissgott U & Bortlik K (1996) Prospects for New Natural Food Colorants. Trends in
Food Science and Technology, 7, 298-302.

- Worrall DM (1996) Dye-Ligand Affinity Chromatography. Protein purification protocols, Totowa, N.J: Humana, 59.
- Yancy & Cecil H (2004) Buyout brings changes to Maryland farm landscape. Southwest Farm Press Web 12 Jan. 2009
<<http://southwestfarmpress.com/news/maryland-tobacco-buyout/>>.
- Yang X, Kathuria SV, Vadrevu R, & Matthews CR (2009) Beta-Alpha-Hairpin Clamps Brace Beta-Alpha-Beta Modules and Can Make Substantive Contributions to the Stability of TIM-Barrel Proteins. PLoS ONE, 4.9, E7179.
- Yanishlieva N & Gordon M, (2001) Pokorny J (ed) Antioxidants in Food: Practical Applications. Cambridge: Woodhead Publishing Limited.
- Zees AC, Pyrpassopoulos S, & Vorgias CE (2009) Insights into the Role of the (alpha plus Beta) Insertion in the TIM-barrel Catalytic Domain, regarding the Stability and the Enzymatic Activity of Chitinase A Form *Serratia Marcescens*. BBA - Proteins and Proteomics, 1794.1, 23-31.
- Zhang K, Cascio D, & Eisenberg D (1994) Crystal Structure of the unactivated ribulose 1, 5-bisphosphate carboxylase/oxygenase complexed with a transition state analog, 2-carboxy-D-arabinitol 1, 5-bisphosphate. Protein Science, 3, 64-69.
- Zhang Y, Liu C, Liu S, Shen Y, Kuang T, & Yang C (2008) Structural stability and properties of three isoforms of the major light-harvesting chlorophyll a/b complexes of photosystem II. International Journal of Biochemistry, Biophysics and Molecular Biology, 1777, 479-87.

Zhou HY & Liu CZ (2006) Microwave-assisted extraction of solanesol from tobacco leaves. *Journal of Chromatography A*, 1129.1, 135-39.